POLITECNICO DI MILANO

School of Industrial and Information Engineering

Master of Science in Electrical Engineering

Impact of EV Charging Station on the Electric Distribution Grid

Thesis Supervisor: Morris Brenna
Department of Energy
Politecnico di Milano

Master thesis of:

Dwaramakki Gaurav
Matricola: 814767

Harinarayanan Manimaran
Matricola: 814802

Academic year 2015-2016

ABSTRACT

Over the past few years, Electric vehicles have become a very important part of the automotive industry as we try to look for a future less dependent on fossil fuels. A lot of research and development has taken place in this field to improve the existing technology and to develop efficient ones. This continued emphasis on research and development has resulted in great improvements in the technology of Electric vehicles.

In this thesis, we discuss about the features of Electric Vehicles, the existing protocols to charge the battery systems, the battery management system (BMS), the different standards used in various parts of the world and about the infrastructure that is needed to charge the Electric Vehicles and about the different modes of charging.

In the next part of the thesis, we have focussed on the Electric Vehicle and its relationship with the Electric Distribution Grid. Aspects related to PHEV characteristics, Load growth, PHEV Penetration level are looked into. The essence of this thesis is to learn about the Impact of the EV Charging Station on the Electric Distribution Grid. Research papers regarding the impact study of EV Charging station on the Milan Electric Distribution network is considered and discussed.

Finally, we look at the Optimisation of EV charging stations which helps in the overall efficiency of the charging process and lessens its impact on the Electric Distribution Grid. In this study we discuss about various control strategies of battery management, charging and the control of inverters.

Contents

1. INTRODUCTION

The high energy usage, environmental pollution and rising fossil fuel prices, current dependent on Internal Combustion Engine (ICE) technology must be reduced and alternative fuel which has the potential to solve environmental pollution; global warming and energy sustainability concerns must be explored. Taken consideration that electricity is the most suitable energy for transportation in the next 30 years when considering risk, emissions, availability, maintainability, efficiency and reliability [1]. The invention of automobiles with ICE began in the late 19^{th} century and the automotive industry ever since has seen only incremental changes. ICE remains the prime mover for automobiles with fossil fuel as the main fuel.

With the increasing concerns over depletion of natural resources (e.g. oil and gas) and air pollution, governments, automakers and consumers worldwide have been working together to adapt a shift to green transportation. This has spurred intense competition and ongoing revolution in the development of electric vehicles (EVs) and hybrid electric vehicles (HEVs) are an alternative to the internal combustion engine (ICE) vehicles with better efficiency and lower CO2 emissions. Among all EVs and HEVs, electrochemical batteries are core components used for energy storage, similar to the fuel tank in ICE vehicles.

Nowadays, EVs represent an interesting solution for the growing dependence from fossil fuels, since they allow a considerable reduction of air pollution. However, the diffusion of EVs is still affected by many issues, which are mainly due to interaction and integration of these types of vehicles with the existing power grid. Moreover, in order to have a wide diffusion on the market of no polluting vehicles, they have to present the characteristics of travel ranges and recharging times comparable to the traditional oil-based fuel vehicles. For these reasons EVs require battery packs characterized by high values of both energy storage capacity and charging rates. From this point of view lithium based batteries represent a very interesting solution, as they are showing a great potential, in recent years, to supply electric vehicles having good performance in terms of acceleration and driving range. Nowadays, new technologies of lithium compounds are available, which permit reaching an specific energy up to 180 Wh/kg and a maximum charging rate of 6 C reducing the charging times up to 10 minutes.

Typically, the charging modes at low power are suitable for charging the battery packs during night time of 7-8 hours, ensuring low power requirements for the grid. In fact, recent studies demonstrate that the daily travel range is less than 50 *km* in 80% of the cases. For this reason such slow recharging would be acceptable for most users ensuring a travel range from 100 to 150 *km* during the daylight.

2. Electric drive vehicles

Electric drive vehicles are very attractive due to low road emissions, can potentially strengthen the power system by providing ancillary services; have a lower operating cost compared to fossil fuels and are more energy efficient. Advanced electric drive vehicles can be categorized into Hybrid Electric Vehicles (HEVs), plug-in Hybrid Electric Vehicles (PHEVs) and all-electric vehicles (EVs).

2.1. Hybrid Electric Vehicles

HEVs can be generally classified as series, parallel and series-parallel (combined hybrid) as shown in Fig. 2 to 4 respectively. In a series HEV, traction power is delivered by the electric motor while the ICE drives an electric generator that produces power for charging the batteries and driving the electric motor as shown in Fig. 2 and Fig. 3 shows a parallel HEV in which the engine and electric motor are coupled to drive the vehicle which allows simultaneous operation of ICE and motor high speeds. Figure 4 shows a series-parallel configuration in which two electric machines are used to provide both parallel and series paths for the power. This means that ICE can be used to drive the vehicle together with the motor, or used for generating electricity to be stored in the battery, depending on the operating conditions and setup. HEVs can be further divided into micro hybrids, mild hybrids, power hybrids and energy hybrids depending on the hybridization factor. Hybridization factor is defined as the ratio of the peak of vehicle electrical power to that of total electrical and mechanical power. Micro hybrids have a hybridization factor of 5-10%; mild hybrids, 10-25% and power hybrids have much higher factor.

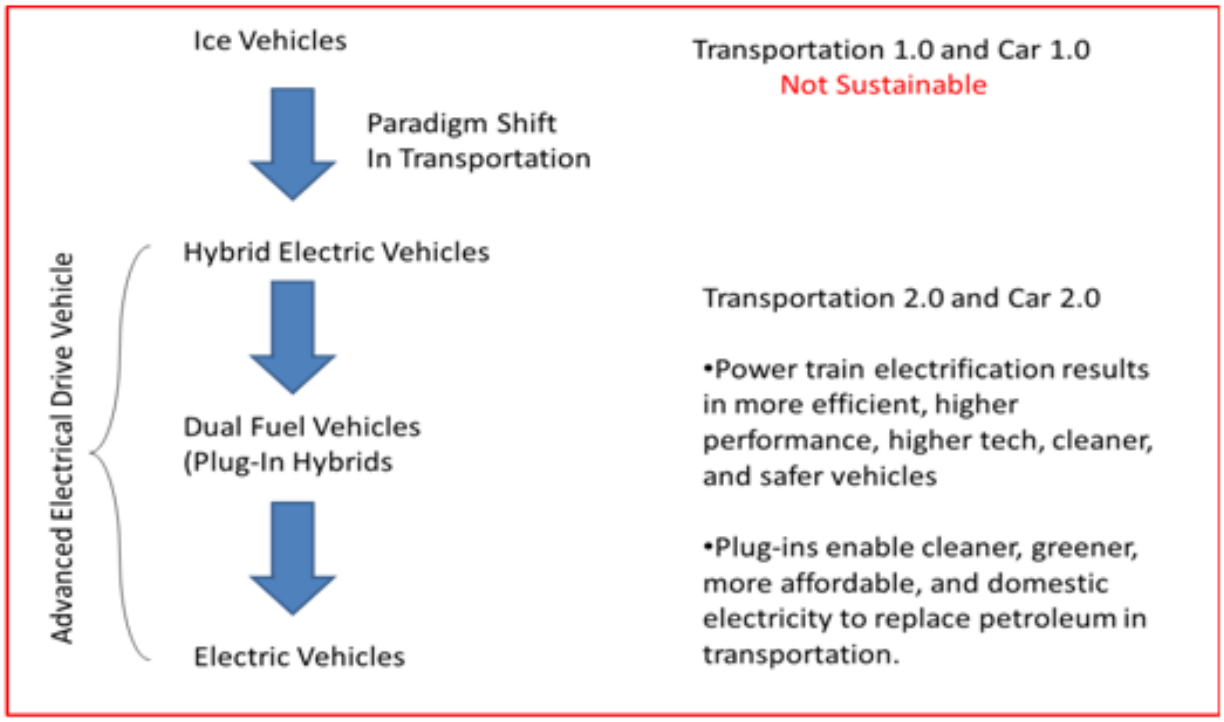

Figure 1: The paradigm shift in transportation from ICE vehicles to advanced electric-drive vehicles *[1]*

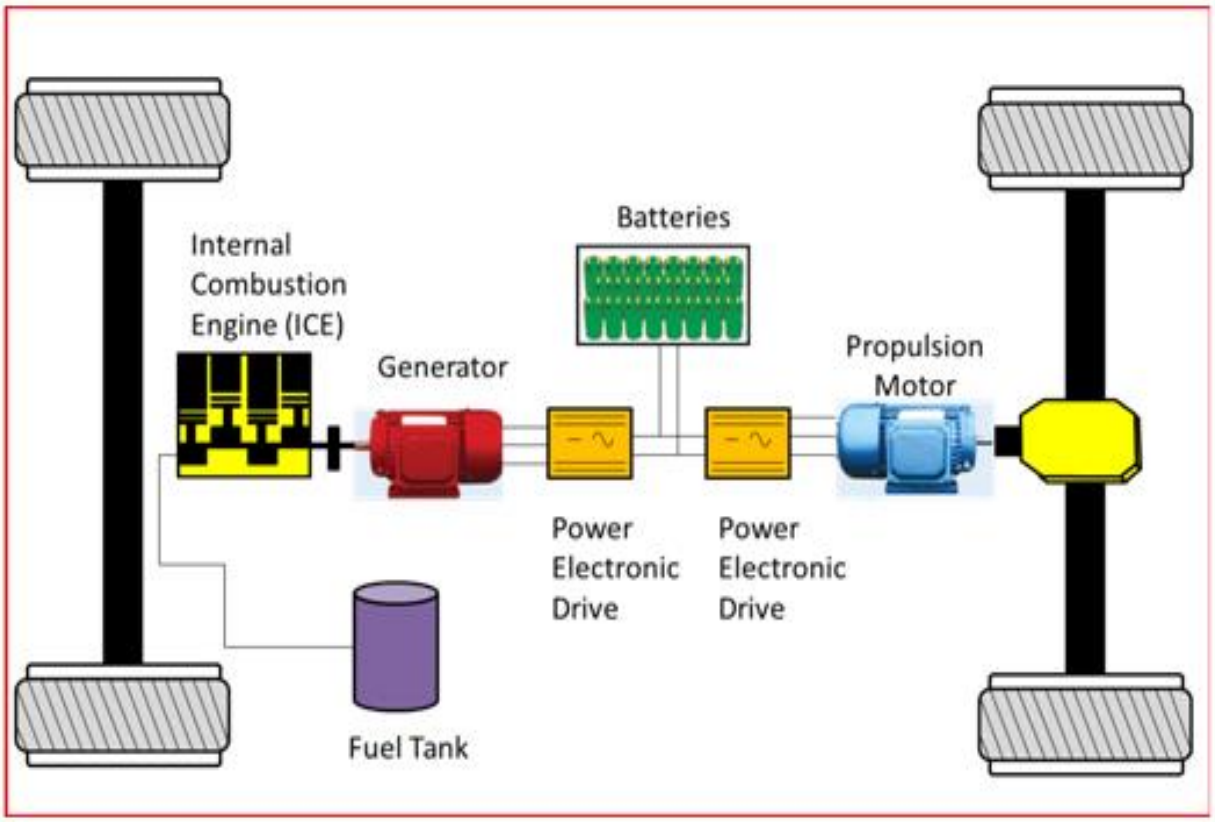

Figure 2: A hybrid electric vehicle with a series hybrid power train *[1]*

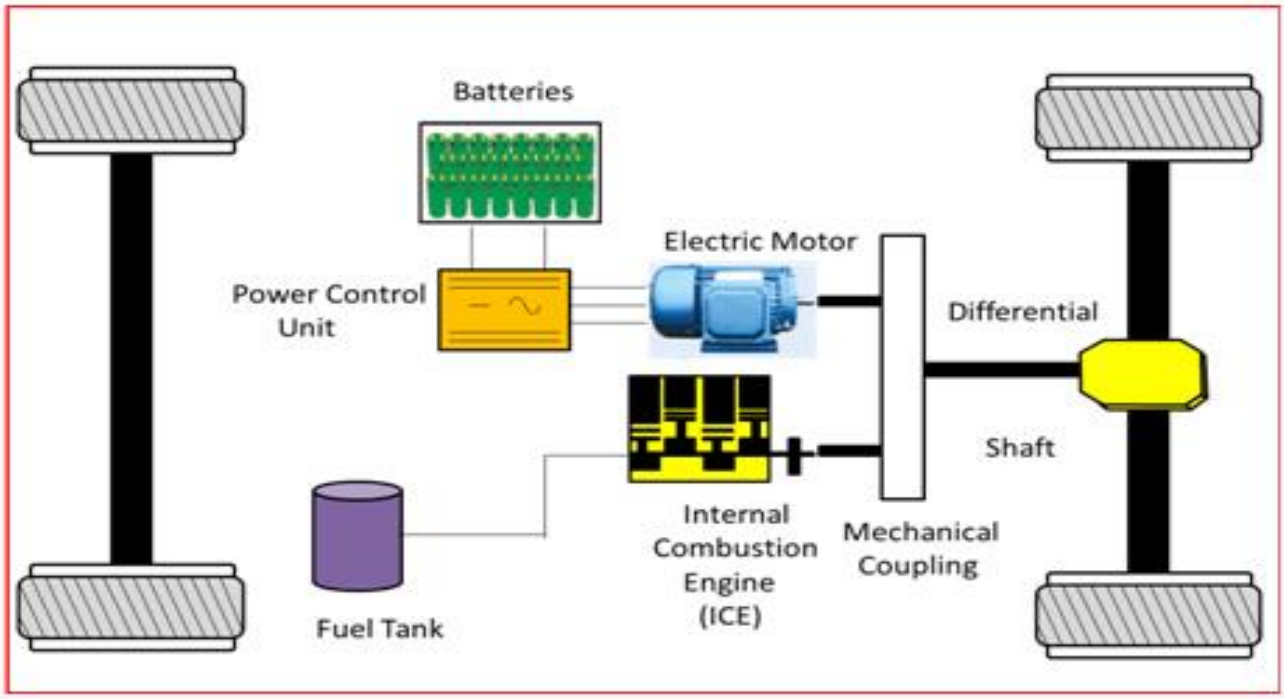

Figure 3: A hybrid electric vehicle with a parallel hybrid power train *[1]*

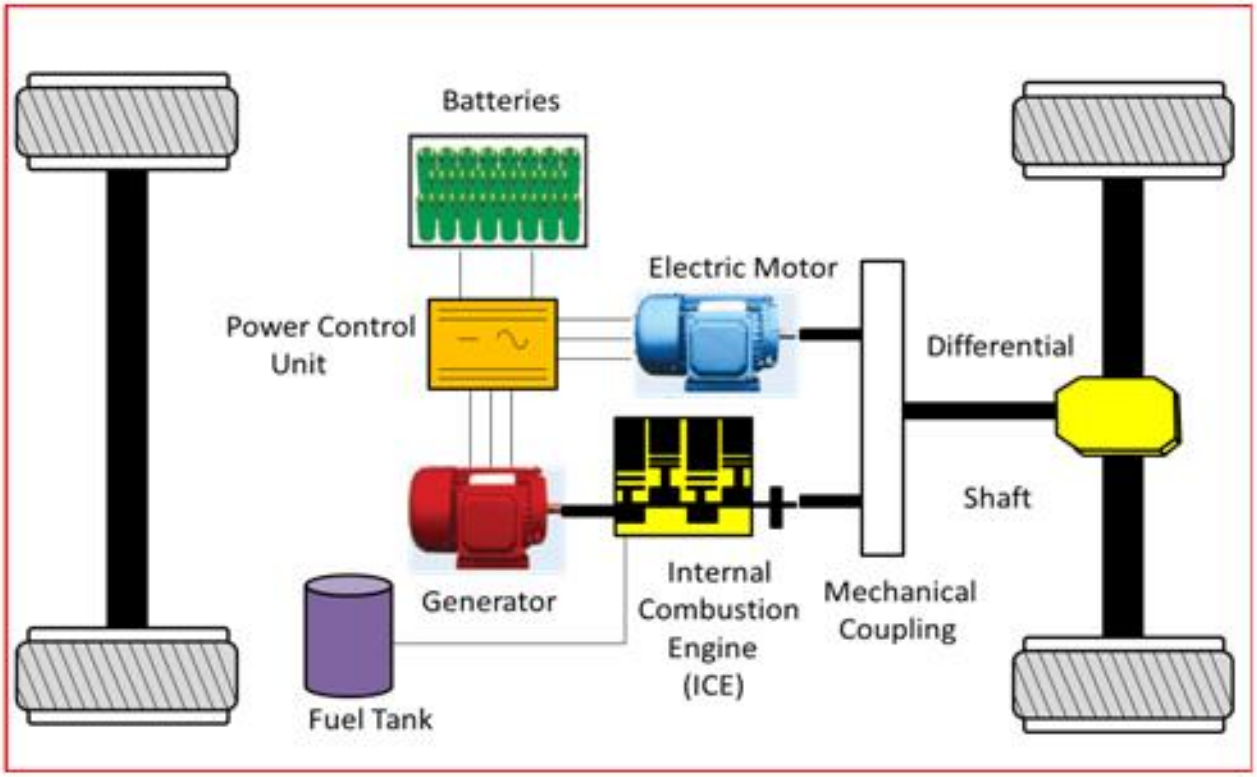

Figure 4: A hybrid electric vehicle with a series-parallel hybrid power train *[1]*

2.2. Plug-in Hybrid Electric Vehicles

Plug-in Hybrid Electric Vehicles (PHEVs) is essentially an HEV with the option to recharge its energy storage system with electricity from the grid (Markel and Simpson, 2006). PHEVs have a high-energy-density energy storage system that can be externally charged and they can run solely on electric power longer than regular hybrids, resulting in better fuel economy. Just like HEVs, PHEVs can have series, parallel and series-parallel configurations. Figure 5 and Figure 6 show a PHEV with series and series-parallel configuration, respectively. PHEVs make use of utility power as the batteries are usually charged overnight. The battery can also be charged on-board to increase the vehicle range.

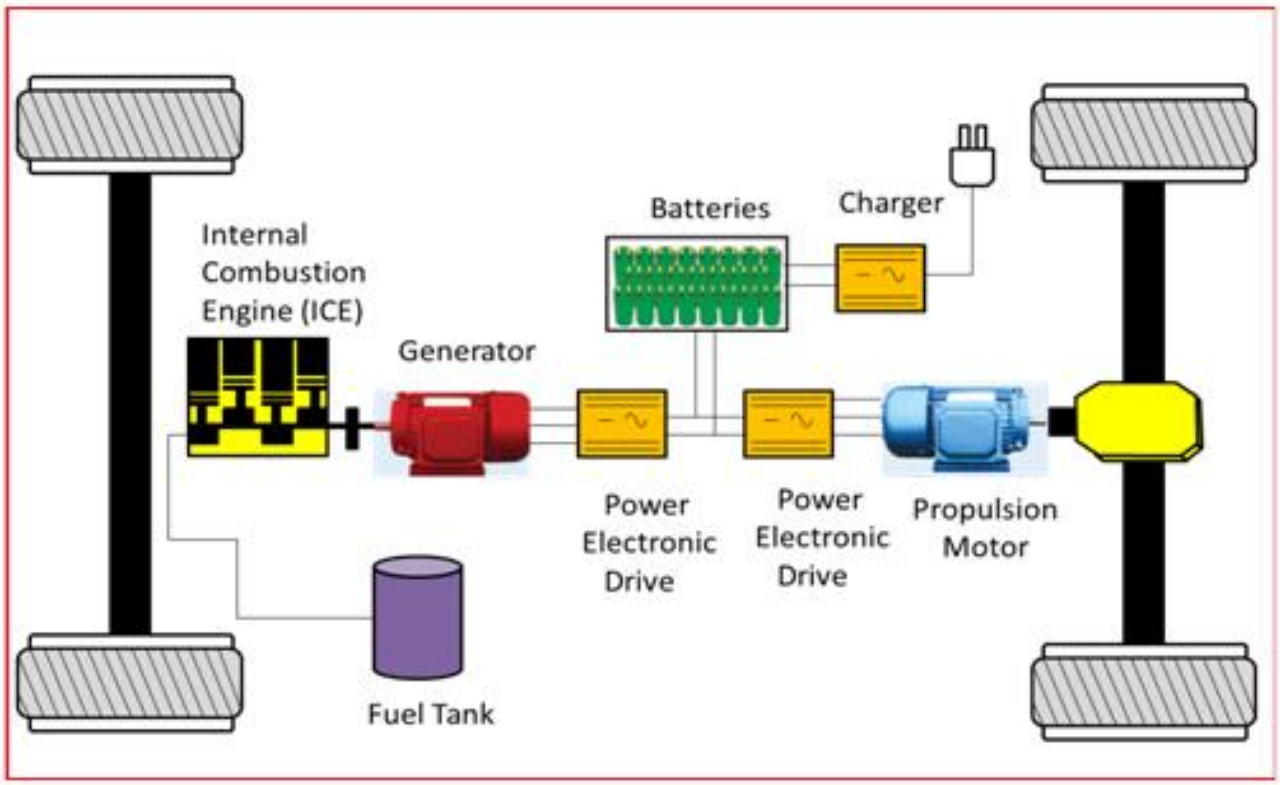

Figure 5: A plug-in hybrid electric vehicle with a series hybrid power train *[1]*

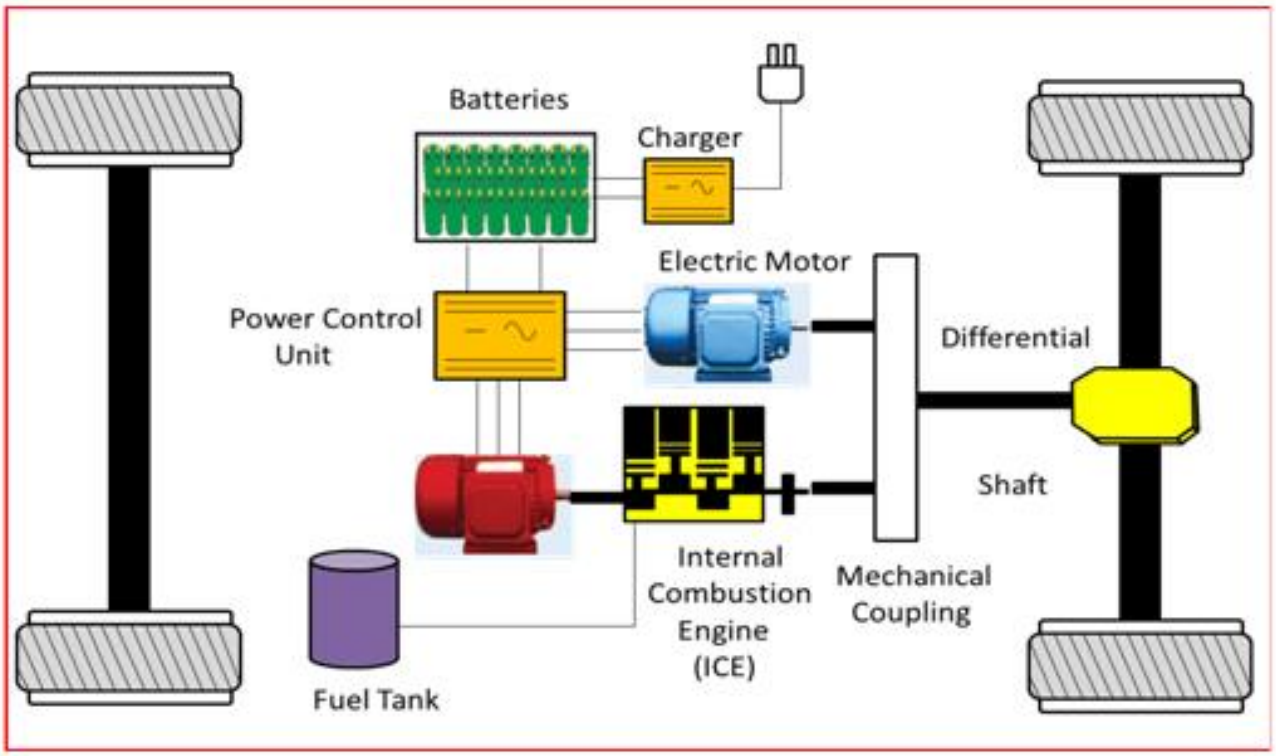

Figure 6: A plug-in hybrid electric vehicle with a series-parallel hybrid power train *[1]*

2.3. Electric Vehicles

All electric vehicles have all-electric propulsion system. A typical EV architecture is shown in Fig. 7.

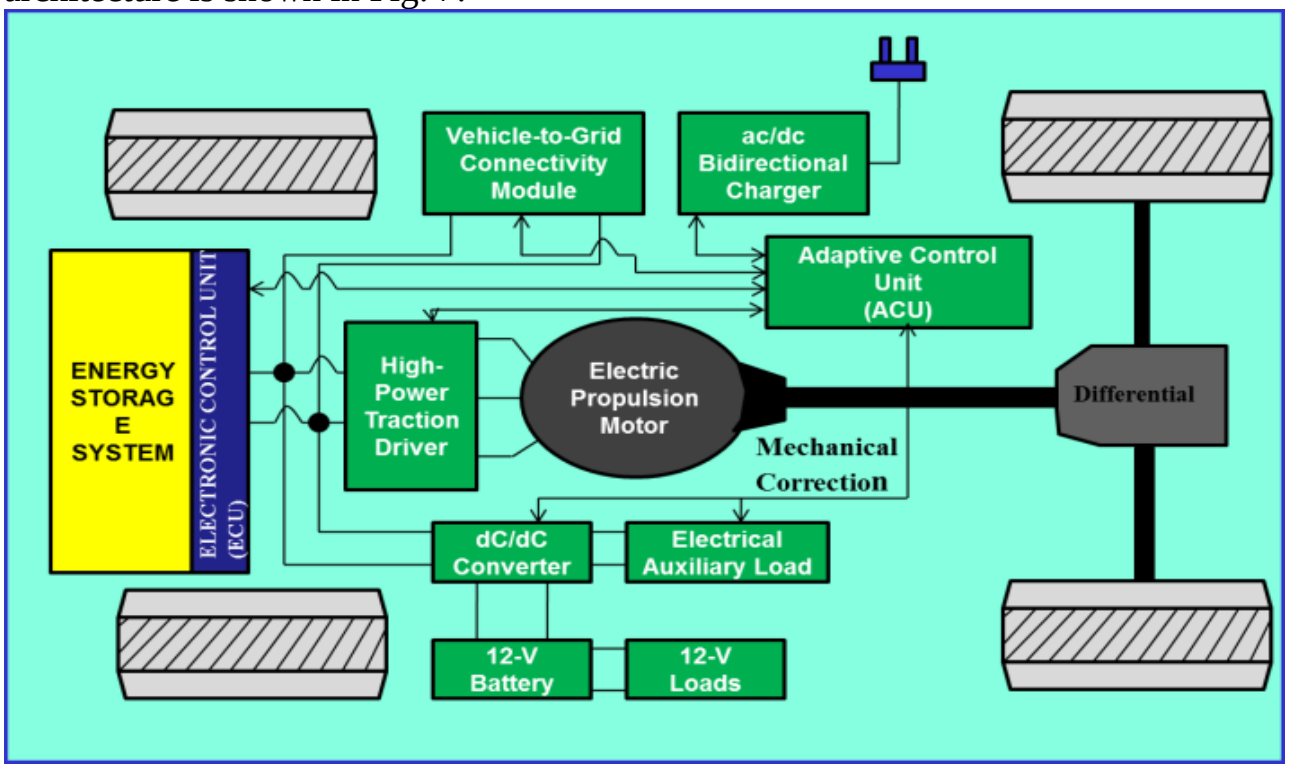

Figure 7: A plug-in hybrid electric vehicle with a series-parallel hybrid power train *[1]*

Unlike HEVs and PHEVs, EVs do not have an ICE to supply the additional power. These EVs rely mainly on external charge from the utility power grid and these types of advanced electric-drive vehicles are expected to affect the electricity distribution network.

Vehicle/ Type	Tesla Roadster (Berdichevsky *et al*., 2006) Battery	Nissan Leaf (Nissan, 2012) Battery	GM Chevy Volt (Chevrolet 2012) Plug-in hybrid	Toyota Plug-in Prius (Prius 2012) Plug-in hybrid	Mitsubishi i-MiEV(Mitsubishi 2012) Battery	Exora REEV (Che Din 2011) Plug-in hybrid
Electric range (Km)	394	161	56	24	160	97
Battery size (kWh)	53	24	16	4.4	16	13.5
On board charger (kW)	9.6	3.3	1.44	1.44	2.3	3.8
Quick charger (kW)	16.8	60	3.3	3.3	50	20
Charging time	On board: 6 h Quick: 3.5 h	On board: 6 h Quick: 0.5 h	On board 10 h Quick: 4 h	On board: 3 h Quick: 1.5 h	On board: 8 h Quick: 0.5 h	On board: 4 h Quick: 0.5 h
Vehicle/ Type	Saga EV (Che Din 2011) Battery	Mercedes-Benz Blue ZERO E-Cell plus (Mercedes 2012) Plug-in hybrid	BMW i3(Autocar 2012) Battery	Honda Fit/Jazz-EV (Honda 2012) Battery	Mazda Demio-EV (Mazda 2012) Battery	Tesla model S (Tesla 2015) Battery
Electric range (Km)	97	100	160	131	200	450
Battery size (kWh)	15.9	18	22	20	20	90
Onboard charger (kW)	3.1	3.3	7.7	6.6	3.3	
Quick charger (kW)	20	20	12	40	50	
Charging time	Onboard:6-8 h Quick: 0.5 h	Onboard: 6 h Quick: 1 h	Onboard: 6 h Quick: 1 h	Onboard: 3 h Quick: 0.5 h	Onboard: 8 h Quick: 0.67 h	

Table 1: Overview of technical data for commercial/ prototype electric vehicle

Power demand of EV is a function of voltage and current and its energy requirement depends on the battery size. The technical information on commercial and prototype EV sin terms of electric range, battery size, charger power and charging time is tabulated and summarized in Table 1. Such information is useful for determining the power demand required by EV. It is estimated that a single EC can increase electricity consumption of a household by 50%. Some EVs consumed more than 5 kW powers which is greater than the consumption of a typical residential house and this consumption is continuous up 10 h subject to the state of charge of the EV's battery. This power consumption is required for EV which is charged using the slow type on board charger.

3. Battery Technologies

A Battery is an energy storage device which uses electro chemical reaction to store electricity in the form of chemical potential during charging. This process is reversed during discharging to provide electricity to a load. Batteries are for high-performances electric vehicles (EVs) should be a nice trade-off between "drive performance" and "high reliability." The former feature includes vehicle autonomy and power output, and the latter includes a long lifetime, a maintenance-free system, high degree of safety, and energy regeneration capabilities. Battery has an important role as energy storage in electricity system utilization, such as portable electronic devices, electric vehicle, and in renewable energy power plant such as in smart micro grid system. Battery with good performance would provide optimal support for the operation of the corresponding system. Battery useful life will be longer if the battery operation is maintained in safety operating area (SOA), either when the battery is charged or discharged. Improper charging and discharging processes could decrease the performance and shorten the battery useful life.

Nowadays, different storage systems for both stationary and on board application are available to these purposes. The main storage systems are based on the following battery technologies.

- lead
- sodium and
- lithium

3.1. Lead batteries

Lead batteries have been largely used for traction applications since the end of the 19th century. Different types of lead-acid batteries have been developed and the main categories are classified as:

- Flooded and
- Valve regulated lead acid batteries (*VRLA*).

The latter mentioned batteries were developed as an alternative to the first ones, in order to maintain the levels of distilled water and also to avoid drying of the cells. This characteristic makes this kind of batteries particularly suitable for road electric vehicle applications. The VRLA batteries are also called 'no maintenance batteries', because they require a minimal attention and maintenance operations by the user. They are characterized by values of energy density in the range of 35÷50 *Wh/kg* and specific power of 150 *W/kg*. As a matter of fact, these kinds of battery are not used anymore for the road electric vehicles, mainly because of the disadvantage of a very low energy density, low performance at high discharging currents, low charging rate, plus the need by the designer of taking into account the material recyclability for the environmental impact. Anyway, they still present some advantages, such as that the temperature does not affect their performance, they are considered particularly secure, their cost is considerably cheap. For these reasons lead acid batteries are still used for many stationary applications, where restrictive constraints in terms of volume, weight and charging rate are not required. [2]

3.2. Sodium batteries

The sodium batteries are characterized by high working temperatures, required for the sodium to be in the molten state, in fact for these batteries the best performance is in the operative range of 520÷620 *K*. The sodium/sulphur batteries represent a low cost and environment friendly solution to be used particularly for stationary applications, since they are characterized by slight low values of energy density and reduced safety issues related to the combination between sulphur and sodium. The sodium-nickel chloride, better known as Zebra batteries (Zeolite Battery Research Africa), is a branch of the sodium batteries and represents a breakthrough in the sodium storage system technology, since they are much safer and present higher energy density than sodium/sulphur batteries. For this reason, Zebra batteries are mainly used to power road electric vehicles, in particular urban transportation means, due to the temperature issues to manage. Although the nickel extraction cost is higher than sulphur, Zebra batteries are still environmental friendly. Moreover, their characteristics of high energy density and low power density make them suitable when combined with supercapacitors to realize hybrid configurations.

3.3. Lithium batteries

Lithium batteries are characterized by high power and energy density, which means high performance in terms of acceleration and driving range when used to power

electric vehicles. The utilization of lithium batteries implies some concerns to be taken into account related to safety issues, mainly due to the high reactivity of the lithium metal. For this reason, lithium "host" compounds are used in lithium-ion batteries for both positive and negative electrodes, without a significant structural change to the host.

Recent developments of lithium batteries have been obtained by taking advantage of new anode and cathode materials to obtain high energy and power densities. The material most commonly used for cathode in lithium ion batteries is either LiCoO2 or Li-Co-Mn mixed oxides. Both these lithium based batteries present interesting performance in terms of high capacity and high voltage per cell. The main disadvantage of these types of cathode materials is due to the cost of cobalt and limited stability during the recharging phases [2]. Recently, other lower cost materials for cathode have been tested and proposed, and in particular the LiFePO4 batteries appear to be suitable for road vehicles applications. Their main advantages are based on their characteristics of low cost and abundance of Fe, high thermal stability, safety and durability in terms of life cycle. The energy density of LiFePO4 is slightly lower than LiCoO2 cathode, but the main limitation is represented by a low electrical conductivity.

A lithium–titanate battery (Li4Ti5O12, which is known in the battery industry as *LTO*) is a modified lithium-ion battery that uses lithium-titanate nanocrystals on the surface of its anode instead of carbon graphite. Lithium titanate is a promising anode material for specific applications that require high rate capability and long cycle life. LTO is interesting as it offers advantages in terms of power and chemical stability, although LTO based batteries have a rated voltage of 2.4 *V/cell*, which is lower than LiCoO2. On the other hand, the lower operating voltage is balanced by significant advantages in terms of safety. Further, these batteries have fast charging rate, in fact they can be safely charged at rates even higher than 10C, which means charging times lower than 10 minutes for this kind of batteries. The LTO based batteries have also the characteristic of an operating temperature range wider than other lithium battery technologies, in particular they have excellent low temperature discharge characteristics with an actual capacity of 80% at 243 *K*. Moreover, their life span and power density are not lower than other lithium batteries, and the recharge efficiency can be even higher than 98%. On the other hand, the energy density of 65 *Wh/kg* for the LTO based batteries is higher than lead acid and NiCad batteries, but it is still lower than other lithium ion batteries.

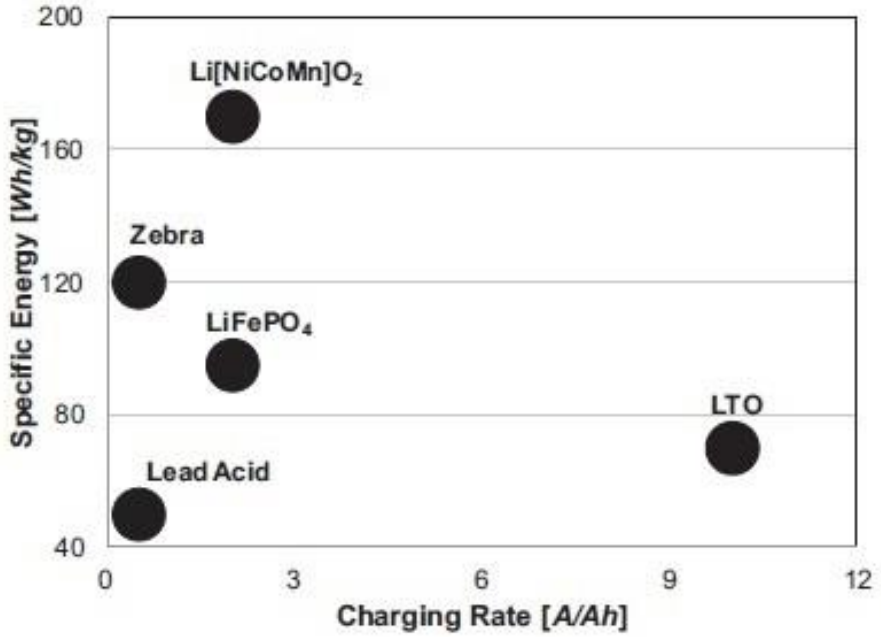

Figure 8: Comparison between different battery technologies in terms of specific energy vs charging rate [2]

4. International Lithium-Ion Battery Standards

Standard lithium-ion battery research currently undertaken a major international standardized International Organization for Standardization (ISO), the International Electro technical Commission(IEC), the American Society of Automotive Engineers(SAE), the German Automotive Industry Association (VDA), the Japan Electric Vehicle Association Standards(JEVS), as well as the Standardization Administration of the People's Republic of China (SAC) in our country and so on.

4.1. ISO Standard

ISO (International Organization for Standardization) is the world's largest developer of voluntary International Standards. International Standards give state of the art specifications for products, services and good practice, helping to make industry more efficient and effective. Three standards of lithium-ion traction battery for Electric vehicles were prepared by Technical Committee ISO/TC22/SC21 (Road vehicles/Electrically propelled road vehicles). ISO 12405-1: 2011 Electrically propelled road vehicles - Test specification for lithium-ion traction battery packs and systems - Part 1: High-power applications, ISO 12405-2: 2012 Electrically propelled road vehicles - Test specification for lithium-ion traction battery packs and systems - Part 2: High-energy applications, ISO 12405-3 Electrically propelled road vehicles - Test specification for lithium-ion traction battery packs and systems - Part 3: Safety performance requirements. The series of ISO 12405 are all test method standards which using the lithium-ion battery pack systems as test object, and set a lot of test items.

However there is no set criterion, test items, test conditions, and the results requirement can determine by the supplier and user through consultation [3].

4.2. IEC Standard

The International Electro technical Commission (IEC) is the world's leading organization that prepares and publishes International Standards for all electrical and electronic related technologies. The IEC is one of three global sister organizations (IEC, ISO, ITU) that develop International Standards for the world. Two standards of lithium-ion traction battery for Electric vehicles were prepared by Technical Committee IEC/TC21 (Secondary cells and batteries). IEC 62660-1: 2010 Secondary lithium-ion cells for the propulsion of electric road vehicles - Part 1: Performance testing, IEC 62660-2: 2010 Secondary lithium-ion cells for the propulsion of electric road vehicles - Part 2: Reliability and abuse testing. Likewise, in ISO 12405 there is no setting limit criterion for all test items of IEC 62660 standards, as well as the series of standards, but the detailed test results obtain through the standards of the test items and test methods. The series of IEC 62660 are standards for testing electrical performance, system reliability and abuse aspects of lithium-ion traction battery [3].

4.3. SAE Standard

SAE International, formerly the Society of Automotive Engineers, is a U.S.-based, globally active professional association and standards organization for engineering professionals in various industries. SAE International provides a forum for companies, government agencies, research institutions and consultants to devise technical standards and recommended practices for the design, construction, and characteristics of motor vehicle components. SAE documents do not carry any legal force, but are in some cases referenced by NHTSA and Transport Canada in those agencies' vehicle regulations for the United States and Canada. SAE J 2929-2011 Electric and Hybrid Vehicle Propulsion Battery System Safety Standard - Lithium-based Rechargeable Cells published by SAC in February 2011 [7]. SAE J 2929-2011 stipulated the discharge current of hybrid vehicles and pure electric vehicles lithium ion batteries during testing process, and explain the state of the testing battery system in detail. In order to better protect the safety of the battery, this standard can be divided into two parts to test the traction battery. One is conventional case may occur in electric vehicle during operation, such as vibration, thermal shock, thermal humidity cycling, etc., for the other is abnormal situation may occur in electric vehicle during operation, such as falls, flooding, mechanical shock, simulated vehicle fire, short circuit, overcharge protection, over-discharge protection, Thermal control system failure protection. The standards not only raised test items and test methods, but also specifies the requirements for the test results.

4.4. UL Standard

Underwriters Laboratories (UL) is a global independent safety science company with more than a century of expertise innovating safety solutions from the public adoption of electricity to new breakthroughs in sustainability, renewable energy and nanotechnology. Dedicated to promoting safe living and working environments, UL helps safeguard people, products and places in important ways, facilitating trade and providing peace of mind. UL 2580 Standard for Batteries for Use in Electric Vehicles published by UL in October 2011 [8]. UL 2580 raise several criteria for battery and battery modules, including enhanced compatibility test for battery and charging system, enhanced imbalances test for a single battery or battery modules, enhanced security assessment insulating lines, and enhanced electrical misuse testing associated applications. In addition UL2580 also increased the production line safety testing standards to the design requirements for basic safety within the battery pack various parts or components, which covers non-metallic materials fire rating, anti UV aging level, corrosion level of metallic materials, flame and electrical insulation requirements for battery casing, etc. And also strengthen the requirements for safety review in battery management system (BMS), cooling systems and the protection circuit design specific to large-scale electric vehicle battery pack, etc.

4.5. UL Standard VDA Standard

The German Association of the Automotive Industry (Verband der Automobilindustrie, VDA) nationally and internationally promotes the interests of the entire German automotive industry. It can bank on a strong power base of members consisting of automobile manufacturers, suppliers and manufacturers of trailers, special bodies and buses. Unlike in many other countries, they are organized under one association, resulting in decisive advantages for the German automotive industry through direct dialogue and rapid decision-making. VDA 2007 Test Specification for Li-Ion Battery Systems for Hybrid Electric Vehicles published by VDA in March 2007. The standard mainly stipulate some test methods and acceptance criteria for the battery performance and durability requirements, including energy and capacity, power, energy efficiency, high low temperature start, self-discharge, standard rating cycle and working cycle, etc. Security testing methods are basically reference Freedom CAR 2005: Electrical energy storage system— Abuse test manual for electric and hybrid electric vehicle applications [3].

4.6. CHINESE BATTERY STANDARDS

To make lithium-ion battery industry more responsive to the development of electric vehicles, and more in line with China's current technical requirements, SAC/TC114 publish a mandatory access electric vehicle product testing standards, QC/T 743-2006 Lithium-ion batteries for electric vehicles [11], based on the relevant international advanced standards and combination of specific safety requirements lithium-ion battery and electric vehicle industry status. This standard test target for the battery cell and the cell module, simultaneously, test item including high and low temperature discharge capacity, room temperature and high temperature charged maintain ability and capacity recovery ability, storage, cycle life, overcharge test, over discharge protection test, Short Circuit test, drop test, heating test, extrusion test, acupuncture test. Specified in the standard security requirements are more comprehensive and rigorous, single battery during overcharge, short circuit, heating, extrusion and prick tests should be no explosion, no fire; over-discharge and drop test, should not explosion, no fire, no leakage. Battery modules required for each module consists of five or more single cells in series, in addition to the drop test is not required, other security requirements and the same single cell. QC/T 743-2006 has played a major role in China's electric vehicle development. With the development of electric vehicles and lithium-ion battery industry, the QC/T 743-2006 was not fully meet the relevant test requirements. So SAC/TC114/SC27 revising QC/T 743-2006, and in the stage of approval [3].

5. Battery management system

Battery Management System (BMS) is needed to treat the dynamics of energy storage process in the battery in order to improve the performance and extend the life of battery. BMS has two operational aspects: monitoring and control. Monitoring aspect cannot be separated from the control aspect. The BMS ensures that the battery will not damage due to overcharging, over discharging or over load power consumption. The BMS will examine the operational parameters of the battery e.g. voltage, current, the internal temperature during charging and discharging and estimate the battery state e.g. state of charge (SOC) and state of health (SOH). [4]

A BMS which flexible enough to protect different types of batteries and can provide all the safety features, has been a recent topic of development and research in electric vehicle and alternative energy systems. BMS should include functions for data acquisition, safety protection, ability to determine and predict the state of the battery, ability to control battery charging and discharging, cell balancing, thermal management, delivery of battery status and the authentication to a user interface,

communication with all BMS components and the most important thing is to prolong battery life.

5.1. Need for BMS

Although battery technology is growing very fast to provide practical solutions for the EVs industry, the progress in technology and materials alone cannot guarantee a solution that will overcome all the concerns. Some of the concerns regarding the integration of the battery storage are as follows:

- Cost—includes manufacturing, labour, maintenance, operation, and replacement costs.
- Lifetime—measured by the charge/discharge cycles and calendar life of the battery.
- Power delivery—measured in terms of charge/discharge rate, energy storage level, ramp rate, and charge/discharge efficiency.
- Environmental impact and safety— measured in terms of the safety/risk factors due to the chemical composition of the battery, operating temperature, etc.

The BMS provides accurate estimations of the status of the battery to the energy management system (EMS) unit. The EMS unit in EVs minimizes the cost involved while maximizing lifetime, safety and reliability. The performance of the EMS is only as accurate as the data provided by the BMS about the battery's SOC, remaining useful life (RUL), round-trip efficiency, etc.., to increase the efficiency and safety of the battery.

In the figure.9 below:

1) The data acquisition (DAQ) module collects the battery data, which includes current, voltage, and temperature at proper sampling frequency and precision.

2) The collected data is sent to the state estimation algorithm module, which includes the online parameters identification module and a state observer. In this module, considering a simple model for the battery dynamics, the parameters of the battery are identified using the input/output data. Afterward, the updated parameters of the battery model are fed to a state observer to estimate the SOC, SOH, and state of life (SOL) of the battery. Since the state observer is designed based on the state-space model of the battery, online identification and updating of the model parameters enhances the accuracy of the estimation. The SOC, SOH, and SOL are the information that the monitoring and management system in the smart grid and the EVs need to know about the battery to perform efficiently.

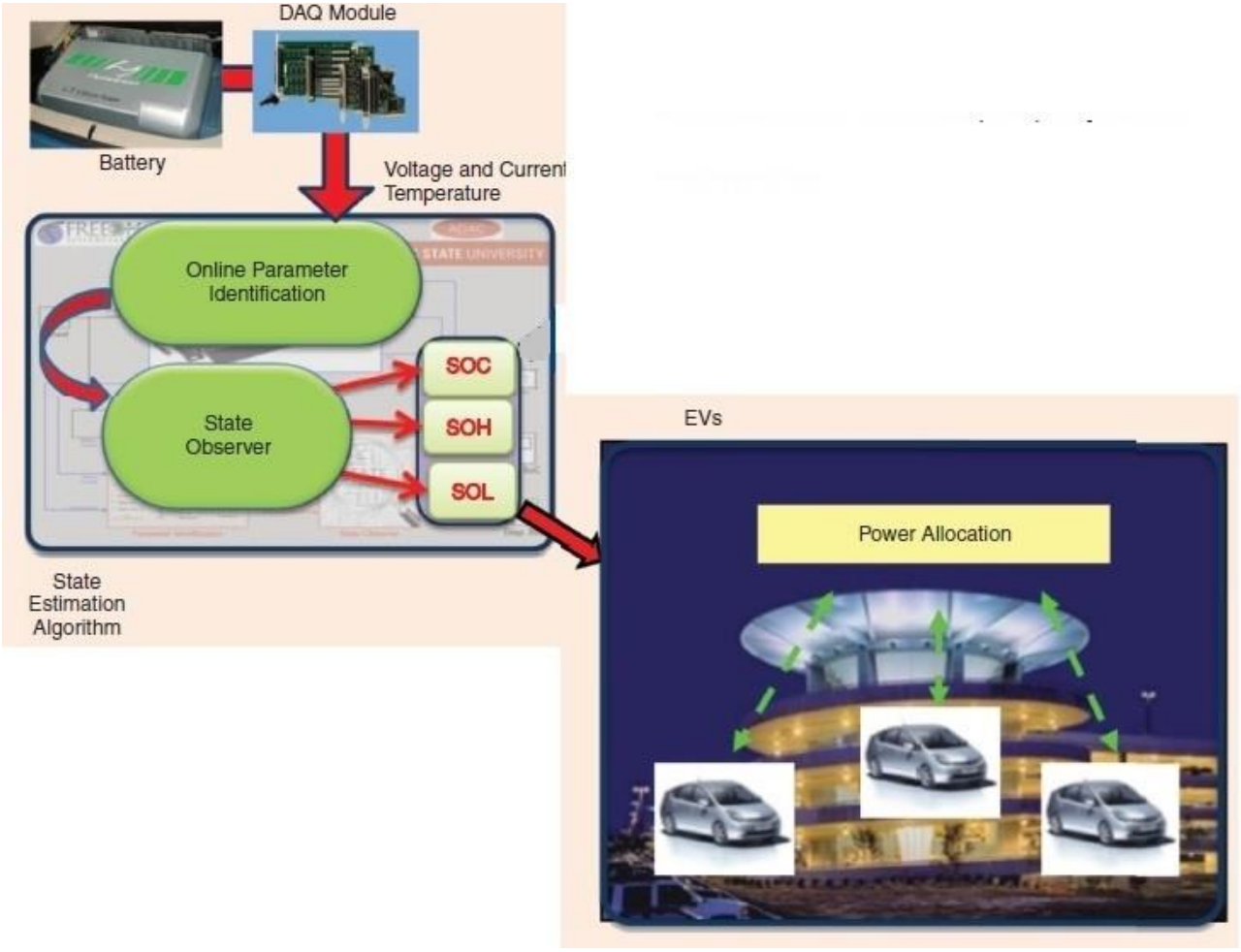

Figure 9: Battery management system algorithms function in electric vehicle *[4]*

3) The smart grid diagram shows a distributed control and energy management among distributed resources, loads, and energy storages in a typical power network in the smart grid. In this network, each component of the grid collaborates with the others to manage the available energy based on the local information and the information from the neighbours.

4) The EVs diagram shows the power allocation of a large-scale EV parking deck to different charging stations based on the state of the batteries and the customer's preference. The EMS module in the parking deck maximizes the satisfaction factor of the customers without exceeding the power constraints. Customer satisfaction is evaluated by the SOC of the vehicle battery at the arrival and departure times and the budget preferences of the customers.

5.2. BMS Architecture

Architectural choices for implementing a BMS are strictly dependent on the physical structure of the battery. In high-power applications, such as EVs and smart grids, usually ten to more than 100 high-capacity elementary cells are series-connected to build up the required battery voltage. The overall cell string is usually segmented into smaller modules consisting of several series connected cells. Thus, the battery can be regarded as being made of three nested layers: the elementary cell, the module, and the pack (i.e., the series of modules). Each layer can serve as an intelligent platform for the effective implementation of a subset of the previously outlined BMS. This general view leads to the BMS hierarchical architecture schematically depicted in Figure. The innermost layer hosts the cell monitoring units (CMUs), one for each cell in the string. The middle layer consists of the module management units (MMUs), one for each module in which the string has been partitioned. An MMU uses the basic monitoring functions of the CMUs and provides higher-level services to the pack management unit (PMU), which supervises the entire battery string. A dedicated and ad hoc designed link can be used to connect each CMU to the relevant MMU. A shared galvanic-isolated controller area network (CAN) bus is the preferred choice to implement communication between the MMUs and the PMU. The CAN bus also embeds the interface between the battery and the other control units of the system hosting the battery. This hierarchical architecture platform is flexible and scalable, as the BMS functions can be freely distributed and, if redundancy is needed, replicated over all three layers of the platform. A simplified instance of the hierarchical platform consists of only the two outer layers. In such a case, the BMS embeds only an MMU for each module and the PMU. This is a relatively common choice, since providing each cell with a dedicated CMU can be expensive. In addition, it may increase the overall self-discharge rate of the battery in a non-negligible way. However, the actual trend is to build up the battery by series-connecting very-high-capacity cells, instead of groups of parallel connected cells with lower capacity. Consequently, the cost and power consumption of a CMU may seem affordable when compared to the cost and self-discharge rate of a very-high capacity cell. The use of the cell layer can be beneficial to the implementation of the BMS monitoring tasks. The CMU can easily act as a gauge measuring the voltage and the temperature of the related cell to provide redundancy to this key BMS function. [4] In addition, the embedded CMU can store valuable information, such as the serial number, the lifetime, and the number of cycles to be evaluated and stored, into the cell itself. This enables easy tracking of the cell history, thus facilitating potential use in a second market application of the smart grid when the progressive degradation of its usable capacity makes the cell no longer suitable for an EV. Along with reducing size and cost, a key point in implementing the CMU is the communication with the MMU. This needs to be isolated because the MMU and the relevant cells belong to different voltage domains. An interesting approach based on a capacitive coupled link among the cells and the MMU that eliminates the need for a wiring harness with the cells and the MMU.

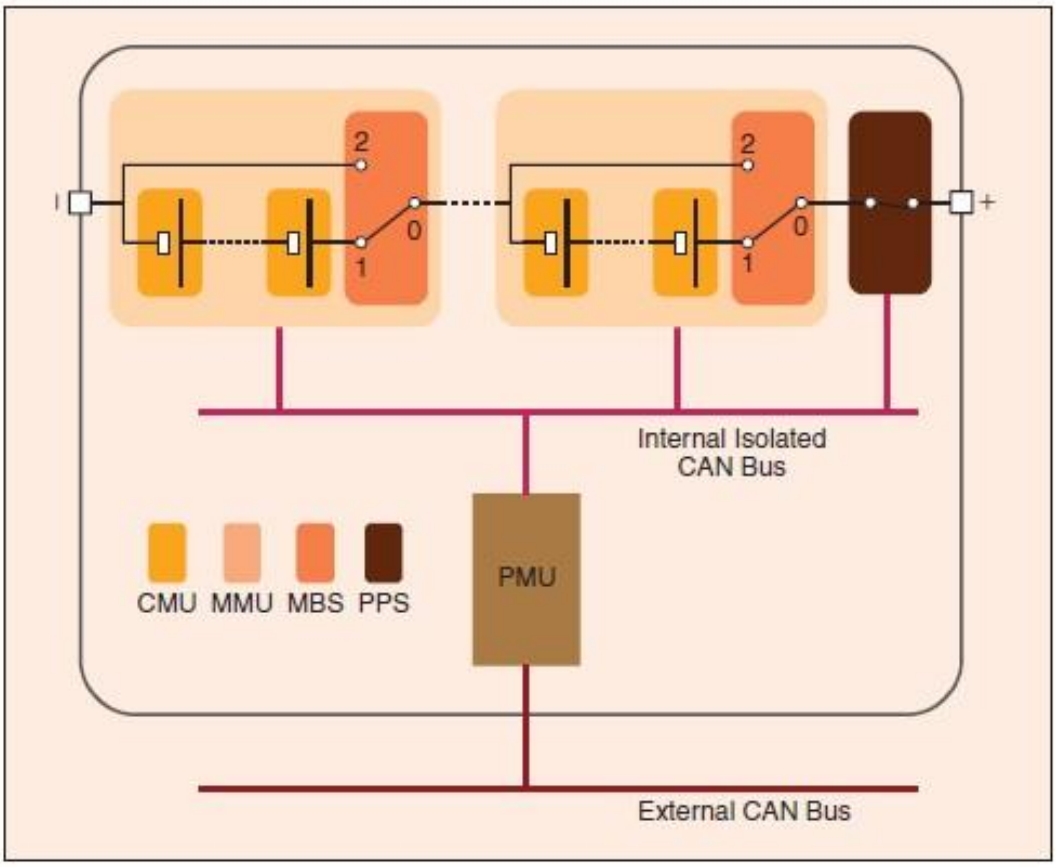

Figure 10: Hierarchical BMS architecture *[4]*

5.3. BATTERY PACK DESIGN

The developed battery pack consists of two independent batteries are parallel connected through two dc/dc converters to a common dc link. Each battery is constituted of 70 LiCoO cells series connected for a nominal battery voltage of about 260 V. Table I reports the characteristics of a single cell and of the whole battery pack. Fig. 1 shows the battery stack: seven packs connected in series constitute the two batteries. The ten cells inside every pack are individually protected and equalized by a suitable electronic circuit. As is known, charge and discharge cut offs for the lithium-ion battery cells must be closely controlled or early cell damage will occur: Overcharge leads to electrolyte oxidation and decomposition while over discharge results in cathode structural changes. The high number of adopted cells (70) stacked in series compounds the problem: under these conditions individual cell monitoring and equalization must be provided.

5.3.1. Cell Voltage Monitoring

According to manufacturer specifications the cell charge must be stopped if voltage exceeds 4.2 V and, additionally, cell discharge will be stopped if cell voltage falls below the 2.7-V threshold. Obviously, from the energy storage point of view, stopping battery charge when the first cell surpasses the voltage threshold is not an efficient solution. This would result in storing an amount of energy clamped by the leakiest cell of the stripe. In order to optimize EV autonomy, a proper charge equalization must be provided. In fact, the voltage profile during discharge may be remarkably different for each cell within a ten-cell stripe battery pack. The cell voltage monitoring circuit consists of a precision temperature compensated voltage reference and of a resistor voltage divider to sense cell voltage. The voltage of each cell is continuously compared with voltage reference to state cell voltage condition. Suitable threshold hysteresis was implemented for both overvoltage and under voltage conditions to prevent oscillation due to battery equivalent series resistance (ESR). Parasitic elements must be taken into account during transient conditions because voltage drop can deceive the protection circuit causing false under voltage. *RC* low-pass filters with suitably large time constant were used to address this issue. Dedicated circuits were designed for overvoltage and under voltage monitoring. High resistance values were used in order to decrease power consumption. Moreover, resistance tolerance is very important to achieve accurate protection: SMD resistors 0805 series with 0.5% tolerance values were used extensively. The normal operating voltage range of each cell is [3V, 4.15 V]. When the voltage exceeds this range, under voltage and overvoltage protection circuits start to operate, sending the actual cell voltage level to the control by an opto-coupler. Specifically, in the overvoltage operation range [4.15 V, 4.25V], the overvoltage circuit produces a linear voltage depending on the charge state of the relevant cell [5]. With a dual behaviour in the under voltage operation range [2.7 V, 3 V], the under voltage circuit produces a linear voltage depending on the charge state of the relevant cell. When two or more cells are operating in a non-optimal voltage, the control board acts as an ex-or and sends the output of the sensing circuit which shows the worst case of charge state. A temperature sensor ensures that the battery pack temperature does not surpass 70C, in order to prevent damage to the cells. The outputs of the above-mentioned protection circuits are sent through a proper interface (implemented with an array of opto-couplers) to the motion control digital signal processor (DSP) allowing a tuning control strategy according to journey characteristics. Each sensor observes the voltage across the relevant cell independently of the position of the cell inside the pack. The reason for the different slopes between overvoltage and under voltage transitions is due to the different priority of intervention. In overvoltage conditions, the DSP must stop the charge at constant current starting the charge at constant voltage. On the other hand, when a cell is in under voltage condition the DSP must reduce the current requested by the user providing less acceleration in

order to guarantee the best autonomy of the vehicle and allowing a larger margin of battery safety.

5.3.2. Cell Equalization

To obtain maximum energy storage, cells must be individually equalized during charge operation. Toward this aim, in the literature several solutions are adopted. The most widely used are critically reviewed in Table II. In spite of higher energy efficiency, the use of reactive switched elements was discarded because it leads to a bulky solution [6]. The switching resistive solution was adopted. As far as the choice of the switch is concerned, the need for good balancing capability and especially for high reliability leads to an automotive technology solution. In order to obtain a simple and reliable solution a protected FET (ProFET) was used in parallel to each cell of the pack to drain current from the cells at the threshold of overvoltage (4.15 V). In overvoltage conditions the battery charge will continue without overcharging the cell because of the shunting operation performed by the ProFET. Battery charging will be stopped when the cell overvoltage monitoring circuit detects a voltage of about 4.25–4.3 V. The ProFET is a smart FET, which includes a high-side drive and is fully protected by embedded protection functions, thus, this solution greatly simplifies the equalization circuit. Table III reports ProFET current capabilities. A dedicated circuit for equalization purposes was designed for each cell inside the battery pack relying on ProFETs. The choice of the components of the control circuit was driven by the need of low power consumption of the board (500 mW). Because of the large number of devices, they were placed on two faces in a four-layer printed circuit board (PCB). The conformation and the size of the board are related to the size of the battery pack composed of ten cells; in fact, the board is mounted on the battery pack, in order to reduce the volume. The size of the board is 201 mm 54mm (7.91 2.12 in). SMT components were used for size and precision purposes. The pads, which provide the voltage of each cell, were placed in order to reach the cell connectors by screwed bars for ease of assembly [5].

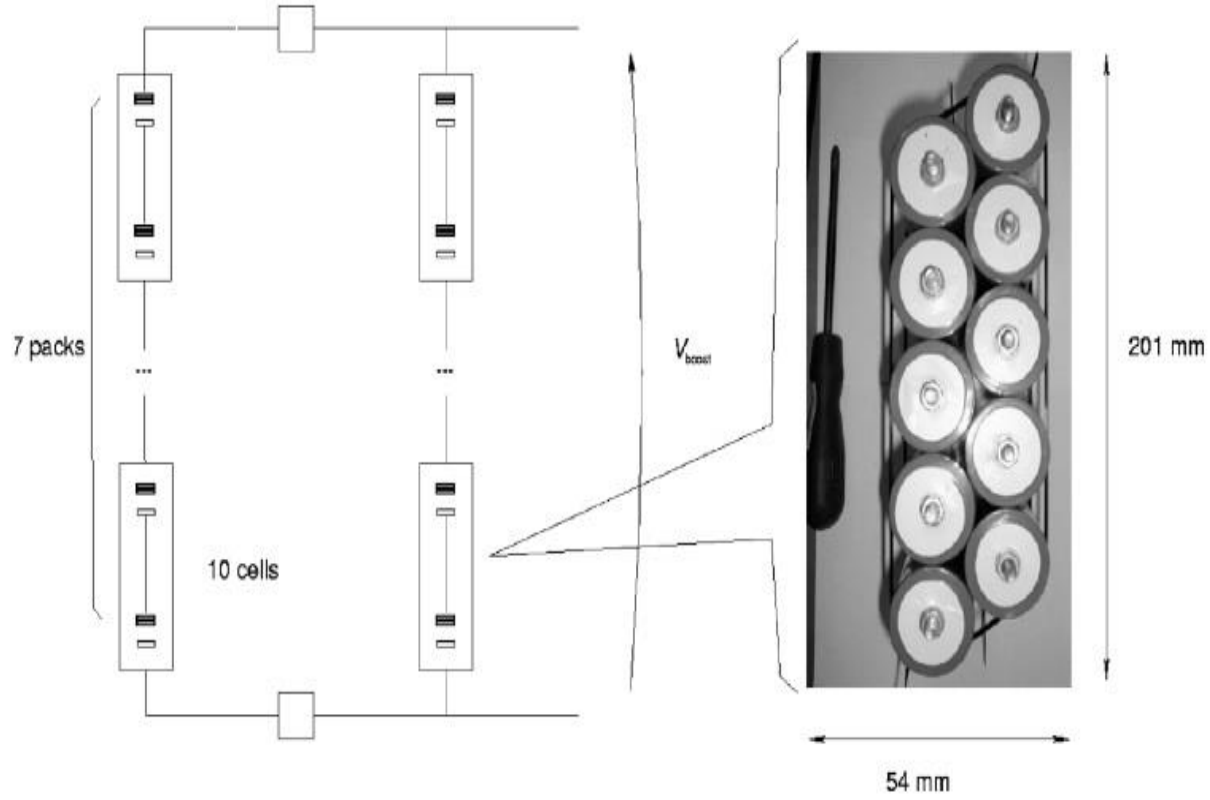

Figure 11: Battery cells hierarchical structure.

Method	Advantage	Disadvantage
Switched Capacitor	Simple Circuit Elements	Low equalizing capability
Variable Analog cell shunting	Good balancing capability. Constant voltage model.	Complex power electronics. Thermal management. Energy efficiency (90%).
Switched Resistive	Good Balance capability. Simple Electronics. Low power Requirements.	Thermal management. Energy efficiency(90%).
Switched Resistive Inductor/Trasf.	Energy efficiency (99%)	Mass. Cost. EMI.

Table 2: Equalization circuit characteristics

Nominal load current	3.1 A
Repetitive Short Circuit Current Limit	12 A

Table 3: ProFET Characteristics

6. Protocols

Fast Charging makes electric cars more useful because of the reassurance drivers get knowing they can quickly recharge, and the faster effective trip speed. It seems that car owners with fast-charge capable cars, with enough fast charging stations around them, feel capable of taking longer trips.

6.1. CHAdeMO Protocols

CHAdeMO is a fast charging protocol co- developed by Japanese automakers and Tokyo Electric power Company (TEPCO). CHAdeMO is the world's first DC fast charging standard designed for modern Electric Vehicles, featuring high density lithium-ion batteries and compact yet powerful magnetic synchronized motors. The R&D of CHAdeMO dates back to 2005. After more than four years of thorough testing and onsite demonstration, the first commercial CHAdeMO charging infrastructure was commissioned in 2009.

CHAdeMo allows up to 62.5 kW, the CCS-Standard up to 90 kW and the Tesla Supercharger (TSC) up to 120 kW. However those given power limits are most likely to increase with further development.

The charging sequence of a DC quick charger according to the CHAdeMO protocol is shown in the figure.12 below.

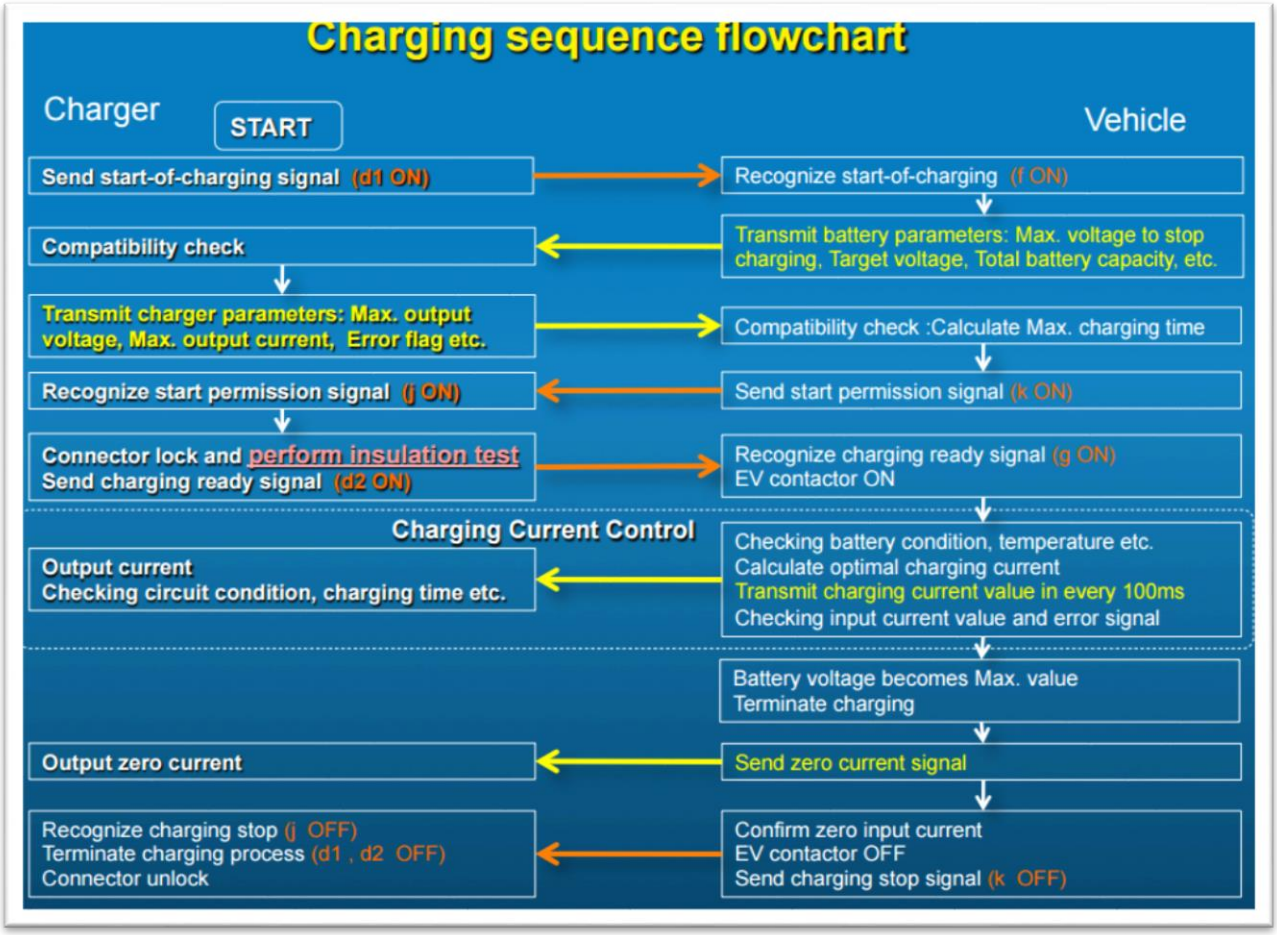

Figure 12: Charging sequence circuit *[7]*

Once the user decides to start the charging process and after the necessary connections are made and the user presses the Start button, the CAN, communication is initiated. Now, the insulation test is conducted. If the insulation test is passed, the conductors K1 and K2 are closed. With the help of the CAN- communication protocol, the charging process starts and stops according to the issues encountered by the system. Once the charging process is completed, the conductors K1 and K2 are opened and the connector is unlocked. With the unlocking process, the CHAdeMO protocol comes to an end.

Connectors of the CHAdeMO protocol were designed by the Japanese Automotive Research Institute (JARI).

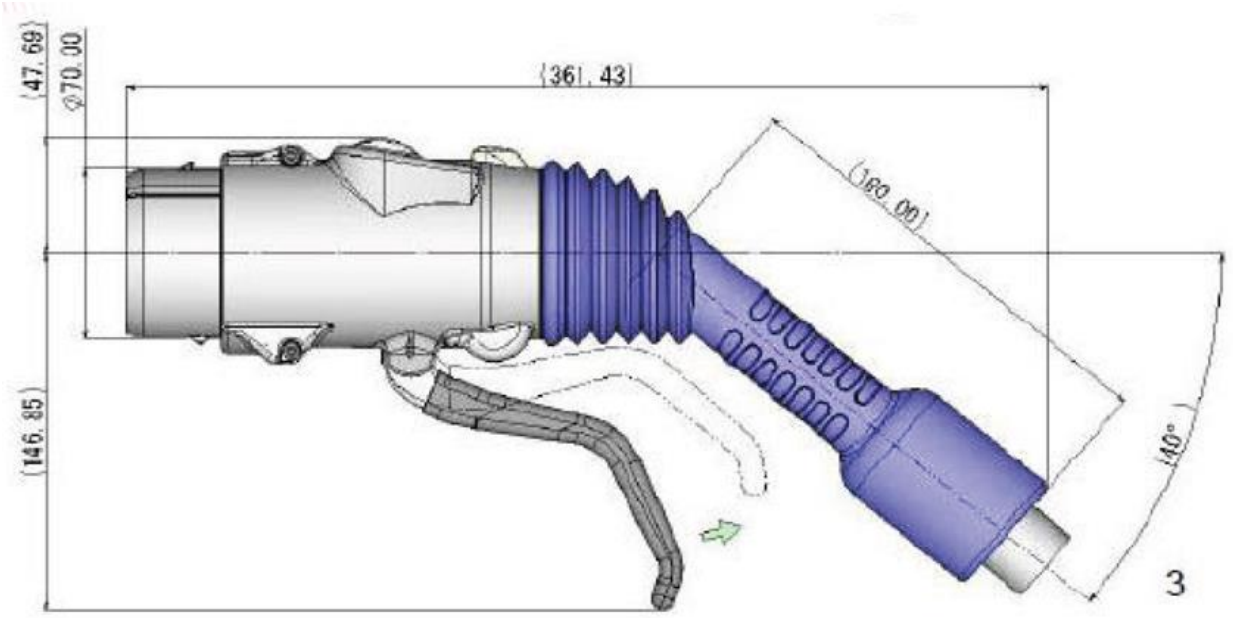

Figure 13: Connector CHAdeMO protocol *[7]*

The above figure shows the connector that is used in the CHAdeMO protocol. The charger interface is round shaped and is 70 mm in diameter. As for normal AC charging, CHAdeMO-compatible vehicles utilize Type 1 or Type 2 connector (IEC62196-2), depending on the local standards. The AC and DC inlets can be independently positioned on the sides or front of vehicles. It is a common practice in electrical equipment industry to differentiate the geometrical design of the connecting interface when higher power level is required. Using a single connector combining AC normal charging and DC fast charging could lead to a smaller geometry on the vehicle side, but might not mean the compactness of the connector held by customers. The independence between the AC and DC inlets of CHAdeMO has a clear advantage of allowing a flexible vehicle design especially considering the wireless AC charging technology in the future. The external diameter is 9mm and the signal terminal external diameter is 1.9mm.

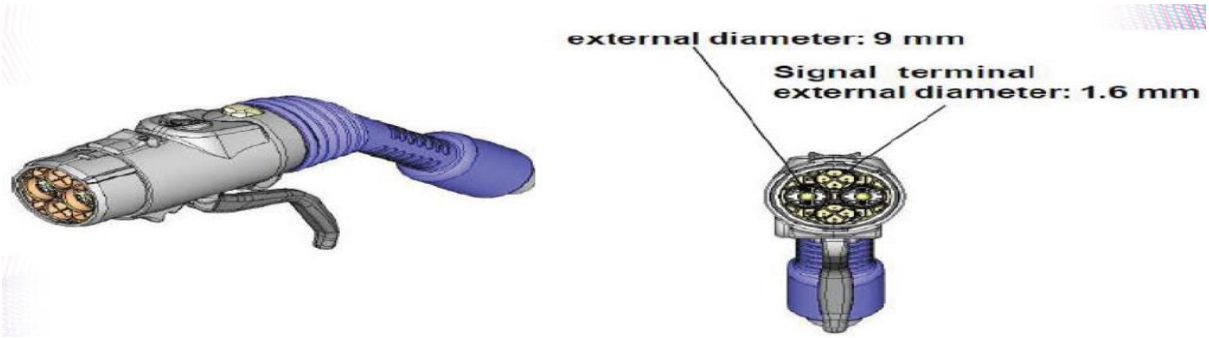

Figure 14: Connector dimension CHAdeMO protocol *[7]*

The JARI connector that is used in the CHAdeMO protocol has 10 pins. The connector interface is as shown in the figure below.

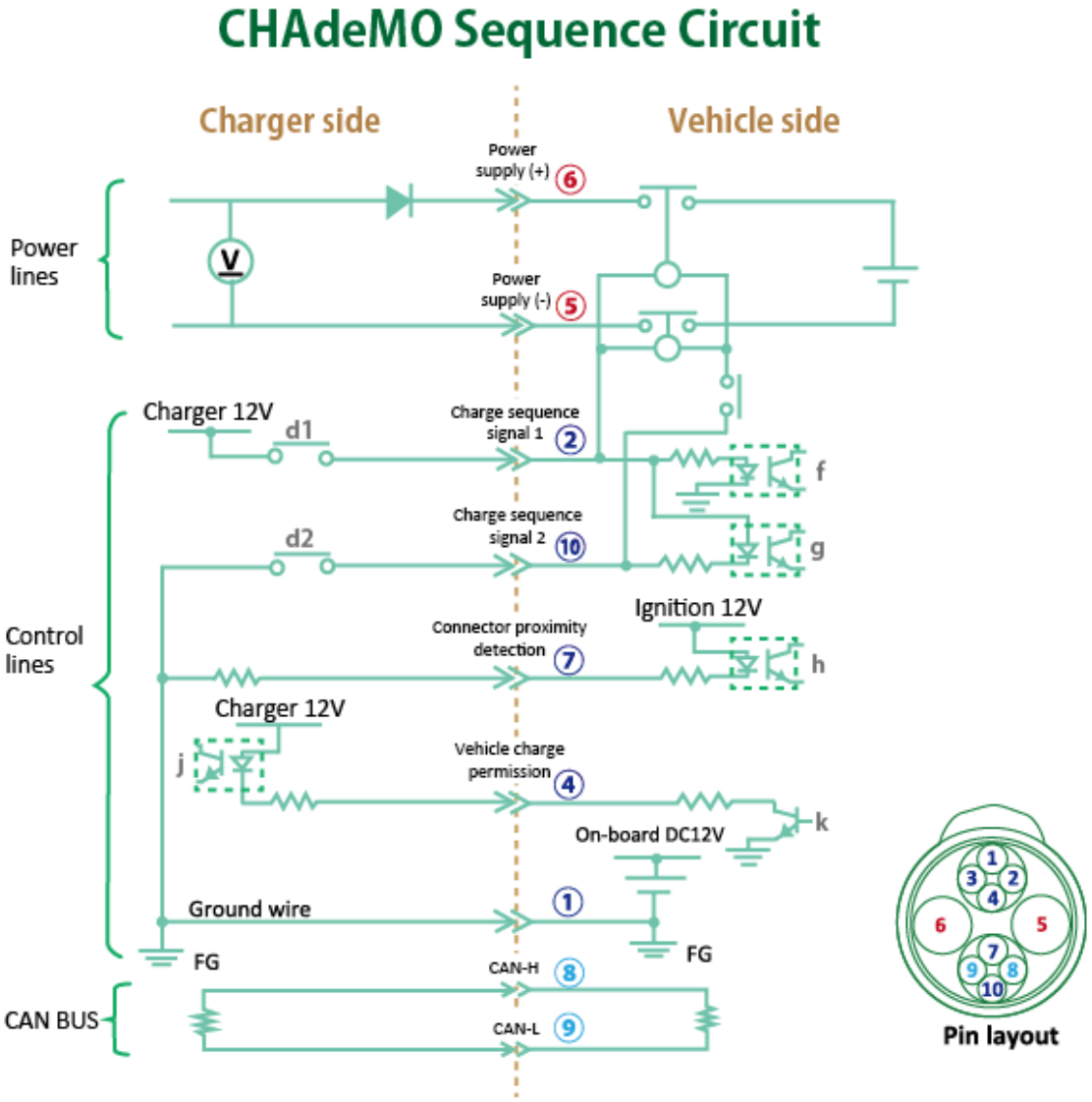

Figure 15: JARI connector for CHAdeMO protocol *[8]*

In the JARI designed connector that is used for the CHAdeMo protocol the Pins 1,2,4,7 and 10 are connected to the control lines. The pins 2 and 10 are connected to Charge sequence signal 1 and 2 respectively. The Pin 7 is connected to the Connector proximity detection and the pin 4 carries the control signal for the Vehicle charge permission. The Pin 1 is connected to the grounding wire. The pins 8 and 9 are used by the CAN communication bus. The Pin 8 is connected to the CAN-H line and the pin 9 is connected to the CAN-L line. The Pin 6 and Pin 5 are connected to the power lines. The pin 6 is connected to the positive terminal of the power supply whereas the pin 5 is connected the negative terminal of the power supply.

The size of the power pins are larger than that of the control lines and the communication lines.

The DC power pins are 8.5 mm in diameter while the ground pins are 2.5 mm in diameter and the pins for the communication lines are 1.5 mm in diameter. Also there is an equal difference when it comes to the cable sizes that are used to connect to the JARI connector used for the CHAdeMO protocol.

The cable size of the ones connected to the power pins are 50 mm^2 while that of the communication system pins are 0.75 mm^2 and the size of the cables used for the control signals are 2.5 mm^2.

The typical layout of a Dc quick charger based on the CHAdeMo protocol is as shown in the picture below.

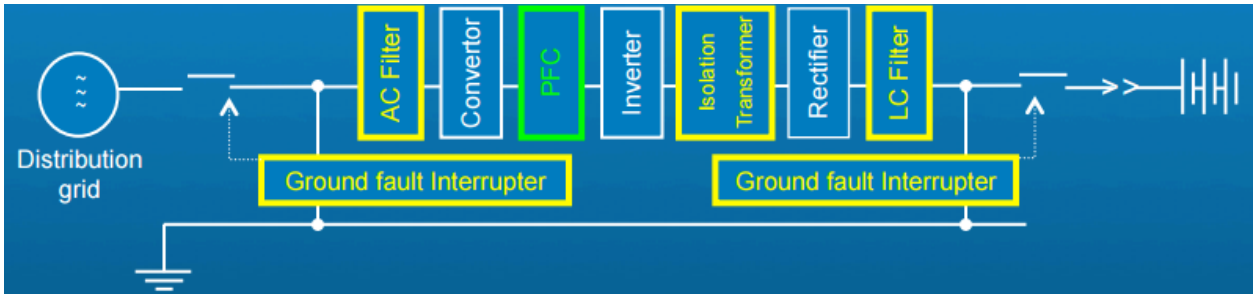

Figure 16: Typical layout of DC quick charger *[7]*

As can be seen from the picture above, it shows the grid connected to a transformer to alter the output voltage followed by fuses for safety reasons and optional power chokes to change the short circuit power of the connection. Here the DC Quick Charger (DCQC) is connected which often consists of a rectifier followed by a dc/dc transformation. To allow the charging process to start, the CHAdeMO protocol for example needs to measure a counter voltage which is given by the voltage source.
The applied diode avoids a power flow into the voltage source when the DCQC charging is active. The power sink is given by the variable resistance Rload. Additionally the communication with the DCQC has to be established. This varies with the given standards and is realized for example as power line communication or CAN communication. Here the controller is responsible for the communication and realises the communication depending on the charger type. Detailed information of the communication as well as the measured values can be recorded and analysed with the computer. The demanded output power can be achieved by the variation of the resistance and the transmitted current or voltage demands [8].

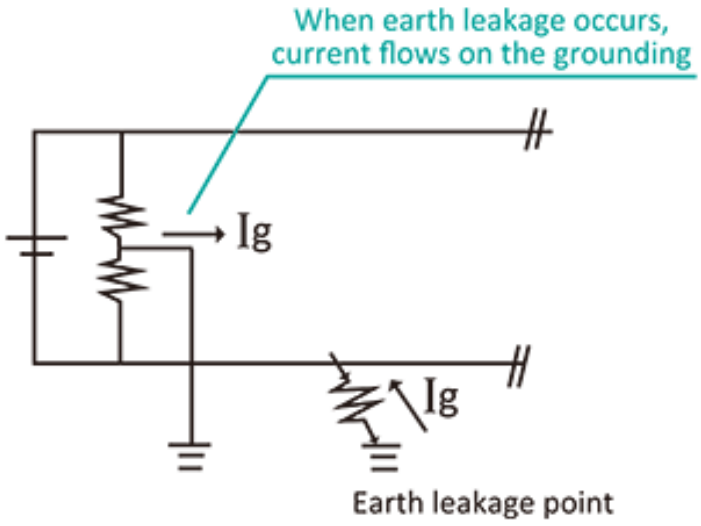

Figure 17: Ground fault interrupter to protect operator *[7]*

The CHAdeMo protocol employs a lot of safety features to protect the user from any sort of injury. Each of the components that are used has its specific functions. The AC filter used in the circuit helps in removing the higher harmonics distortion to protect any adverse effect from the distribution grid. The Power Factor corrector (PFC) is employed to increase the conversion efficiency. The isolation transformer is a very important equipment that is used in the circuit. The isolation transformer helps to separate the battery circuit from the grid for operator safety. The LC Filter reduces the ripple noise from output current to protect the battery system.

The CHAdeMo protocol also has a rapid Ground Fault interrupter to protect the operator from fatal electric shocks in case of any fault in the system. A leakage current monitoring device is installed at the DC side as well as the AC side and it shuts down input power to the charger as soon as leakage current is detected. The electrical shock protection in the DC-2 zone stipulated under IEC60479-1 was realized by combining the leakage current monitoring and immediate automatic disconnection. The analog communication makes fail safe design. The EV and the charger redundantly watch the charging conditions. And the Isolation test prevents inadvertent short circuits. One very important feature employed in the protocol is the isolation transformer which prevents any sort of electrical shock.

As seen from the figure below, RCD (1) [Residual Current Device] monitors between grid and ELB [Earth Leakage Breaker] of the charger. The earth Leakage breaker of the charger monitors ELB of charger and primary side of transformer. Earth fault detector (③) of charger monitors between secondary side of transformer and vehicle. The presence of an isolation transformer depends on the converter used as well.

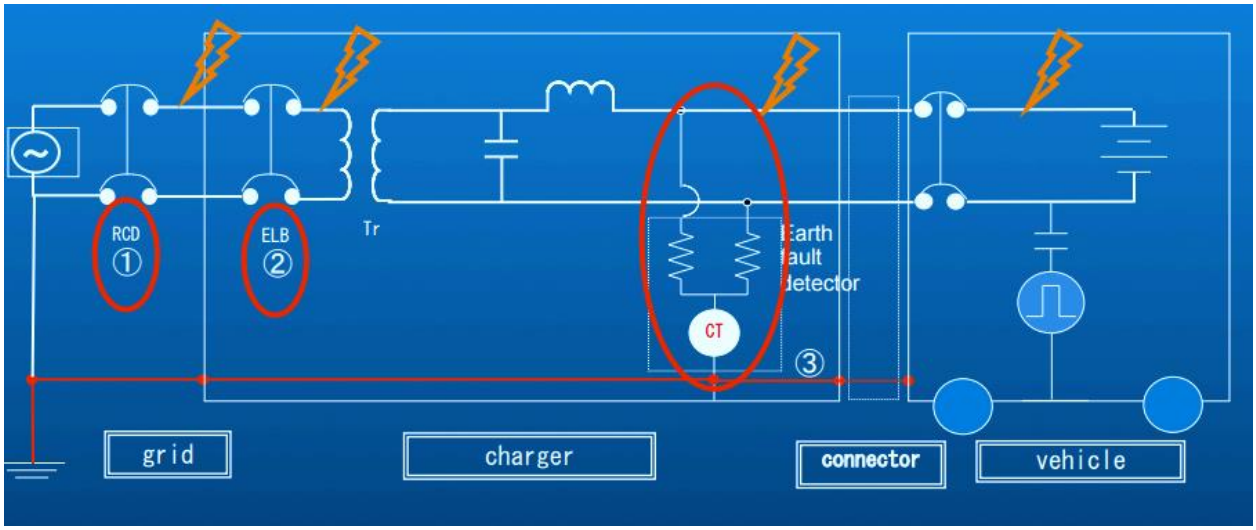

Figure 18: Isolation between the converters *[8]*

When discussing about the DC Quick Charging, one question that often comes to mind is about the effect it will have on the battery. Will the DC quick charging system degrade the life of the battery?
The main cause of the battery degradation is the high temperature and over voltage. Hence, depending on the type of the battery, the temperature and the voltage must be limited. The CHAdeMo protocol has a built in Battery Management system (BMS) which watches the temperature and the voltage in real time. Some of the observing parameters of the BMS are the total voltage of the battery, Cell voltage, Battery Temperature and the input current.

In CHAdeMO protocol the charging process is controlled by the Electric vehicle (EV). The computer unit on the EV decides the charging speed based on the BMS observation. The charging current signal is sent to the charger using the CAN bus. The charger then supplies the DC current following a request from the EV [8]. As the CHAdeMO quick charger can change charging speed based on the characteristics and conditions of each battery, the damage that can be caused to the battery is very less. There can be no negative impact to the battery if the charging speed is well controlled. Advanced batteries which can absorb more power get fed at a much higher rate.

6.2. Efficiency of the DC Quick Charger

According to CHAdeMO specifications the DCQC has an efficiency of more than 90%. At the nominal point the assessed DCQC reaches an efficiency of up to 94%. However at power of 35.5kW or below, the efficiency decreases to below 90%.

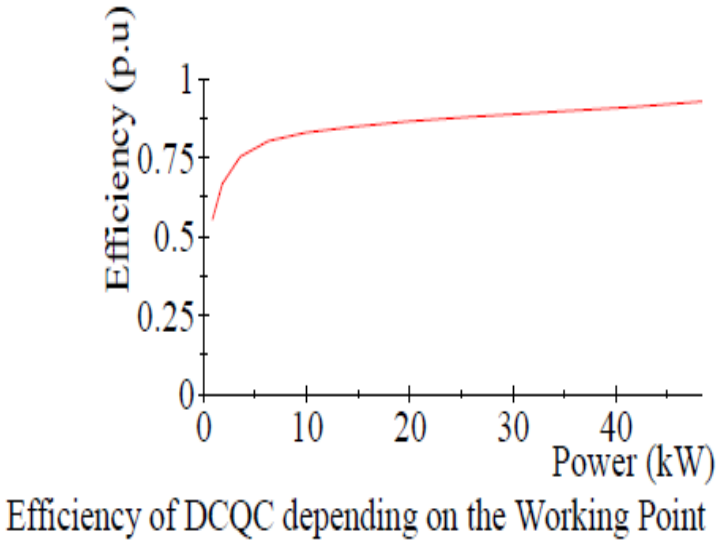

Figure 19: Efficiency of DCQC depending on the working point *[8]*

In the extended charging mode, the charging power can decrease to 3.5kW (e.g. with the Mitsubishi i-MiEV), which leads to an efficiency of 75%. The extended charging mode describes the charging process from 82% to 96% of battery charging status with the Mitsubishi i-MiEV. The following Figures show the DC Power and AC-Power within both Charging Phases, the first Charging Phase form State of Charge (SOC) 0% to 82% and from 82% to 96% SOC.

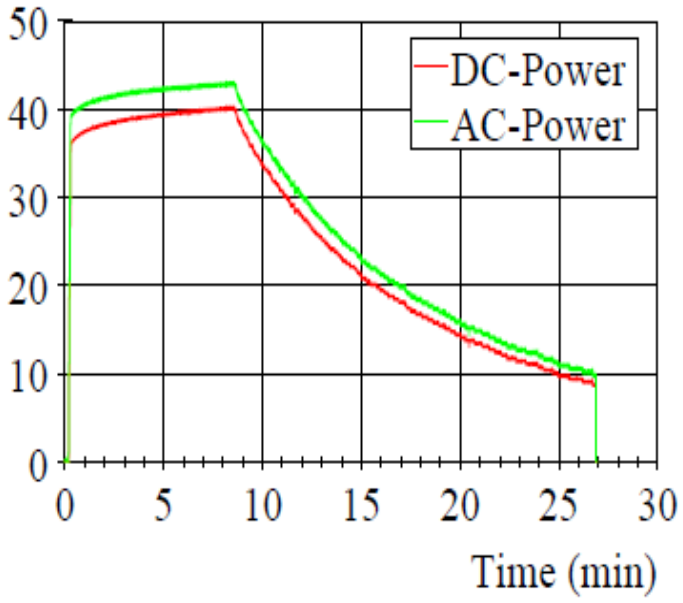

Figure 20: DC-Power and AC-Power for a Charging Process from 0% SOC to 82% SOC *[8]*

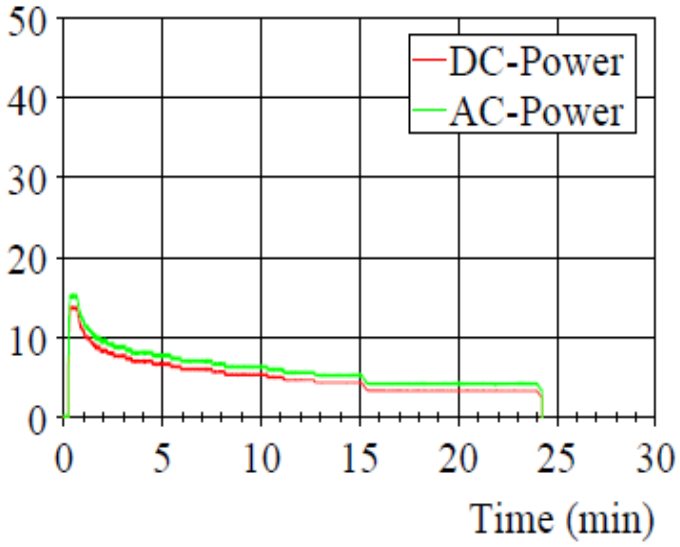

Figure 21: DC-Power and AC-Power for a Charging Process from 82% SOC to 96% SOC *[8]*

The efficiency throughout the charging processes is illustrated in the Fig below and reaches a maximum of 96% at the maximum power flow in charging phase 1 between 5 min and 10 min, and decreases in charging phase 2 down to 76%. The utilization ratio of charge phase 1 is 92.3%, the utilization ratio of charge phase 2 is 84.2%.
The overall utilization ratio herewith results in 90.9% without taking into account stand-by time [8].

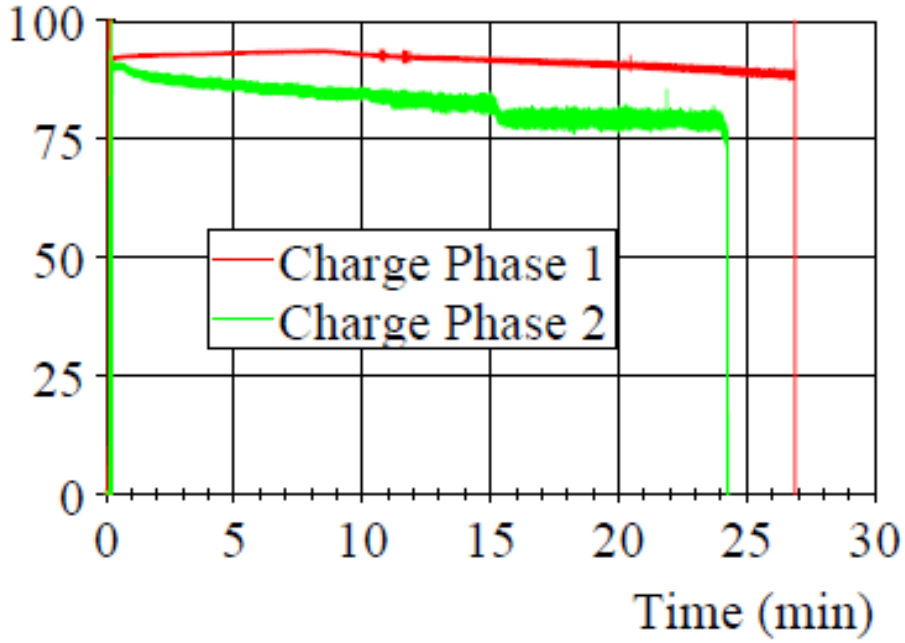

Figure 22: Efficiency of DCQC in Charging Phase 1 (SOC 0% to 82%) and Charging Phase 2 (SOC 82% to 96%) *[8]*

7. Protocol Standards

7.1. SAE Standards

Society of Automotive Engineers (SAE)

SAE International is a global association of more than 128,000 engineers and related technical experts in the aerospace, automotive and commercial-vehicle industries. The Society is a standards development organization for the engineering of powered vehicles of all kinds, including cars, trucks, boats, aircraft, and others. SAE standards are mainly used in the United States. A thorough description of the SAE standards is given in this chapter.

Electric Vehicle and Plug in Hybrid Electric Vehicle Conductive Charge Coupler-J1772

According to the SAE, J1772 was the first and only such standard in the world to reach the industry consensus. The standard spells out the physical and electrical characteristics of the connector and the vehicle electrical inlet. It enables the charging at 120 or 140 volts with a connector of standardized dimension and function to optimize the ease of use for consumers while at the same time solving the problem that several unstandardized charging interfaces otherwise would have entailed for the automakers, their suppliers and other parties including consumers.

Both IEC and JESV adopted the design of SAE J1772 standard for single-phase charging. For developing the later three-phase high-power charging, IEC has classified single-phase charging coupler as Type-1, one/three-phase charging coupler as Type-2, while the Type-3 would be compactable to both one and three phase supply. The China GB standard adopted IEC Type-2 charging coupler for single-phase charging.

Figure 23: SAE J1772 Type connector

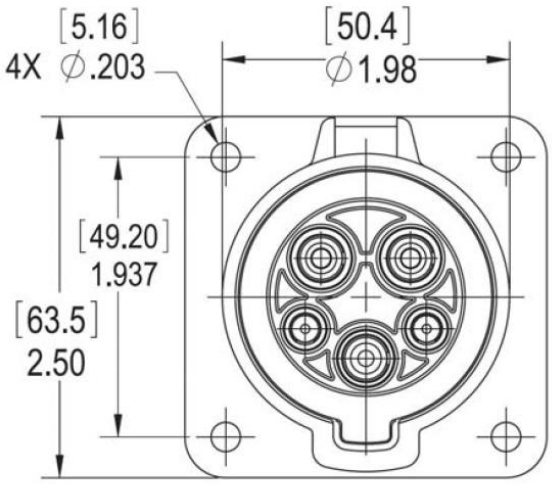

Figure 24: SAE J1772 Pin Configurations *[9]*

The above 2 pictures show the SAE J1772 connectors. There are 5 pins in this type 1 connector. The different functions of the pins are as follows.

Contact #	Connector Function	Vehicle Inlet Function	Description
1	AC Power (L1)	Charger 1	Power of AC level 1 and Level 2
2	AC Power (L2)	Charger 2	Power of AC Level 1 and Level 2
3	Equipment Ground	Chassis Ground	Connect EVSE grounding conductor to EV/PEV chassis ground during charging
4	Control Pilot	Control Pilot	Primary control conductor
5	Proximity Detection	Proximity Detection	Allows the vehicle to detect the presence of charge connector.

Table 4: SAE J1772 Connector pins

The dimensions of the SAE J1772 are given in the second picture. The top end to bottom end is 63.5 mm in length. The width of the charger is 50.4 mm. the pins are in a circular shaped structure. The distance from one end of the circular shaped structure to the bottom end is about 49.20 mm.

The control pilot is a very important equipment. It is the only equipment which informs about the proper operation of the charger circuit when connecting the EV/PEV to the EVSE.

The important operations performed by the **control pilot** are given below.

- Verification of vehicle connection
- Indication of EVSE standby state
- Indication of EVSE state- ready to supply energy
- Indication of EV/PEV state- ready to accept energy
- Determination of indoor ventilation
- Checking of the EVSE current capacity

7.1.1. Proximity Detection

The coupler provides a means to detect the presence of the connector in the vehicle inlet, as soon as the connector is inserted into the vehicle inlet. Detection of the connector will occur at a point where damage to coupler, EV/PEV, or EVSE could occur if the EV/PEV were to be intentionally moved. Proximity detection can be used to provide a signal to activate the EV/PEV charge controller and engage the EV/PEV drive interlock system. It can also be used to provide a signal in the vehicle charge control strategy to help reduce electrical arcing of the coupler during disconnect.

7.1.2. Digital Data Transfer

Communication of digitally between the EV and the EVSE is required for DC charging and it must be established before the charging process can begin. However in AC level 1 and Level 2 charging the digital data transfer is only optional.
The digital data transfer is still a under development and a lot of stress in being given at the moment.

7.1.3. Communication between the PEV and the Utility Grid

The requirements and the specifications for the communication between the EV and the utility grid is laid down by SAE J2847-1. The primary purpose of the SAE J2847-1 standard is to optimize the energy transfer from the grid to the EV so that the vehicle operators of sufficient amount of energy while driving the vehicle and the stress in the grid in minimized at the same time.

This specification supports the Forward Power Flow (FPF) energy transfer to charge the vehicle's rechargeable energy storage system. (RESS) aka batteries.
SAE J2847-1 also enables other applications between vehicles and the grid such as vehicle participation in a utility controlled charging plan or participation in a home area

network of communications-capable electrical devices. This protocol is extensible, thus enabling new applications and additional messages to be added to the existing message set.

7.1.4. Messages

The messages documented by SAE J2847-1 are required to implement the functionality as per SAE J2836-1 and apply to the customer when she/he enrols in one or more of the following utility programs. These programs are as follows:

- Time-of-Use (TOU) Rates/Tariffs/Programs (Load Shifting)
- Direct Load Control Programs (Demand Response)
- Real Time Pricing (Demand Response/Load Shifting)
- Critical Peak Pricing (Load Shifting)
- Optimized Energy Transfer Programs (Regulation Services/Demand Response)

7.1.5. Loss of Communication/power

In the event that reliable data communication between the PEV/EVSE and Energy Management System cannot be established or are interrupted during the session, but the power remains, the PEV/EVSE shall have the discretion to revert to a default state in which it charges at the maximum rate allowed by the SAE J1772 Pilot signal and in the event that power is lost during the charging session, the PEV/EVSE may resume charging upon restoration of the power.

7.1.6. Energy Request/ Response Messaging

These messages are intended to support the functionality whereby the vehicle can request a certain amount of energy at a certain delivery rate and an off board charge scheduling system will respond to the PEV/EVSE with messaging indicating the available energy schedule. The off board scheduling system may be an intelligent HAN based Energy Management System which manages the power allocated to multiple devices (including PEV) in the home or premises. Some of these messages are described as follows:

- Energy/Power Available- These messages “Energy Available” and “Power Available” are sent together. They represent the amount of energy and the rate of energy transfer that the vehicle should expect to draw for the present charging cycle. The home or premises based Energy Management System determines based on the information from the utility and based on the “Energy Request”, “Power Request” and “Time Charge is Needed” information the amount of

energy it can deliver to the vehicle (in kWh) and the rate of energy transfer (in kW).

- Energy Delivered- The energy delivered message is transmitted by the EUMD at the completion of a charge cycle and represents the amount of energy (in kWh) delivered to the EVSE/PEV system. This message can be used both for the billing purposes by the utility and for display purposes in the PEV or in-home display.

- Energy Request- This message refers to the amount of energy in kWh that the vehicle expects from the utility. The amount is computed by the vehicle and is determined based on several parameters including the charger efficiency, battery condition, and current battery state of charge (SOC). The expected response to this message is "Energy Available".

- Power Request- Sent together with the "Energy Request" message, by the vehicle, it indicates the maximum expected energy transfer rate in (kW) for the energy requested in "Energy Request". This quantity is determined by the vehicle based on the observed PWM available line current and the charger's present capability depending on battery conditions. This value is used by the Energy Management System to determine a charging schedule for the vehicle.

- Power Schedule- Each "Power Schedule" message consists of the signals Event ID, kW, Start Time and Duration. An alternative to the "Energy Available/Power Available", each power schedule message indicates the particular energy delivery rate (in kW) beginning at Start Time (in UTC) and lasting for a time specified by Duration in minutes.

7.1.7. Identification Messaging

The identification messages are required for identifying the vehicle, the driver and the charging location to the utility for the billing purposes and also for the verification that the valid vehicle (registered in a utility PEV program) is connected.

- Communications Authenticated- Sent by the utility to the vehicle, this message indicates of communication establishment between these two entities, after the validation of the customer, premises and EUMD IDs by the utility

- Customer ID and/or PIN- The customer ID and PIN will uniquely identify a customer to the utility for billing purposes among others. In case of a shared vehicle, fleet cars or rental cars, these values will be used to determine the access to features that may or may not have been prearranged with the meter provider.

- EUMD ID- Equivalent to a MAC address, this id will be validated and required by the utility at the start of a session between a vehicle and the utility.

- Premises ID- This ID uniquely identifies the customer's premises and charging location and especially useful in PEV roaming scenarios, where a PEV charges from a different location, then the cost of charging could be added to the driver's bill (based on customer's ID and subtracted from the premises owner bill (based on premises id).

- Vehicle ID- It uniquely identifies a vehicle. Vehicle ID can be the same as vehicle identification number (VIN) or HAN MAC address.

- EVSE ID- Required to uniquely identify the EVSE, as multiple vehicles may be attached to multiple EVSEs behind any single EUMD

- Smart PEV Present- In the scenario, wherein the SAE J2847-1 message support is present both in EVSE and in PEV, then it will be assumed that the PEV will be the default controlling device of the connection session.

7.1.8. Load Control/ Demand Response Messaging

These set of messages are intended to allow the utility to send a request to an EVSE/PEV to reduce or shed its load whenever there is a present or anticipated future need for a reduction in the network load. A customer has the option to decline and not to comply with load control/demand response requests, but doing so might incur increase cost due to noncompliance with the utility rate program. Some of these messages are as follows:

- Cancel Load Control- The message contains the Event ID and the Cancel Time. While the Event ID serves to identify which load control information is supposed to be cancelled, the Cancel Time specifies the time when the load control event should be cancelled.

- Load Control- The load control frame consists of the Event ID, Start Time, Duration, Criticality Level and Load Reduction Request. While most of these IDs are self-explanatory, the Criticality Level indicates the severity of the load control event and the Load Reduction Request is a percentage which indicates how much of the load should be reduced. These frames are sent by the utility and the PEV/EVSE can populate a table in memory with scheduled events and to plan charging.

- Report Event Status Request- This message allows the utility to request an update from the PEV on the status of a load control event.

- Report Event Status Response- This message consists of the signals Event ID and status. While the Event ID corresponds to the utility initiated load control event, the status field shall be a state encoded value that indicates whether the PEV is following the request or not.

7.1.9. Price Messaging

The pricing messages are intended to provide a framework for the PEV/EVSE to request pricing information from the utility and for the utility to provide this pricing information. The pricing messages are formulated to allow for either "real time" variable pricing or 'tiered/register" pricing. Through real time pricing messages, the utility could publish pricing schedules that change frequently and that reflect the instantaneous bulk rate of electricity, on the other hand, tiered or register pricing messages would allow the utility to specify the price of electricity for certain fixed times of the day.

- Define Rate Time Period- This message consists of the following signals: RTP ID, Start Time, Duration and Day and allows a utility to define a pricing period or tier which represents a particular block of time on a particular day of the week. The RTP ID provides a unique identifier for the defined pricing tier/period that allows the utility to reference a particular period.

- Price of Rate Time Period-This message is used to assign a price to each defined period. This allows the utility to update the prices in the periods/tiers without having to redefine the structures of the periods.

- Publish Price- This message consists of the Event ID, Price, Start Time, and Duration. Here the Event ID uniquely identifies the current frame of real time pricing information, price represents the price of the electricity, the Start Time represents the time at which the stated price takes effect and the Duration represents the duration of the price.

- Request Scheduled Prices- Upon connection or upon loss of memory, the PEV may need to request an update to its stored real time pricing information. This frame consists of Start Time and Number of Prices [10]. The Start Time indicates the time starting at which the PEV wishes to receive pricing data and the Number of Prices indicates the number of "Publish Price" frames the PEV wishes to receive.

7.1.10. Timing Information messaging

This set of messaging is used primarily by the PEV or EUMD to communicate timing requirements and history to the utility and/or premises HAN based energy manager.

- Charging Profile- This is a periodic message and contains the following signals: Present Rate of Charge and Current Time. It is intended to be used by the utility for the statistical data gathering and future planning purposes.

- Time Charging to Start/Time Charging to End- This message intends to provide the estimated duration of charging and are formulated by the vehicle, charger, or energy management system using other available parameters such as pricing, user preferences, etc. as inputs.

7.1.11. Vehicle Information and Charging Status Messaging

It is expected that the vehicle will continuously monitor many other parameters which can be useful to a customer for display purposes and to the utility for the statistical purposes.

- Usable Battery Energy- Provides the usable energy of the battery in kWh and can be used for in-home display purposes.

- Battery SOC Start/Battery SOC End- These messages state the start and end state of charge of the battery before and after the charging begins. This signal is to refer the usable capacity only.

- Customer Mode Preference- This message is intended to convey how the customer has selected to charge the PEV. The customer could choose from various options like (charge now, charge based on pricing information, charge based on energy request or on yet to be defined customer selections.

7.2. Other SAE Standards

Although, there are many SAE standards that pertain to the PEVs and some of them are currently being formulated, it will not be possible to describe them all here. But here is the list of some of the important ones.

- Communication between Plug-in Vehicles and off board DC Charger-J2847/2
- Use Cases for Communication between Plugin Vehicles and off board DC Charger-J2836/2

- Communication between Plug-in Vehicles and the Utility Grid for Reverse Power Flow-J2847/3
- Use Cases for Communication between Plugin Vehicles and the Utility Grid for Reverse Power Flow- J2836/3
- Recommended Practice for a Serial Control and Communications Vehicle Network- J1939
- Power Quality Requirements for Plug-in Vehicle Chargers [10]

7.3. Combined Charging System (CCS) Standards

Combined Charging System is a standard supported by a total of 7 different U.S and Europeans carmakers which was designed to be the new de facto standard for all North American and European electric cars. It is more compact and less mechanically complicated than CHAdeMO, since it simply adds two high-powered DC connectors underneath the standard J1772 (U.S.) and Type 2 (European) AC charge connectors. It shares the same communication and signal pins used for low-power AC charging, resulting in just one charging port capable of both AC and DC rather than the two discrete charging ports called for with CHAdeMO.
The SAE CCS (Combined Charging Standard) or "Combo" standard was developed in a SAE committee process that was open to all automakers to participate. For a variety of reasons (including the belief that the SAE J1772 coupler was generally considered to be the accepted AC Level-1 and Level-2 charging standard in the U.S.), the members of the SAE committee wanted to create an upward compatible coupler for DCFC. Some of the advantages to this approach are the reduction of cost and complexity of two separate interfaces (J1772 using the Control Pilot, CHAdeMO using a CAN bus) and the avoidance of the need for a large door for two separate connectors. An upward compatible interface was created by adding higher capacity DC+ and DC- pins and updating the spec to incorporate power line carrier (PLC) communications modulated on the Control Pilot signal to support DCFC.
The CCS standard allows for a single gas-filler sized fender opening, a lower cost, and an upward compatible coupler to the existing J1772 AC coupler that is pervasively deployed. CCS advocates' position seems to be that one charging interface standard is better than two for reducing costs to help make PEVs cost competitive, that there are an infinitesimally small numbers of electric vehicles on the road today as a nascent technology so the industry should not be bound to a less optimal older standard, and that there are methods to accommodate the transition to CCS.

The most important requirement for a modern E-Mobility charging infrastructure is a reliable and standardized connection for charging stations and vehicle sockets. The vehicle can be recharged with both alternating current (AC) and direct current (DC). If AC is used for charging, the energy is supplied directly from the existing low-voltage network to the integrated AC/DC converter in the vehicle. In the

case of DC charging, the AC/ DC converter is located within the charging station, thereby reducing the load on the vehicle. The combined AC/DC charging system type 2 enables both AC charging and faster DC charging on the move. The combined AC/DC charging system type 2 is the ideal charging interface for everyday charging situations in Europe. The electric vehicle is designed for both established AC charging and for DC charging on the move. The combined DC connector transmits DC current up to 125 A. It is inserted into the vehicle inlet very easily and with very little force.

The combined DC connector for Type 2 charging is shown below.

Figure 25: Combined DC connector TYPE 2

The combined DC connector type 2 has 5 pins (3+2) for DC charging. It is usually very easy to handle and the insertion forces to be applied are low as well. It complied with IEC 62196 specifications. The charging plug is locked in the vehicle to prevent arcs caused by removal when under load. The plug is designed to withstand the highest pull-out forces. The integrated temperature monitoring protects against fire in the event of faulty contacts.

Predefined charging mechanisms and sequences are performed for both AC and DC charging. For both charging types, the signal and control contacts, CP and PP, are used for communication and control.

Similar to the connector shown in the above picture, there is a connector which combines the AC and DC pins for type 2. This type of a connector has 9 pins.

The combined AC/DC charger for type 2 is as shown in the below picture.

Figure 26: Combined AC/DC Charger for Type 2

The technical data for the combined AC/DC charging is given in the table

Parameter	**Vehicle inlet**	**Connector**
AC Unit Type 2		
Nominal Voltage	Up to 480 V	-
1/3 Phase Nominal Current	up to 32 A	-
Standard	IEC 62196-2, IEC 62196-3 (draft)	IEC 62196-3 (draft)
DC Unit Type 2		
Nominal voltage	Up to 850 V	Up to 850 V
Nominal Current	Up to 125 A	Up to 125 A
Standard	IEC 62196-2, IEC 62196-3 (draft)	IEC 62196-3 (draft)
Degree of Protection		
IP protection when plugged in	IP44	IP44
IP protection when not plugged in	IP20	IP20
IP protection when covered	IP55 (road position)	IP24 (with protective cap)

Table 5: Technical Data of Combined AC/DC connector

7.4. Tesla Supercharger

Tesla Supercharger is a system for Ultra-fast charging of batteries developed by the American EV company Tesla Inc. Superchargers consist of multiple chargers working in parallel to deliver up to 120 kW of direct current (DC) power directly to the

battery. Typically, it uses its on-board charger to convert alternating current (AC) from a wall charger to DC that's stored in the battery. As the battery nears full charge, the car's on-board computer gradually reduces the current to the optimum level for topping off cells.

As the battery reaches about 80% of it charge, the current is gradually decreased so that it avoids excessive spillage from the battery cells. The supercharger is well known for its high speed charging. Typically it takes about 30 minutes for the completion of total charging of the battery.

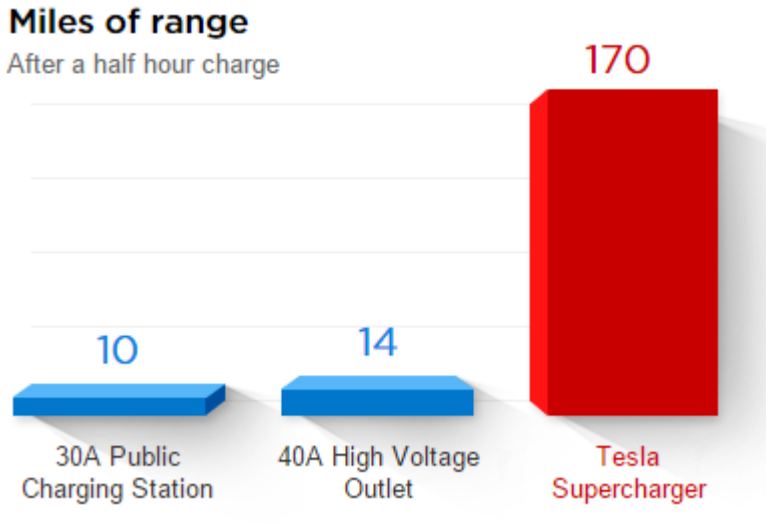

Figure 27: Miles range

The main problem with this particular type of system is that only car models of Tesla Inc. can be used for charging and the diffusion of this Supercharger technology isn't very widespread. Hence it places a huge constraint to the rapid expansion of the charging stations. Even though, of late there has been an effort to make the patents of Supercharger technology held by Tesla Inc. public in an effort to encourage other manufacturers to follow a common protocol and thus help in the expansion and operability of Electric vehicles [11].

8. Charging infrastructure

EV charging devices are mainly composed by electronic components, which can be on board or off board, to provide energy for the vehicle storage system with the existing power supply infrastructures. Typical on-board chargers reduce the charging power because of their weight, space and cost constraints and they are generally used to charge battery packs taking a long period of time. Whereas, off-board battery chargers are less affected by size and weight constraints. This means that EVs with off-board battery chargers can take advantage of fast and frequent high power charging phases, in order to extend the effective driving range and reduce the recharging times, until they are comparable with the refilling times of traditional oil based vehicles. On

the other hand, the disadvantages of these charging systems include an extra cost for the increased power of the power electronic and a more complex communication system with the recharging vehicle. These devices can be characterized by unidirectional or bidirectional power flows. The former case presents limited hardware requirements and simplifies the interconnection issues. The latter case allows the battery to be charged by the grid and to feedback power into the grid, and allows a power stabilization for the grid by means of a proper power conversion unit.

8.1. Types of charging stations

EV charging stations when categorised in terms of voltage rating, power rating and place of application, can be classified into three different types of charging stations, namely,

Figure 28: Domestic charger at residential area

Figure 29: Off-street and robust charger at commercial and office area

Figure 30: Rapid charger at strategic location

In this document, the charging stations discussed will be focusing on conductive chargers due to the fact that the inductive charging method is still under development. According to Daimler's Head of Future Mobility, inductive chargers are at least 15 years away and the safety aspects of inductive charging for EVs have yet to be looked into in greater detail. Most rechargeable EVs and equipment can be charged from a domestic wall socket. However, a charging station may be required due to the following reasons:

- Charging can be provided for multiple EV owners at one time,
- The facility may have additional current or connection sensing mechanisms to disconnect power when the EV is not actually charging,
- Readily provide option for suppliers to monitor or charge for the electricity actually consumed.

8.2. Charging Modes

The IEC 61851-1 Committee on "Electric vehicle conductive charging system" has then defined 4 Modes of charging, concerning:

- The type of power received by the EV (DC, single-phase or three-phase AC),
- The level of voltage (for AC in range between single-phase 110V to three-phase 480V),
- The presence or absence of grounding and of control lines to allow a mono or two-way dialogue between the charging station and EV,
- The presence and location of a device protection.

Different recharging modes are classified as in the international standard IEC 61851-1 are as follows:

8.2.1. Mode 1

Charging refers to the connection of an EV to the AC supply network through a single phase AC line not exceeding 250 *V* AC or a three phase AC line not exceeding 480 *V* AC. at 50-60 *Hz*, using national plug and socket system not exceeding 16 *A* with protective earth conductors, depending on the country and standardization. This low power vehicle charging mode is the slowest mode and can refills a battery during the night reaching the full capacity before the morning. This type of overnight recharge ensures a low electric load for the grid and the car is recharged economically using a low cost night rate power. This recharging mode is mainly used at home and office, since no additional infrastructures are required.

8.2.2. Mode 2

Charging refers to the connection of an EV to the A.C. supply network with the same voltage limits as for the Mode 1, using standard wall sockets and plugs not exceeding 32 *A* with protective earth conductors. The difference with the Mode 1 consists on the fact that the vehicle inlet and connector present a control pin. The supply network side of the cable does not require a control pin as the control function is provided by an integrated control box with the further function of in cable protection device. This recharging mode is primarily used for dedicated private facilities.

8.2.3. Mode 3

Charging refers to the connection of the EV to the AC supply network using an electric vehicle supply equipment (*EVSE*), not exceeding 63 *A*, where the control pilot function is extended, as for the mode 2, to a control equipment permanently connected to the AC supply. In this case, connectors with a group of control and signal pins are required for both sides of the cable. This recharging mode is typical of public charging stations and is generally supplied from three-phase AC mains at 50/60*Hz*. It is also called ‘semi-fast’ charging solution since it is possible to charge a battery in few hours when the driver is at work or during every day activity.

8.2.4. Mode 4

It has been implemented by the CHAdeMO consortium and is characterized by the use of off-board chargers where the control pilot function is extended also to the equipment permanently connected to the AC supply. The supply AC power is converted in the charging station to DC and the plug ensures that only a matching electric vehicle can be connected. Typical charging times of the mode 4 are in a range from 20 to 30minutes. In this case the charging time is limited by the allowable current of 125 *A* and voltage of 500 *V* of the CHAdeMO standard connector. Combining high

power converters with the latest battery technologies this charging mode could allow a recharge from 0 to 80% of battery SOC in less than 5 minutes (ultra-fast charging).

Actually, the market situation still presents a discrepancy with reference to the above mentioned modes since EVs manufactures usually prefer to equip their vehicles with a Mode 1 one-phase on board charger. In this case the standard 16 *A* sockets can be used, de-rated to a constant load of 10÷12 *A*, limiting the recharging power in a range from 2.3 to 2.8 kW. Nevertheless the future market trend is to present the possibility to recharge the battery pack both in mode 1÷2 and in mode4 by means of the installation of two different sockets on the car for the two different types of plug, as already done for the Nissan Leaf and the Mitsubishi i-Miev. For this reason there is a growing interest in studying different charging architectures for the mode 4 [12].

Table synthesizes the main characteristics of the charging modes, according to IEC 61851-1

Charging Mode	**Max Current per phase**	**Charging Time**	**Vehicle Battery Charger**
Mode 1	16 *A*	4÷8 *h*	On Board
Mode 2	32 *A*	2÷4 *h*	On Board
Mode 3	63 *A*	1÷2 *h*	On Board
Mode 4	400 *A DC*	5÷30 *min*	Off Board

Table 6: IEC 61851-1 Charging Modes

8.3. AC and DC Charging Architectures

Two different charging architectures are proposed with AC or DC bus [23]. Nowadays the electric energy production and transmission infrastructures are designed to work in AC and most of the electric loads, such as lights, electric motors, domestic appliances, are supplied in AC. In particular a charging AC architecture for EV should be based on an AC bus to enable and at the same time to manage the energy sharing among battery chargers, RESs, and the electric grid. A block scheme of this architecture is proposed in Fig., where the electric energy can be shared through bidirectional power converters. This architecture would be suitable to realize a smart charging scenario presenting different strategies of V2G energy management, obtained with a proper EV aggregation agent.

The growing interest towards distributed power plants, RESs, EVs, DC electronic equipment brings to reconsider a new energy management strategy. As matter of fact, the EV storage systems need to be recharged in DC, generally requiring the connection to the AC bus by means of low efficiency AC-DC converters. Moreover, distributed electric generation with RESs is mainly realised in DC, in this case the electric energy needs to be converted in AC, for the interconnection with either

the electric grid or the AC bus, and then converted again in DC to supply the great part of the electric loads and to recharge the battery packs of EVs.

These energy conversions AC-DC (in particular DC-AC-DC, in case of PV power plants) present the disadvantages of high losses. A proposed solution for these kinds of issues consists in a DC bus based architecture, which requires fewer AC-DC power conversion stages and thus reduces losses and hardware costs. As shown in Fig. , the proposed architecture utilizes just one high efficiency AC-DC converter, also called Grid Tie Converter, to realize a DC bus, connecting the charging EVs through bidirectional DC-DC converters instead of equivalent AC-DC converters required by the AC bus architecture, with great advantages in terms of energy efficiency and costs. Moreover, the DC bus makes possible RESs generation systems to be connected directly through a simple DC-DC converter, avoiding the double conversion losses (DC-AC-DC). It was estimated that this architecture presents conversion losses reduced from about 32% to less than 10%.

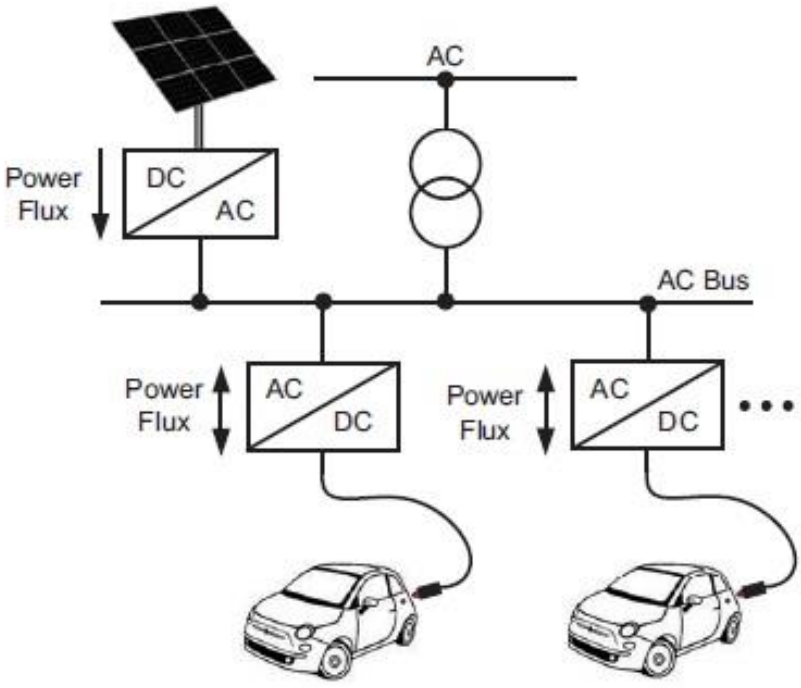

Figure 31: EV Charging Architecture with AC Bus

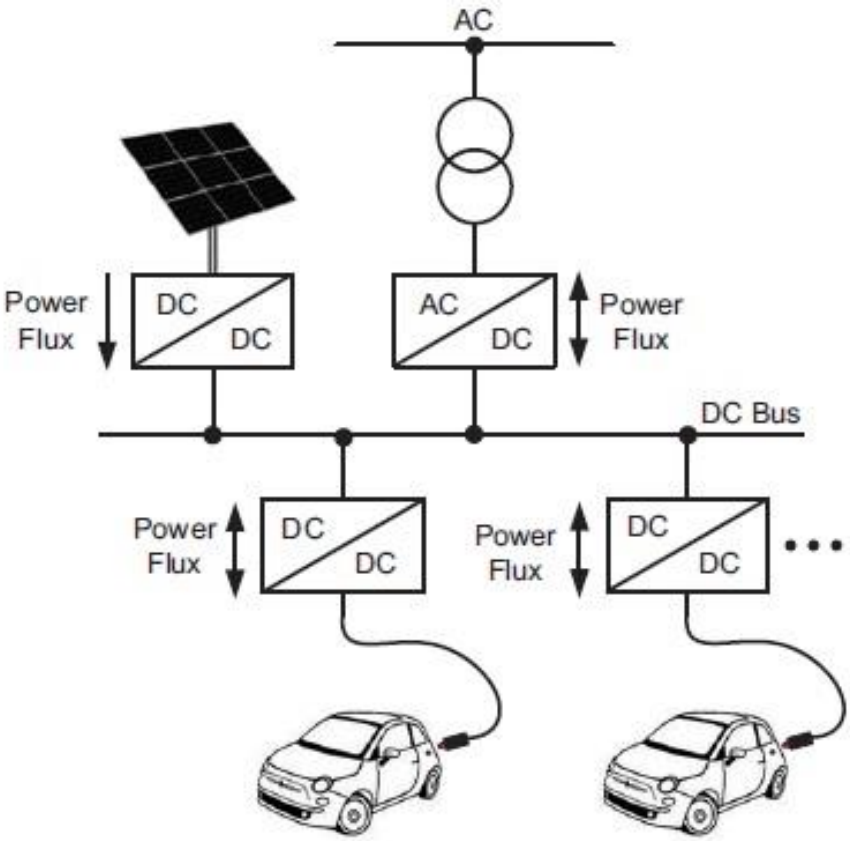

Figure 32: EV Charging Architecture with DC Bus

8.4. ULTRA FAST CHARGING ARCHITECTURE

The main objective of the ultrafast charging is the reduction of charging times up to less than 5 minutes. In order to satisfy this objective the electricity distribution system is required to supply power peaks, and therefore that system needs an over-dimensioning of cables, power transformers, devices, etc. The working conditions become more and more critical when many different vehicles are charged simultaneously. Starting from the architecture shown in Fig., a first possibility of reducing the above impact of the ultra-fast charging on the grid is based on decoupling the load from the AC supply network, by means of stationary energy storage systems. In this case the energy storage system works as a power buffer interposed between the grid and the charging vehicles. This configuration could also allow reducing the sizing, of the grid tie converter, in terms of power. As shown in Fig., the charging architecture is characterized by two-stage conversion with an AC/DC and DC/DC converters. The typical scheme of a buffered EV charging architecture can be seen as a three-port DC bus architecture, connecting the main network, the electric vehicle and the energy storage buffer. The charging power coming from the grid tie converter depends on the power available from the battery buffer, and on the efficiency of the DC/DC converters.

Two different energy management strategies for the just described ultrafast charging architecture can be evaluated, which affect the design of the AC/DC converter

and of battery buffer: load levelling and load shifting strategy. For the first case, the average charging power is supplied by the main grid whereas the power peaks are supplied by the battery buffer. For the load shifting strategy, the battery buffer stores energy during the night, when the grid overall load is minimal, and it releases energy for the EV charging during the day, when the grid is heavily loaded. This way, the AC/DC converter can be downsized, taking into account that its function can be limited to the low power charging operations, during the buffering phase, and to support the discharge power from the battery buffer, during the high power charging of the vehicle.

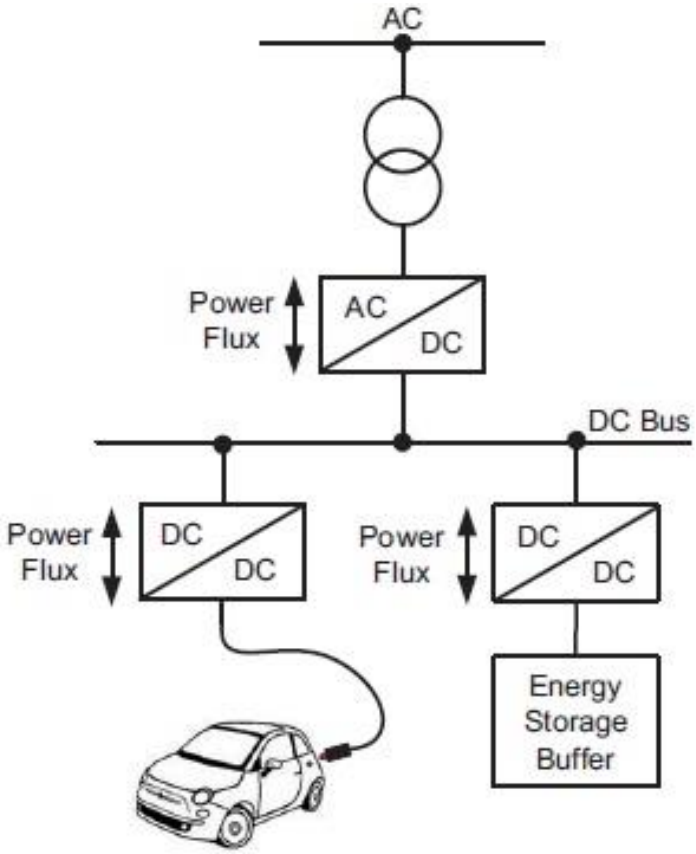

Figure 33: EV Charging Architecture with Buffer

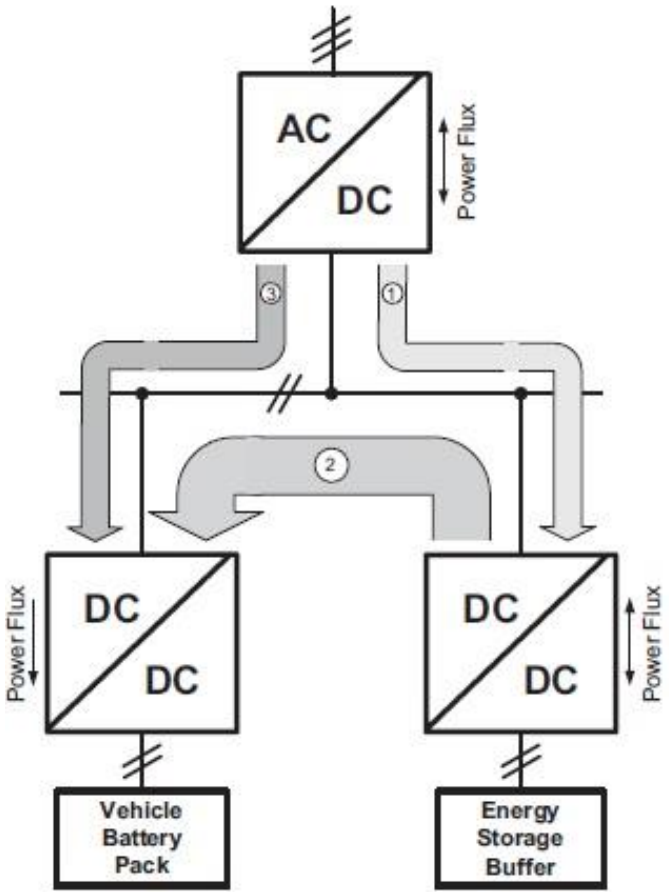

Figure 34: Main power fluxes in buffer architecture

- The flux (1) represents the charge at low power, when no vehicle is connected to the charging station, from the grid into the energy storage buffer to guarantee the energy availability for the following high power EV charge.
- The flux (2) and the flux (3) are involved in the high power charge for the EV, when most of the power comes from the buffer and the amount of the power supplied by the grid with the flux (3) is the same of the flux (1), based on the rated power of the AC/DC converter.

By means of the proposed architecture, an ultra-fast recharge, from 0 to 80% of SoC, was evaluated as possible in 5 minutes, for an electric vehicle with a 22kWh battery pack (i.e. Mitsubishi i-Miev), using both the buffer and the grid power. In this case a recharging infrastructure, based on a 22 kW AC/DC converter and a 210 kW DC/DC high power converter, was proposed with an energy buffering time (time taken to recharge the battery buffer) of about 45 minutes for a LiFePO4stationary battery pack. This kind of battery pack was proposed as energy storage buffer to take advantage of the characteristics for these batteries to be discharged at very high rate, without a remarkable loss of actual capacity with respect to their nominal value. On the other hand, the battery pack of the recharging vehicle could be conveniently chosen using the lithium-titanate technology, taking advantage of its high charging rate capability [13].

8.5. European Standards and trend

European electricity companies, particularly distribution system operators (DSOs), are investing in the necessary infrastructure to stand-in a single European market for EV. European standards are indispensable to safeguard that drivers enjoy convenient EU-wide charging solutions that avoids a multiplicity of cables and adaptors and so retrofit costs. In June2000, the European Commission issued a standardization mandate to the European standardization bodies CEN, CENELEC and ETSI (M/468) concerning the charging of EVs. The mandate stressed the need for interoperable plugs and charger systems to promote the internal market for EV and to discourage the imposition of market barriers. The Focus Group set up to respond to M/468 delivered a comprehensive and valuable report. However, given that the mandate objective was to achieve interoperability, not the adoption of a single connector, no recommendation has been made with regards to the choice of the AC mains connector. As a consequence, two types of connectors have been assessed as appropriate for the European situation. The choice between them is left to the market and will depend on the different National regulatory frameworks. Today the only standards available at European level, dealing with the charging system, plugs and sockets, are contained in the IEC 61851. The actual standards provide a first classification of the type of charger in function of its rated power and so of the time of recharge, defining three categories here listed:

- Normal power or slow charging, with a rated power inferior to 3.7 kW, used for domestic application or for long-time EV parking;
- Medium power or quick charging, with a rated power from 3.7 to a 22 kW, used for private and public EV;
- High power or fast charging with a rated power superior to 22 kW, used for public EV.

In function of the amount of power, different main connections are possible and they are summarized in terms of electrical ratings in Table

Charge Method	**Connection**	**Power [kW]**	**Max current [A]**	**Location**
Normal power	1-Phase AC connection	3,7	10-16	Domestic
Medium power	1- or 3-phase AC connection	3,7 – 22	16-32	Semi-Public
High power	3-phase AC connection	> 22	> 32	Public
High power	DC connection	> 22	> 3,225	Public

Table 7: Electrical Ratings of Different EVs Charge Methods in Europe

Recognising that there is a need to offer customers a high power charging possibility that allows them to recharge the EV battery within a limited timeframe, only the high power connection would satisfy this aim. Two technologies are at hand for high-power charging: DC off-board charging or AC on-board charging.

DC off-board charging is more common today, due to the introduction of the first generation of Japanese electric cars on the European automotive market. Nevertheless, European automotive manufacturers have expressed their intention to promote EV with an on-board charger, which would be compatible with a high-power range AC supply arrangement. For the DC connection, a Japanese socket (CHAdeMO protocol), with a maximum power level of 50 kW, is currently the only available product on the market and is thus being rolled out in several European countries although it is not internationally standardised yet.

The European Automotive Industry is however promoting the combined charging system with the Combo connector, which features a single inlet for AC and DC charging on the side of the EV and can potentially deliver high-power charging of up to 100 kW in future. The Combo connector is currently under development and going through the IEC standardisation process.

The European Commission has decided that all electric vehicles must have installed the "Type 2" connector, showed in Fig. This should resolve a central problem regarding EV charging stations: lack of interoperability.

Figure 35: CHAdeMO connector

Figure 36: CHAdeMO Type 2 connectors

This connector can also be used in three-phase 400 V, having seven contacts in total. Type 2 connector can reach enough high values of charging power: up to 43 kW with fixed cable (63A/400V), up to 22 kW with detachable cable (32A/400V).

The technological choice between on- or off-board chargers will be determined by what suits the EV on the market and the relative cost of both systems for the infrastructure provider. For the electricity industry, it does not matter much whether the conversion from AC to DC is done on- or off-board. In any case, high-power charging is likely to be a premium-priced service for the electric vehicle driver, the use of which should be encouraged only when charging time is critical, i.e. in the middle of a journey. In such cases, limiting or interrupting charging for load management purposes (except for emergencies) is unlikely to be acceptable to EV customers. For the electricity industry, the limited possibilities of load management therefore make high-power charging less attractive.

8.6. American Standards and trend

For many years, the Society of Automotive Engineering (SAE) has been working on standard J1772. Today SAEJ1772 in its last version defines EV charging system architecture: it covers the general physical, electrical and performance requirements for the EV charging systems used in North America. In function of the rated power, voltage and current the charging systems for EV in North America are classified into three categories, which are AC Level 1, AC Level 2 and DC Level 3. In particular:

- For Level I, the charger is on-board and provides an AC voltage at 120 or 240 V with a maximum current of 15 A and a maximum power of 3,3 kW;

- For Level II, the charger is on-board and provides an AC voltage at 240 V with a maximum current of 60 A and a maximum power of 14,4 kW;
- For Level III, the charger is off-board, so the charging station provides DC voltage directly to the battery via a DC connector, with a maximum power of 240 kW.

Table summarizes the electrical requirements of the three charging systems in North America.

Charge Method	**Nominal AC Supply Voltage [V]**	**Maximum Current [A]**	**Maximum Power [kW]**	**Charger Location**
AC Level 1	120	12	1.44	On-board 1-phase
AC Level 2	240	32	7.7	On-board 1 or 3 phase
DC Level 3	208- 600	400	240	Off-board 3-phase

Table 8: Electrical Ratings of Different Charge Method in North America

SAE J1772 defines the standardized connector that covers the general physical, electrical, communication protocol and performance requirements for the EV conductive charge system and coupler. The SAE J1772 connector is considered a "Type 1" implementation of IEC 62196-2 providing a single phase coupler.

In function of the power level of the charger, the time of charging changes and with it the type of use of the charging system. For this reason the three power levels of charging are also classified in low, primary and fast method in function of the charging time.

Figure 37: IEC 62196-2 “Type 1”connector with Pinout

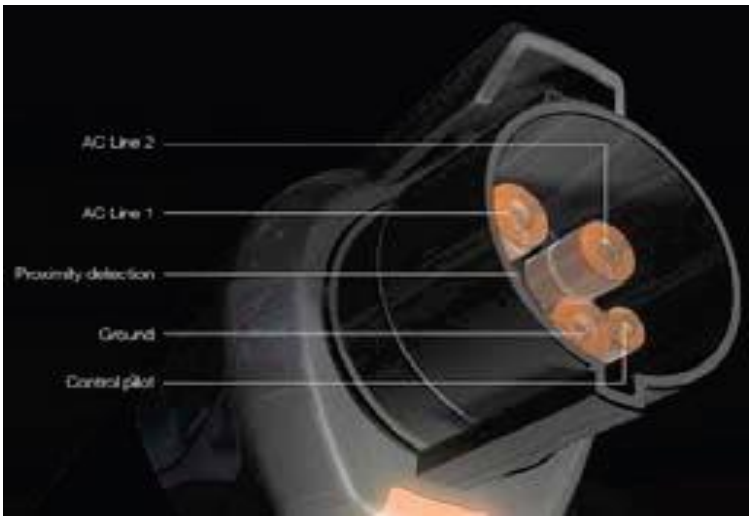

Figure 38: IEC 62196-2 "Type 1"connector with Pinout

Another classification can be made in terms of type of outlet used in the charging station. The American standards define three types for the three levels:

- Level 1 charging method, the slowest one, uses a standard 120V/15A single-phase grounded outlet, such as NEMA 5-15R. The connection may use a standardJ1772 connector into the EV AC port. For home or business sites, no additional infrastructure is necessary;
- Level 2 charging method, the primary one for dedicated private and public facilities, requires dedicated equipment for home or public charging;
- Level 3 charging method, the fastest one and used for commercial application, typically operates with a 480 V or higher three- phase circuit and requires an off-board charger to provide regulated AC-DC conversion.

Standards for DC plugs and hardware are in progress. The Japanese protocol CHAdeMO is gaining international Recognition.

SAE defines also the communication standards for the EV charging stations. A first group contains the standards and technologies between EV and Electric Vehicle Supply Equipment (EVSE) that is required for energy transfer monitoring and management, billing information, and authorization. The standardization is required for fast adoption of EVs and proper functioning of EV network components. The main standards on communication are presented in Fig.

- SAE J2993: it covers the required functionalities and system architectures for electric vehicle energy transfer system;
- SAE J2836/1 & J2847/1: it specifies use requirements and use cases for communications between EVs and the power grid, mainly for energy transfer.

The main focus is on grid-optimized energy transfer for EVs to make sure that drivers have enough energy while minimizing the stress on the grid;

- SAE J2836/2 & J2847/2: it specifies the requirements and use cases for the communications between EVs and off-board DC charger;
- SAE J2836/3 & J2847/3: it specifies use cases and additional messages energy (DC) transfer from grid to electric vehicle. Also supports requirements for grid-to vehicle energy transfer;
- SAE J2931: it specifies the digital communication requirements between EV and off-board device.
- SAE J2931/1: it specifies power-line communications for EVs [14].

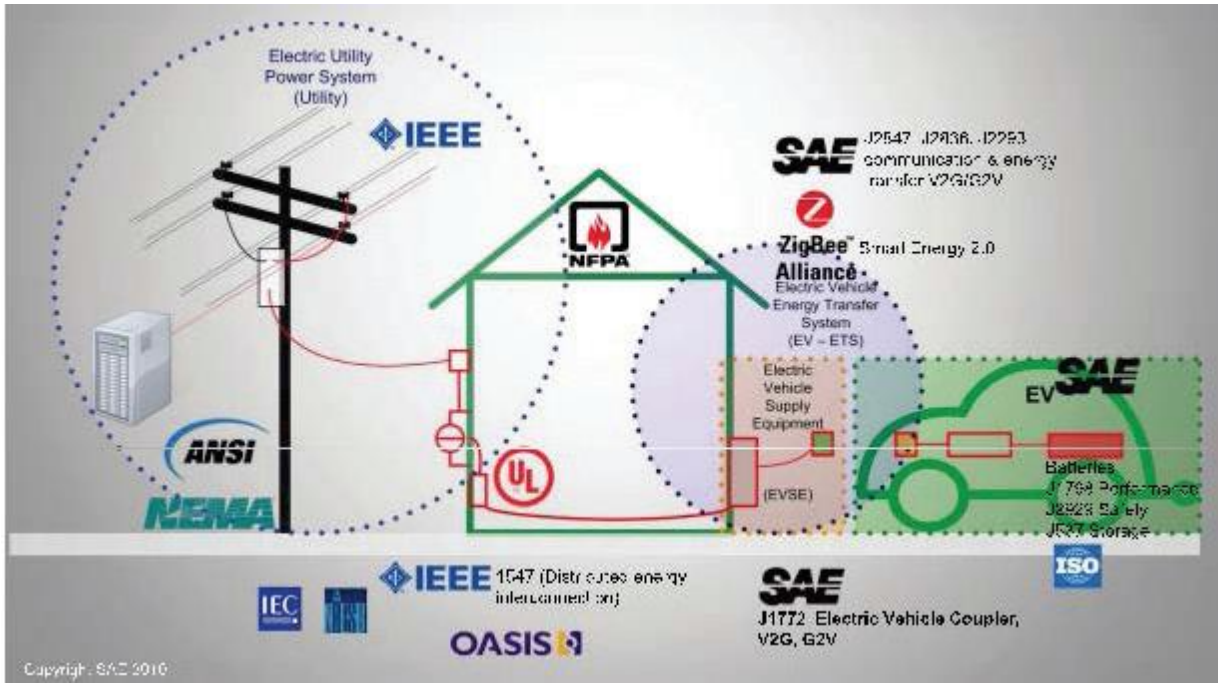

** used with Permission SAE International*

Figure 39: Overview of EV Energy Transfer Standards*

9. Impact on Distribution grid

Plug-in electric vehicles (PEVs) have uncertain penetration in electric grids due to uncertainties in charging and discharging patterns. This uncertainty together with various driving habits makes it difficult to accurately assess the effects on local distribution network. Extra electrical loads due uncoordinated charging of electric vehicles have different impacts on the local distribution grid.

Plug-in electric vehicles introduce a new concept of benefiting from electricity as the economic clean transportation technology. They have considerably less contribution in greenhouse gases, and they can reduce the dependency of expensive

fossil fuels. However, due to the effects of PEVs on power sector and the electric network operation, utilities need to concern reliable and safe operation of the network in presence of PEVs.

A number of studies have discussed economic costs and benefits of PEVs on customers. While, recently the more important question grabs electric utilities awareness: "What impacts will PEVs have on the electric distribution network?". According to a study the following aspects of PEVs impact on electric network:

- Driving Pattern
- Charging Characteristics (Vehicle demand Profile)
- Charging timing (When they plug-in and the magnitude and duration of charging cycle)
- Vehicles penetration

Recently, a number of researches attempt on studying the expected PEVs impacts on electric distribution grids. Previous studies focused primarily on either technical impacts on distribution grids, or economical assessment and economic incentives of PEVs. Researches that attempt on PEV's impact develop analytical methods to evaluate the following features of the distribution network

- System thermal loading
- Voltage profile
- Losses
- Unbalanced
- Transformer loss of life
- Harmonic distortion
- Demand response
- Resource scheduling with PEVs and renewable generation, and CHPs.

In order to plan an electric power delivery system, the transmission and distribution planner must know how much power it is expected to be served. Many distribution planners view voltage, along with loading, as the factors they must engineer in designing an acceptable distribution system. Not only voltage profile, but also power losses are essential to the distribution grid operator as well as grid customers. So, peak load, total losses, and voltage deviation are the most important specifications of distribution system which should be investigated in the widespread presence of PHEVs [15].

To evaluate the impacts of PHEVs on the distribution system, it is preliminary necessary to thoroughly explore the PHEV characteristics including battery capacity, state of charge (SOC), the amount of energy required for charging the battery, and charging level. The capacity of PHEV battery depends on the type of vehicle and the

driving range of vehicle in the electrical mode designated as “all electric range (AER).” SOC is defined as percentage of the charge remained in the battery. The amount of energy required for charging PHEV depends on the energy consumed by the vehicle in daily trips subsequently associated with daily miles driven and operation mode of PHEV, i.e., electric motor or combustion engine [16]. Also, charging level directly affects the duration time of charging such that lower charging level increases the duration time of charging a PHEV.

In conclusion, PHEV characteristics can be generally divided into two categories. The first category relates to those characteristics of PHEV which are known based on the car manufacturer data or power system structure. The features such as battery capacity are placed in this category. The second class comprises of those properties that depend on travelling habits of the vehicle owner. Features such as daily miles driven and starting time of charging PHEV reside in this category. Thus, investigating PHEV owners’ behaviour, along with manufacturer data, is an important key to study the effects of PHEV deployment in distribution systems.

In recent years, considerable efforts have been concentrated on the investigation of the impacts of PHEV on the distribution system. In almost all of the literatures, different assumptions have been made to simplify the investigations. Three time zones were determined for charging PHEVs, without considering vehicle owners’ behaviour as one of the most important factors to extract substantial parameters of PHEVs.

9.1. PHEV CHARACTERISTICS AND ASSUMPTIONS

New generation of vehicles such as PHEVs, which have an electric motor together with an internal combustion engine, are recently becoming more popular and would broadly be seen on the roads in the future. As noted earlier, the PHEV characteristics should be specifically studied before investigating their impacts on the distribution system. It is assumed that PHEVs are charged to their capacity once per day after their last trip arrival time. In this section, the PHEV characteristics and related assumptions required to study the impacts of PHEV on distribution system are described and analysed through the following subsections.

9.1.1. PHEV Battery Capacity

The capacity of battery is the key factor to determine the number of miles driven by a PHEV in the electric mode. The Pacific Northwest National Laboratory (PNNL) has estimated the electrical energy consumption per mile (ECPM) and battery capacity for a PHEV33 of different vehicle types (PHEVx indicates a PHEV with AER = x), as shown in the table below.

Vehicle Type	ECPM [kWh/mile]	Size of PHEV 33 battery [kWh]
Compact Sedan	0.26	8.6
Mid-size sedan	0.30	9.9
Mid-size SUV	0.38	2.5
Full-size SUV	0.46	55.2

Table 9: ECPM and Battery Capacity for PHEV33 of Different Vehicle Types

As noted earlier, AER is the possible distance driven by a PHEV with a full charge battery. So the product of ECPM and AER results in the battery capacity.

$$C = ECPM \times AER$$

Where C is the usable capacity of the PHEV battery.

Type	Vehicle Type	PHEV30	PHEV40	PHEV60
1	Compact Sedan	7.8	10.4	10.4
2	Mid-size sedan	9	12	12
3	Mid-size SUV	11.4	15.2	15.2
4	Full-size SUV	13.8	18.4	18.4

Table 10: Size of Battery for Various PHEVs (Kwh)

The above table shows the battery capacity for PHEVs with AER of 30, 40, and 60 miles according to (1). Referring to this table, PHEVs have a wide range of battery size, from 7.8 kWh to 27.6 kWh [15]. Since the energy required for charging a PHEV depends on the battery capacity, it is necessary to determine the types and AERs of PHEVs to analyse their impacts.

9.1.2. State of Charge (SOC)

SOC is a measure of the amount of energy stored in a battery. It is similar to the fuel gauge in conventional internal combustion cars. In this paper, SOC refers to the percentage of energy remained in the battery when PHEV arrives home, after daily trips. Although many papers, [17] [18]assumed that a PHEV travels in the electric mode until the battery becomes empty and then switches to the charge sustaining mode, the electric motor and internal combustion engine are optimally working together. So, PHEV can operate in blended mode in which the internal combustion engine helps the electric motor provide the required energy to run the vehicle. Therefore, in charge

depleting mode, either the entire or a fraction of the required energy is supplied by the battery. To cover all the possible PHEV operations, a factor λ for each PHEV is defined. This factor represents the percentage of distance that PHEV drives in the electric mode. Accordingly, the SOC of a PHEV would be

$$SOC = \begin{cases} (1 - \frac{\lambda d}{AER})100 & \lambda d \leq AER \\ 0 & \lambda d \geq AER \end{cases}$$

Where E_c is the required energy to fully charge the battery. E_c represents the chemical energy consumed in the battery. The actual electrical energy is calculated by

$$E_g = \frac{E_c}{\eta}$$

Where η is the efficiency of charging PHEV battery and E_g the actual energy which should be transferred from the grid to charge the battery. For further clarification, consider a PHEV with mid-size SUV type and AER equal to 40 miles. So, referring to Table II, battery capacity would be 15.2 kWh. Assume that this vehicle drives 32 miles in a day with λ = 80%. Thus, SOC is calculated as $\left(1 - \frac{(0.8\ x\ 32)}{40}\right)\ x\ 100 = 36\%$ And E_c would be 9.73 kWh. Assume that the efficiency of the charger is 88%. Thus, E_g would accordingly be 9.73 / 0.88 = 11.06 kWh.

9.1.3. Charging Level

Due to various power system structures and different charging stations, so far a number of charging levels to charge PHEV battery have been considered. For instance, charging level is assumed to be 4 kW for all PHEV based on Belgian standard outlet (230 V, 4.6 kW). Another reference has considered 120 V/15 A and 240 V/50 A, respectively, as normal and rapid charging levels. The ORNL report assumed two charging scenarios; the first one is 120 VAC circuit supplied through a 15 A circuit breaker charged at a peak rate of 1.4 kW, and the other one is 240 VAC with a 30 A circuit breaker charged at a peak rate of 6 kW. In, a more reasonable assumption was taken into account for charging level in which different charging rates are specified by a factor of the battery capacity (C), i.e., 0.2C, 1C, and 2C. Accordingly, 0.2C is named slow charging rate at which it takes 5 hours to reach the full charge battery when the battery is initially empty.

9.1.4. Load Growth

Most utilities represent their customer demand on a class by class basis, using smooth, and 24-hour peak load curves. These curves represent the demand characteristics of customers in each class, i.e., residential, commercial, and industrial. With the presence of PHEVs, the total load of a residential distribution network includes the daily household loads and the charging of PHEVs. To investigate the impacts of PHEVs, especially on the load curve, it is important to account the level of load growth during the time period of study. The system load increases as the new customers are added to the grid or the existing customers add new appliances or replace their existing equipment's with devices that require more power. In conclusion, energy usage within an electric utility system grows for two reasons; new customer additions and new uses of electricity. These two factors should be predicted to study PHEV impacts on the load curve in different years.

9.1.5. PHEV Distribution in the Network

To plan the future distribution network with the widespread presence of PHEVs, it is essential to have a precise prediction of PHEV distribution in the network. At first, the number of vehicles, whether PHEV or not, in the network should be estimated. Then, based on the specific PHEV penetration level, the number of PHEVs is determined. Distribution system operator would have no control over the location of future PHEV charging points, and no direct control over the duration and frequency of PHEV charging. Thus, PHEV is randomly distributed along the houses based on the number of PHEVs in a given year. As mentioned before, periods of charging are related to the PHEV owners' interest. Obviously, PHEV characteristics should be determined to study the impacts of PHEVs on the distribution systems.

9.2. Determining PHEV Characteristics and Assumptions for Investigating PHEV Impacts

PHEV characteristics, depended on vehicle owners' behaviour, are extracted from 2009 NHTS by analysing four created files. These data include daily miles driven, starting time of charging, number of vehicles per house, and vehicle type of houses. It is usually assumed that the PHEV owners plug in their vehicles when they arrive home after their last trip in a day. Therefore, the last trip arrival time of the vehicles can be the starting time of charging and is considered here. Other associated reports and references are used to determine AER, PHEV penetration level, daily load profile, and residential load growth. All of these data are required to thoroughly model and analyse PHEV impacts on the distribution system [15].

9.2.1. Daily Miles Driven

As mentioned before, SOC of PHEVs and the energy required to charge the battery subsequently depend on the miles driven by vehicles. Figure below represents individual and cumulative distribution of vehicles on the basis of their mileage in weekdays of summer.
Individual bar curves in figure indicate that the common mileage of vehicles is in the range of 20–25 miles. It can also be seen from this figure that about 55% of the vehicles drive less than 30 miles per day.

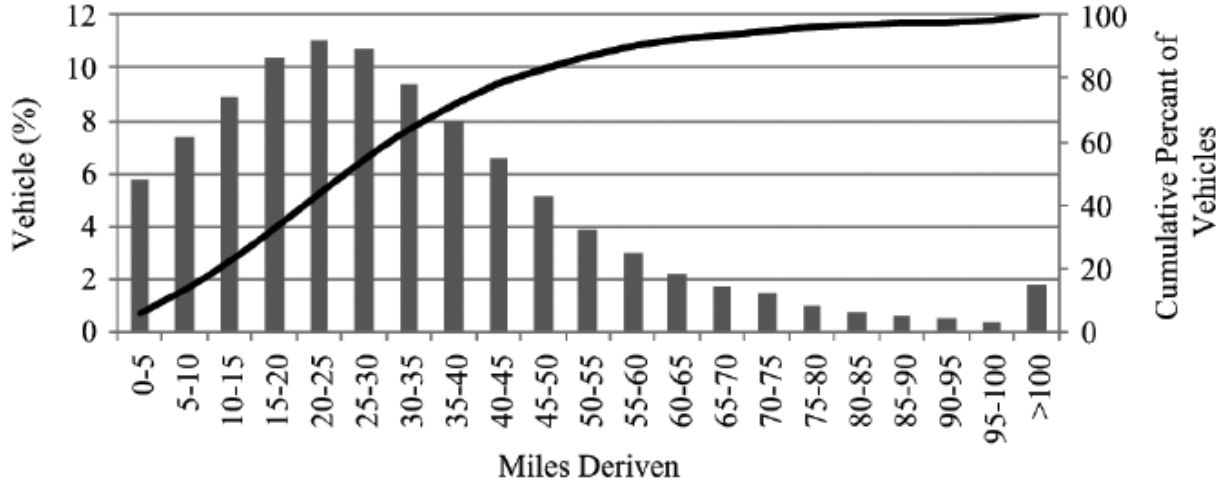

Figure 40: Percentage of vehicles versus daily miles driven for the weekdays of summer

9.2.2. Last Trip Arrival Time of Vehicles

It is commonly noted that an owner of a PHEV starts to charge the batteries of the vehicle as soon as reaching home at the end of the last trip of the day. Figs. 2 and 3, respectively, show the percentage of vehicle home arrival time at weekdays and weekend of summer. It is clear that there is a noticeable difference between people's driving pattern at weekdays and weekends. At weekdays, majority of people come home between 16:00 and 21:00, after their working hours. On the other hand, at weekends, people often stay home or go shopping without regular scheduling.

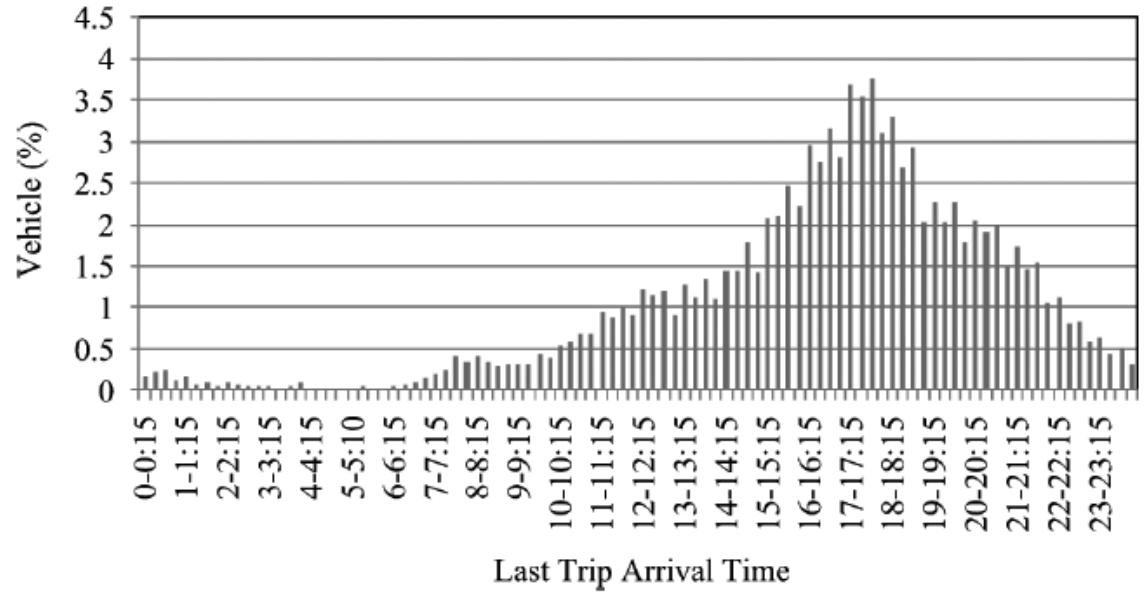

Figure 41: Percentage of vehicles versus their home arrival time for the weekdays of summer

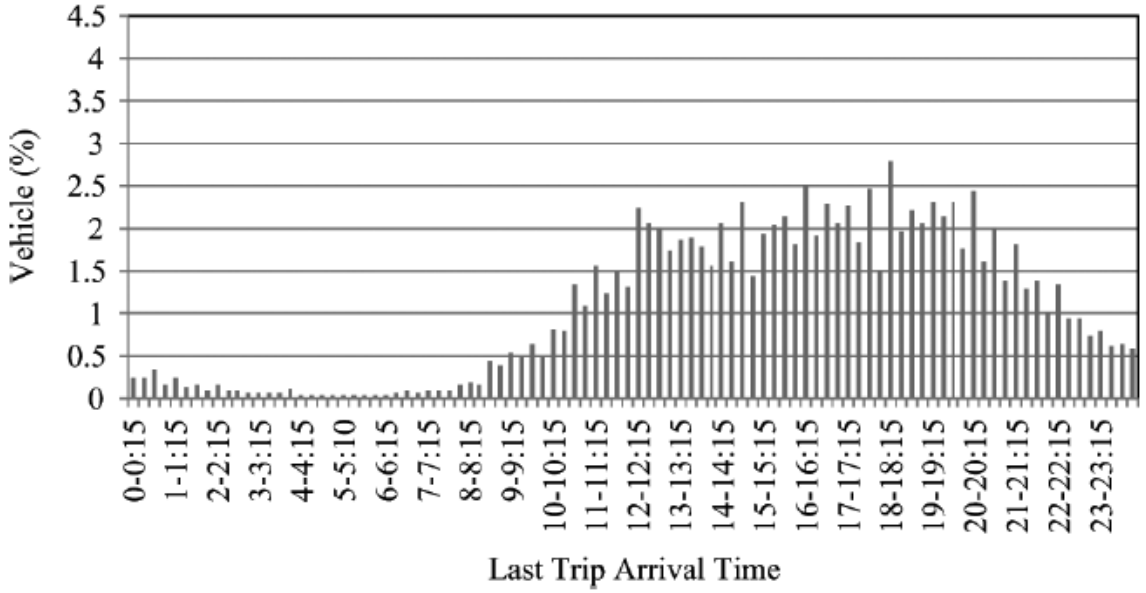

Figure 42: Percentage of vehicles versus their home arrival time for the weekends of summer

9.2.3. **Number of Vehicles per House**

As the PHEV penetration level is one of the most important factors affecting the impact of PHEV on distribution system, estimation of the number of PHEV distributed in houses is important. It is worthwhile to compare the number of vehicles reported in 2009 NHTS and 2001 NHTS report, as shown in Table below. This table certifies that the percentage of houses which have a specific number of vehicles does not change significantly from 2001 to 2009. Referring to Table below, the average number of vehicles per house in 2001 and 2009 is 2.12. This result is close to what was claimed for Washington State, i.e., in average 2.3 vehicles per house.

No. of vehicles in each house	Percentage of houses in 2009 NHTS	Percentage of houses in 2001 NHTS
Zero vehicle	3.40%	3.43%
One vehicle	25.26%	22.17%
Two vehicles	42.61%	45.45%
Three vehicles	18.74%	19.27%
Four vehicles	6.57%	6.45%
Five vehicles	2.18%	2.16%
>Five vehicles	1.24%	1.07%

Table 11: Percentage of houses with different number of vehicles

9.2.4. Vehicles Type Analysis

As emphasized before, type of PHEV has a direct impact on the size of battery as well as energy consumed by the PHEV. It can be realized from Table XII below that the most common vehicle is type 1, i.e., compact sedan.

Vehicle type	1	2	3	4
percentage	51.48%	10.35%	23%	15.17%

Table 12: Types of PHEVs and their Usage Percentage

9.2.5. AER

2009 NHTS does not have data on AER of PHEVs, 2009 NHTS does not have data on AER of PHEVs, and the penetration of PHEVs with different AERs is assumed to be the same as Table XIII below. Based on the type and AER of each PHEV, the size of battery is extracted.

PERCENTAGE OF PHEVS WITH DIFFERENT AERS

	PHEV30	PHEV40	PHEV60
Percentage	21%	59%	20%

Table 13: Percentage of PHEVs with Different AERs

9.2.6. PHEV Penetration Level

The number of PHEVs depends on the PHEV penetration level. PHEV penetration level is estimated in three levels: low, medium, and high. The medium penetration level between 2010 and 2050 is depicted in the figure below.
Accordingly, in medium PHEV penetration level, 35% of total vehicles will be PHEVs by 2020. PHEV penetration rate increases up to 54% and 62% by 2035 and 2050, respectively. It should be noted that the residential load is significantly grown along with the increment of PHEV penetration levels during these years.

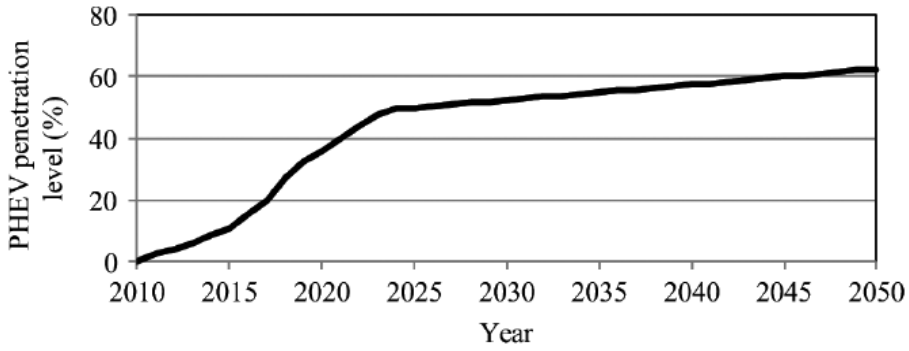

Figure 43: PHEV Penetration level

9.2.7. Daily Load Profile

The load profile covers 24 hours on a 15-min time basis as shown in Fig for an arbitrary day during summer and winter. These load profiles, assigned to each house, are used in the PHEV impacts studies.

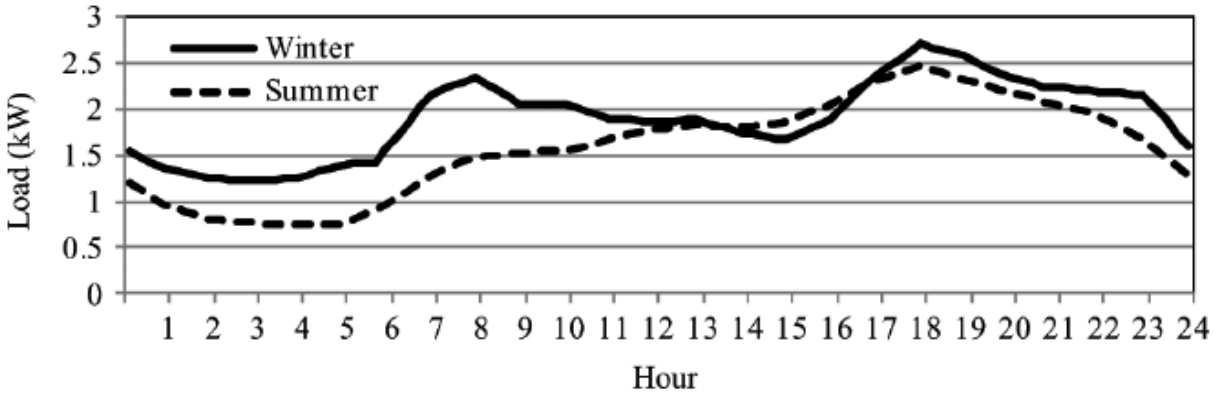

Figure 44: Load profile

9.2.8. Load Growth

The mean incremental growth rate of annual residential electricity consumption will be 1.3%, due to new uses of electricity. The number of houses is assumed to increase similar to the Fig below. Note that the daily load profile determined in the previous subsection belongs to 2010; so the load growth for future years is calculated based on that of 2010 [19].

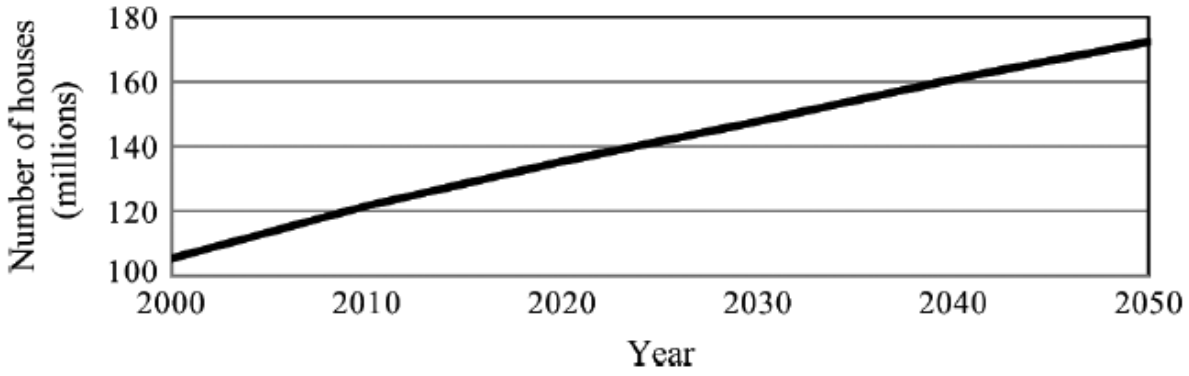

Figure 45: Load Growth

9.3. Impact Study

This section represents the impacts of PHEVs on different terms of distribution system including system power consumption, total system losses, and voltage deviation at load points. In the previous section, the PHEV characteristics and related assumptions were precisely extracted from the accessible reports. In this section, the impacts of charging PHEVs for the weekdays of winter and summer are explored. Since the load profiles have lower peak and average at weekends than weekdays, PHEV impacts are just studied at weekdays. The proposed approach is general and is not case dependent. The following assumptions are just sample cases and are either reasonably justified or extracted from available reports and publications.

9.3.1. Description of System under Study

The IEEE 34-node test feeder is studied here. This radial network is shown in the Fig below. The network medium voltage is 24.9 kV and low voltage is 230 V. So, this network is represented as a residential radial network.

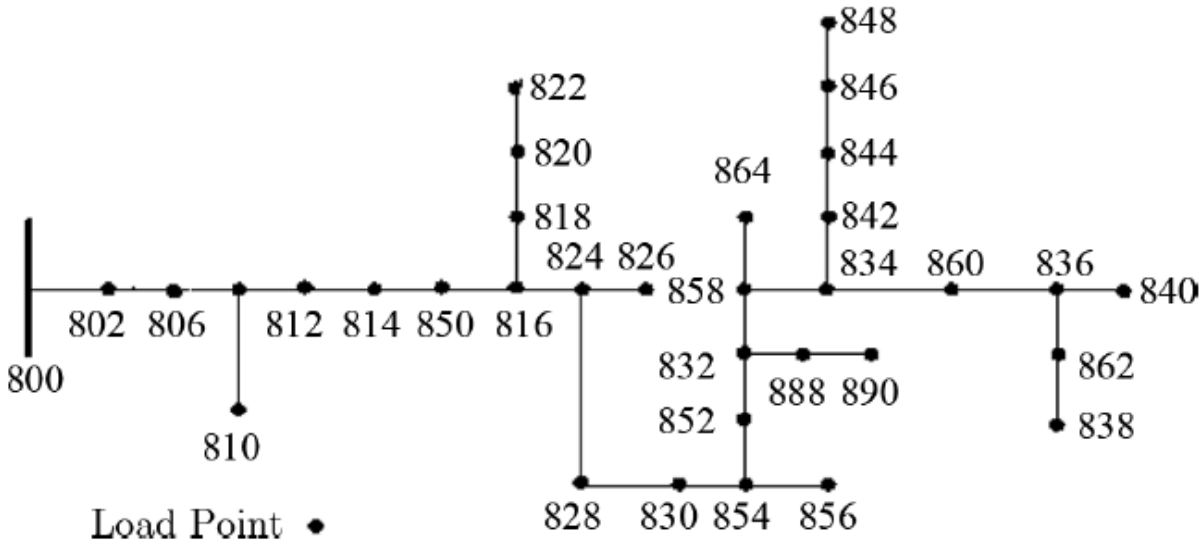

Figure 46: IEEE 34-node test feeder

The network contains 33 load points. Eight points, 810, 818, 820, 822, 826, 838, 856 and 864, are single phase and the remaining 25 are three phase. Two houses are assigned to each phase of load points. Therefore, the total number of houses is equal to 166. The number of vehicles in the mentioned radial network is equal to 352. These vehicles are assigned randomly to the houses based on the percentage noted in the table in the earlier section. Also, the type of vehicle is assumed randomly from the earlier stated data. Daily miles driven and last trip arrival time of vehicles for the weekdays of summer and winter are extracted from presented data. To determine when a vehicle is plugged into the outlet and how many miles are driven by each vehicle. These data are subsequently determined for PHEVs. Although the distribution of factor λ, due to the lack of data, cannot be accurately predicted, it is reasonable to assume that more than half of the daily trips are taken on the electric mode [16].

This leads to have λ, a random number between 0.5 and 1. So, daily miles driven, type of PHEV, AER, and factor λ are incorporated to calculate the energy consumption of the PHEV. Household load profiles are assumed to be the same as the ones presented in the previous section. Due to impacts of reactive power on lines congestion, power losses, and voltage magnitudes, the reactive power consumption of household load and PHEV battery should be considered.

To this end, the average power factor of a typical household and PHEV battery are respectively assumed to be 0.9 and 0.95. The charging level of PHEVs should also be determined. As mentioned before, it is more realistic to consider charging rate as a coefficient of the battery capacity rather than using a definite charging rate. So, the charging rate of a battery with large capacity is reasonably higher than a lower capacity battery. The charging level of 0.2C (C represents the usable capacity of the battery) is considered here, which means that an empty battery will be fully charged in about 5 hours. Referring to the Table earlier furnished, the lower and upper bands of charging rate are $0.2\ x\ 7.8 = 1.56\ kW$ and $0.2\ x\ 27.6 = 5.52\ kW$, respectively.

This range of charging level is commonly available in most single-phase 230 V outlets in residential households without having to reinforce the wiring. The fast charging is not considered, because it requires a higher voltage connection and is not already available in houses. Also, dc/ac and ac/dc conversion efficiency for the battery is assumed to be 88%.

Load flow analysis is performed to calculate the total load, feeder power loss, and voltage deviation in different load points of the network. In this section, load flow analysis is executed by open-source distribution system simulator (Open DSS). Open DSS is an electric power distribution system simulator for advanced analysis of distribution systems [17]. Open DSS is a multi-phase simulator tool in which each phase of load points can be specified separately. Also, power flow is simulated sequentially over successive time steps (e.g., 15 min) considering all circuit dynamic

facilities (e.g., regulators). These Open DSS capabilities provide interactions of the variations of PHEV load patterns and seasonal conventional load.

9.3.2. Case Studies Definition

The following case studies are conducted to investigate the impacts of PHEV:

Case I: single year study; this case focused on determining the effects of different PHEV penetration levels on the performance of distribution system, i.e., voltage deviation, system losses, and peak to average ratio (PAR), in a single year, 2020.

Case II: short-term study; the impacts of PHEV on distribution system performance within the period of 2020 and 2026 are investigated.

Case III: long-term study; this case is devoted to the investigation of the impacts of PHEV between 2020 and 2050, just, on the load curve.

As mentioned before, some of the PHEV characteristics are randomly distributed. So, for a more accurate analysis, for each scenario study, about 3000 samples are taken over these parameters to achieve a precise average for PHEV consumption in 15 min time interval. In the following subsections, the mentioned cases are deeply studied.

9.3.2.1. Case I

This investigation is effectuated in year 2020, in which the low, medium, and high penetration levels are respectively 11.3%, 35% and 45%.The load of each house grows 13.8% ($(1.013^{10}-1) = 13.8\,\%$) compare to that of year 2010. The number of houses is assumed to be 166, as mentioned before. The case with no PHEV is taken as a reference case. The following figures show the results of PHEV charging impacts on the distribution system in summer and winter.

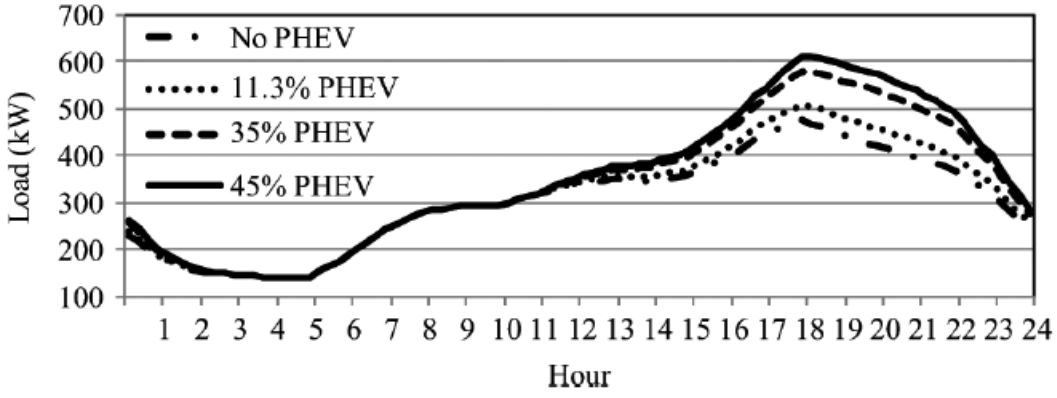

Figure 47: Impacts of PHEV charging on total load curve for different PHEV penetration levels in summer of 2020

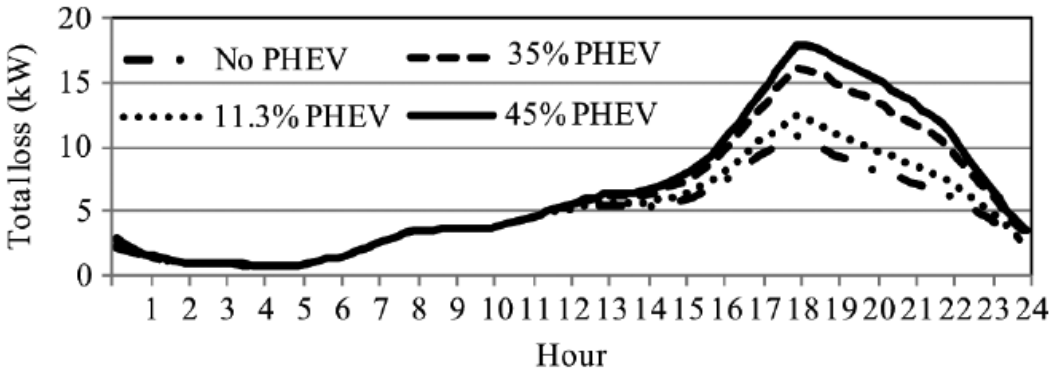

Figure 48: Impacts of PHEV charging on total losses for different PHEV penetration levels in summer of 2020

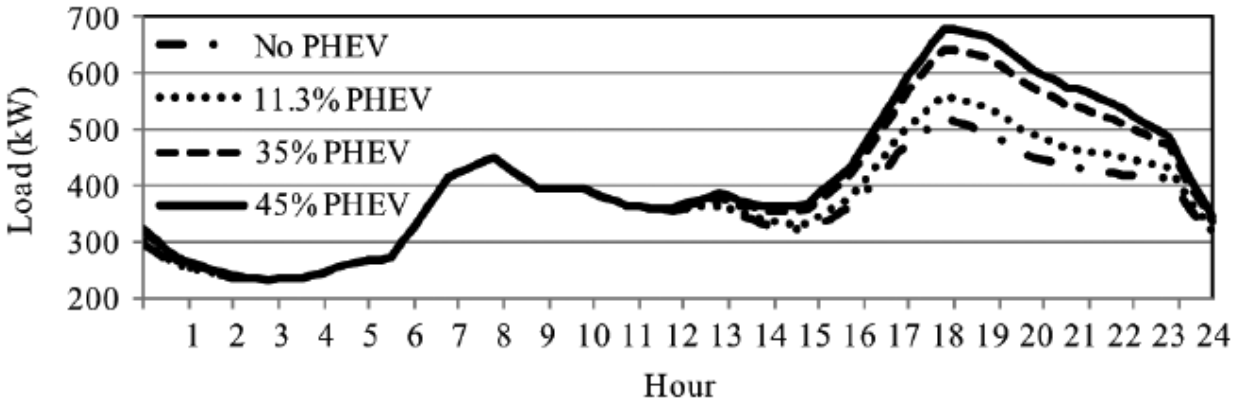

Figure 49: Impacts of PHEV charging on total load curve for different PHEV penetration levels in winter of 2020

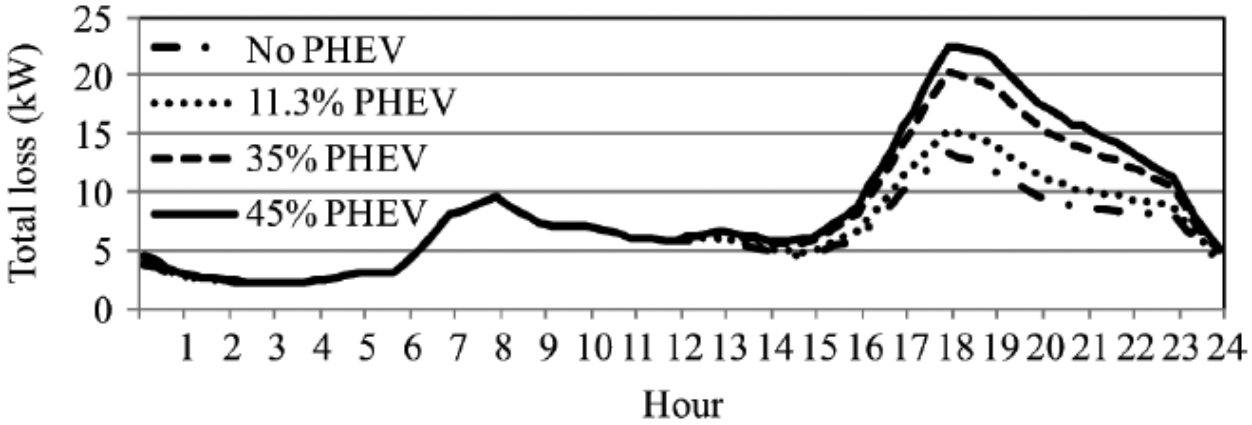

Figure 50: Impacts of PHEV charging on total losses for different PHEV penetration levels in winter of 2020

The table below illustrates various specifications of the grid with different PHEV penetration levels.

	Season	No PHEV	11.3% PHEV	35% PHEV	45% PHEV
Peak Load [kW]	Summer	474	507	576	607
	Winter	520	558	638	674
PAR	Summer	1.56	1.61	1.70	1.73
	Winter	1.42	1.48	1.59	1.63
Total losses [%]	Summer	1.35	1.42	1.58	1.66
	Winter	1.52	1.59	1.75	1.83
Max. Voltage Deviation [%]	Summer	3.12	3.34	3.82	4
	Winter	3.46	3.72	4.27	4.53

Table 14: Specifications of the Grid with Different PHEV Penetration Levels

The first two rows of Table present the impacts of PHEVs on the peak load. Table demonstrates that growing PHEV penetration level leads to a significant peak load increment, since majority of people arrive home after their last daily trip between 16 and 21 and plug-in their vehicles at this time which coincides with the households peak load. These facts are also be seen in the above graphs which show the feeder load curve in summer and winter of 2020, respectively. The results shown in these 2 graphs imply that load demand with PHEVs does not change noticeably from 3:00 to 11:00 compared to the reference load curve. This point shows that no PHEV charges when the load level is low. So, although the average load increases due to PHEV charging, the peak load increases more than that and it causes PAR increment as presented in the above Table. It is desirable to have PAR close to one. Higher PAR might result in substantial cost increment for utilities in long-term since it requires new investment in generation and transmission capacities to serve higher peak load. Also, utilities take disadvantages of peak increment in short-term due to the operation cost rising. Unlike peak load, PAR is lower in winter than summer. The reason for this is that, load curve in winter is smoother than summer as shown by fig 47 and 48, fig 49 and 50 and the third row of Table show total system losses during a day in summer and winter of 2020 with different PHEV penetration levels. The results verify the loss increment due to PHEV penetration level growth. It is worthwhile to draw a comparison between PHEVs power consumption, which can be concluded from Figs. 47 and 48 and loss variation curves sketched in Figs.49 and 50. It can be deduced that charging PHEVs takes place simultaneously with the peak of loss curve. This occurrence results in the increment of loss contribution in the peak load.

With regards to the fourth row of Table, increasing the number of PHEVs also causes an increase in voltage deviation; 45% PHEV penetration leads to more than 25%

increment in the maximum voltage deviation, for both summer and winter, compared to the reference case. However, this deviation can likely be limited to its cap, using voltage regulators in the network.

9.3.2.2. Case II

In this case, three definite years are selected to probe the impacts of medium PHEV penetration level between 2020 and 2026:

- Year 2020: PHEV penetration level is 35% and the load profile of each house grows 13.8% compared to that of 2010 shown in Fig. 5.
- Year 2023: PHEV penetration level is 47% and the load profile of each house grows 18.3% compared to that of 2010.
- Year 2026: PHEV penetration level is 50% and the load profile of each house grows 23% compared to that of 2010.

It is assumed that the topology of the test feeder is not changed during these years. However, the number of houses increases according to the earlier Fig and these houses are randomly distributed among the existing load points. Simulation results for this case is presented below.

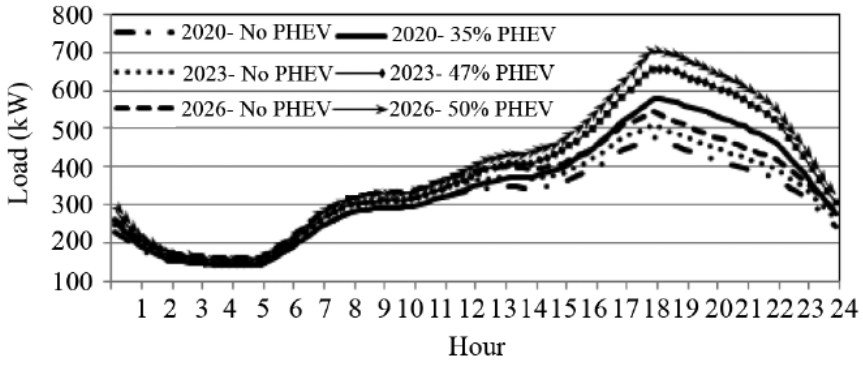

Figure 51: Impacts of PHEV charging on total load curve for medium PHEV penetration levels in summer of different years

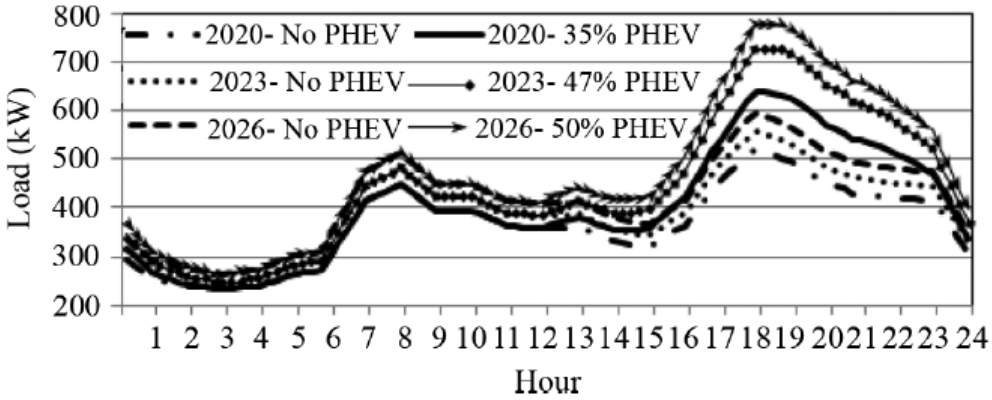

Figure 52: Impacts of PHEV charging on total load curve for medium PHEV penetration levels in winter

	Season	2020		2023		2026	
Penetration level		0%	35%	0%	47%	0%	50%
Peak load [kW]	summer	474	576	503	644	533	689
	Winter	520	638	551	715	584	763
PAR	summer	1.56	1.70	1.56	1.74	1.56	1.75
	Winter	1.42	1.59	1.42	1.63	1.42	1.64
Total losses [%]	summer	1.35	1.58	1.45	1.79	1.56	1.95
	Winter	1.52	1.75	1.65	1.97	1.78	2.15
Max voltage deviation [%]	summer	3.12	3.82	3.38	4.40	3.58	4.70
	Winter	3.46	4.27	3.76	4.94	3.96	5.26

Table 15: specifications for short term simulation in summer and winter

The cases without PHEV are the reference cases for each year. The figures and table bring miscellaneous impacts of PHEV charging on the 34-node test feeder in a typical weekday of summer and winter, presents the peak load, PAR, total losses, and maximum voltage deviation of load points for summer and winter. Figs depict the feeder load curve including losses, with and without PHEV for short-term study in summer and winter, respectively.

The following results can be concluded:

- The second and third rows of Table VII show, respectively, the peak load and PAR of the network for different years. The peak load and PAR increment, compared to the reference cases, are higher in 2023 than 2020 and do not change significantly from 2023 to 2026. The reason for this is that, the growth rate of PHEV penetration level is higher within 2020–2023 than that of period 2023–2026 and majority of PHEVs charge at the time of household peak load.

- The fourth row of Table 2 describes the ratio of total power losses to total load in the reference case of the same year. With the PHEV penetration level increment, power loss rises significantly.

- The last row of Table 2 shows the maximum voltage deviation among the nodes during 24 hours. The results certify that PHEV charging causes an increment in the voltage deviation of load points. Also, the increment of PHEV number leads to a more voltage deviation. The table also shows that the voltage deviation is higher in winter than in summer due to the higher load demand of winter.

9.3.2.3. Case III

This case provides important information about peak load demand in a long-term investigation between 2020 and 2050, notwithstanding that the feeder structure is changed during these years. The PHEV penetration levels during these years are simply extracted from Fig. d. Also, based on the previous mentioned data, the number of houses increases 27.5% and load of each house grows 47.3% from 2020 to 2050. The results are depicted in Figs. 14 and 15 for summer and winter weekdays. As expected, the peak load increases due to the PHEV presence and PHEV penetration level increment. The presented results indicate that the PHEV charging coincides with the peak of household energy consumption.

As expected, the peak load increases due to the PHEV presence and PHEV penetration level increment. The presented results indicate that the PHEV charging coincides with the peak of household energy consumption. In both summer and winter curves, represent that PAR increases before year 2026, since in this period, the rate of PHEV penetration level is high, and PHEV charging is coinciding with peak load curve. This occurrence causes the peak load increment to be more than average load increment. Obviously, PAR lessens in the next years due to the higher increment of average load than peak load.

9.4. Sensitivity Analysis

The distribution of λ would significantly affect the consequent result of the load curve. As mentioned earlier, the distribution of factor λ cannot be accurately predicted. Therefore, a sensitivity analysis on the impacts of different values of is constructed here to investigate the impacts of all the possible PHEV operation modes on the network load profile. Doing so, different values of λ, i.e., 0.5, 0.6, 0.7, 0.8, 0.9, and 1, are considered for all the PHEVs in a single year, 2020, with different PHEV penetration levels. Table XVI illustrates the impacts on peak load of factor λ. Higher implies that PHEVs drive more on electric mode, so the battery of PHEVs would likely require more power from the grid to be fully charged. Consequently, as presented in Table XVI, peak load increases on the basis of λ increment.

Also, a higher penetration level of PHEV leads to a more increment in peak load versus λ growth.

λ	11.3% PHEV		35% PHEV		45% PHEV	
	summer	Winter	summer	winter	summer	winter
0.5	498	549	553	613	578	642
0.6	501	552	563	627	590	657
0.7	504	555	571	633	599	668
0.8	507	557	679	642	611	681
0.9	510	559	584	649	618	690
1	512	562	591	655	828	897

Table 16: Impacts on peak load of factor λ

10. Impact of PEV charging stations on the Milan Distribution Grid

For estimating power demand of a FC station, it is necessary to make an assumption on the number of EVs that need to be charged in each station at any time of the day. Considering the Italian case and data available from the census made by ISTAT, that people owning a private parking place shall be more inclined to buy EVs and to charge their vehicle during the night (car not used and cheaper energy rate), makes possible to estimate that in Italy at the most 64% of the energy for charging EV circulating in 2030 would be allocated during the night and that at least 36% would be allocated during the day. Then we take the further assumption that 6% of EV will charge (during the day) connected to a LV network and a 30% will use a FC stations connected to the MV network [20] [21]. Moreover, taking into account the daily average journey of a present car (about 35 km) and the energy demand per kilometre (0.15 kWh/km), the daily average energy demand of each EV is expected to be around 5 kWh/day. With this figure and making the hypothesis that the daily average travel in 2030 will be the same as today, it's possible to calculate the daily demand of the whole Italian EV fleet, which in 2030, should be around 55 GWh/day. In metropolitan areas, for a number of reasons, penetration of EV will be higher; additionally, due to the limitation of space, traditional gas stations will become the most suited spots to place future fast DC chargers.

This scenario was adapted to the metropolitan area of Milan (provincia di Milano). In this area there are about 1100 gas stations which, in our 2030 scenario, will have to become "hybrid", hence refuelling both ICE vehicle and providing FC for about 300,000 vehicles (that is between 120 and 150 vehicles fast charged everyday by each "hybrid" refuelling station). Hence the energy that should be provided by the average urban "hybrid" refuelling station of the city of Milan should be about 1.2 MWh per day.

Number of Electric Vehicles	~ 300,000
Distance/ day	30 km/ day
Fuel Consumption (pure electric)	0.15 kWh/ km
Number of refuelling stations	~1100
Average Energy per day provided by a refuelling station	~ 1200 kWh/day

Table 17: Estimation of the average energy per day provided by a FC station

Additional considerations were made to identify the profile of the power demand to the network. The FC will be more requested when people are moving, especially when they go to work in the morning or they come back home in the late afternoon, therefore it will be proportional to the "mobility diagram" in the Figure below.

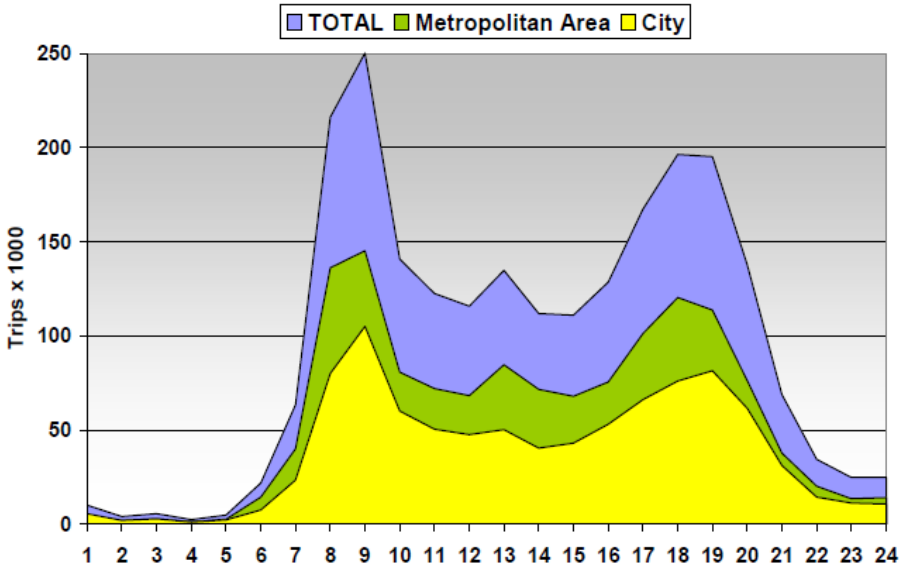

Figure 53: Mobility diagram of the metropolitan area of Milan *[21]*

Scaling FC requests to the electric demand of the average "hybrid" refuelling station in the metropolitan area of Milan, we find the average power request to the network as displayed in the next Figure.

Direct connection of FC stations to an already congested grid, may result in inconvenience like feeders overloading and voltage drops. For that reasons, a cost benefit analysis may, in some cases, prove convenient the use of storages for shaving peak power demand and eventually to provide additional network services, included optimization of intermittent-not-programmable energy resources, such as renewable energy.

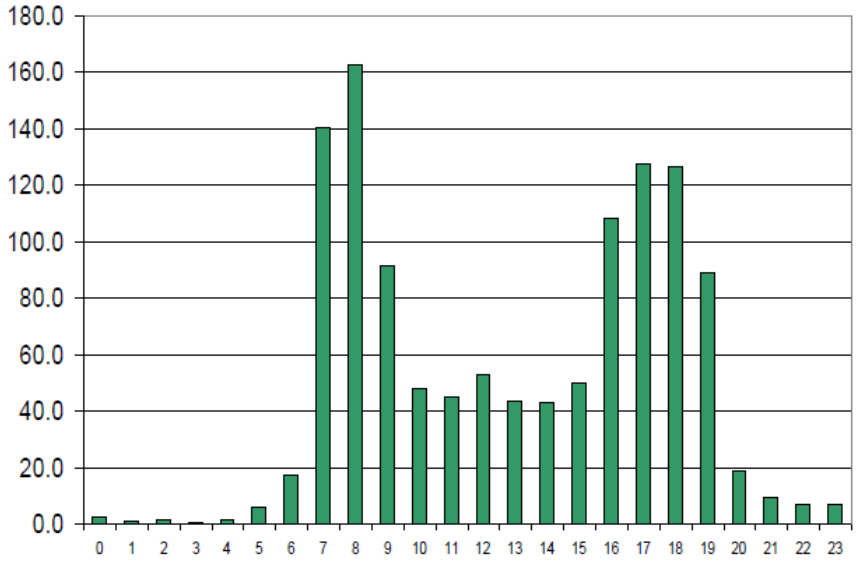

Figure 54: Power request the network of the average "hybrid" refuelling station of the metropolitan area of Milan

10.1. Storage Facility to Shave Peak Power Demand

Storages in FC stations allow accumulating the energy that has to be used for charging EV at high power. There are two main approaches for using storages. The first approach aims both at optimizing the power request from the grid, but also at limiting the capital investment in buying storages [22]. The second approach aims at accumulating energy when tariffs are low (e.g. during the night) or to shave excess production from intermittent-not-programmable energy resources, such as renewable energy. This second case requires *high capacity storages* and gives also the capability to provide ancillary services: like injection of active and reactive power and voltage regulation [23].

10.1.1. Optimizing the Power Request from the Grid

This approach aims at minimizing capital investments both in the connection of the charging station to the network and in the energy storage. The optimization applied to the average FC station of the metropolitan area of Milan shows the profile in Figure.55. It requires a 60 kW connection combined with a 210 kWh energy storage [24]. The Figure.55 displays the state of the average FC station. Green bars represents the energy in storages, blue bars represent the power that is requested from the electric network, and yellow bar is the actual power that is requested to charge EV at any time of the day [25]. Such figures shall be scaled for station smaller or bigger than the average. This means that bigger stations may require power and energy storages two

or three times bigger, but also that for many FC stations (smaller than the average size) a LV connection and even smaller storages may be enough to provide the requested service.

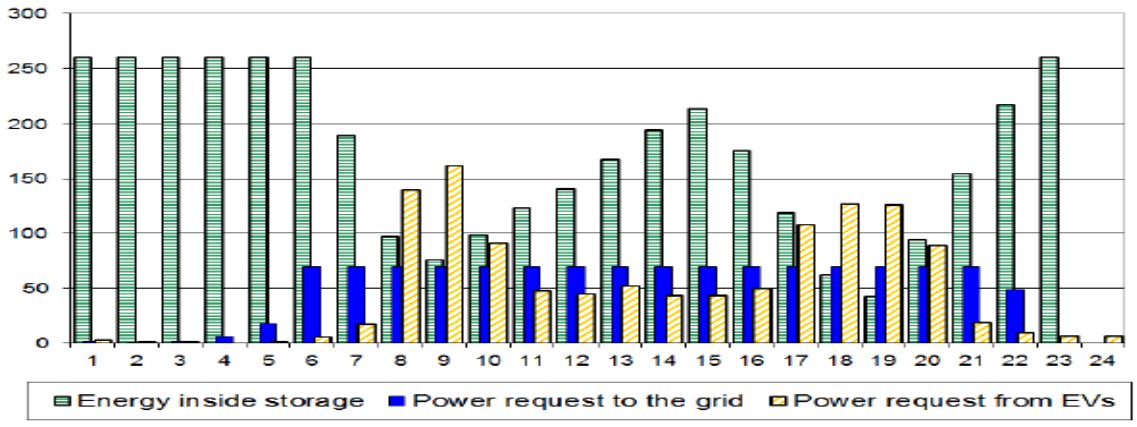

Figure 55: Lower capacity storage: Energy in the storage, power request from the grid end from the EV fleet

10.1.2. High Capacity Storages

This approach aims at accumulating all the energy that is required for charging EV when the price of energy is low or when there is an excess production from intermittent-not-programmable energy resources, such as renewable energy. Optimization of the investment brings to high capacity storages able to accumulate during night time all the energy that is requested during the day. The Figure below represents the actual state of the storage (green bars), power that is requested from the electric network (blue bars) and power requested to charge EV (yellow bars) at any time of the day. The optimal size of the storage for this purpose is equal to the average energy that is needed to charge EVs during the day.

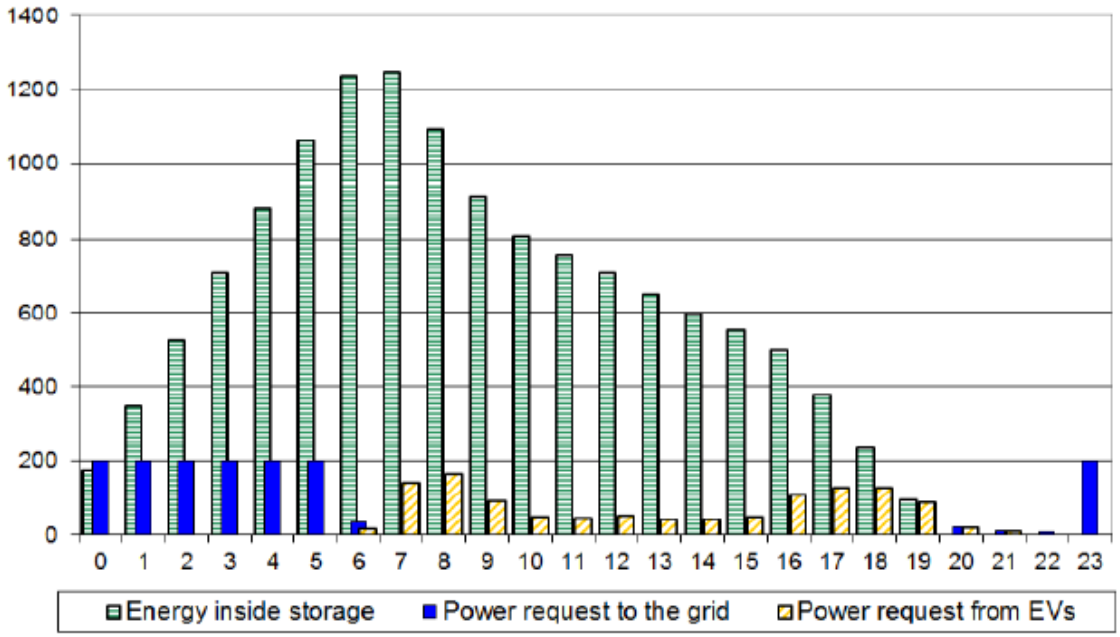

Figure 56: High capacity storage: Energy in the storage, power request from the grid and from the EV fleet

Unfortunately such system is very expensive. It may become convenient in case price of storages drops to 150 €/kWh as in the case shown in the next Figure, where a comparison between different plants' cost is displayed. Reducing the price of batteries, plants with storages becomes more convenient than plants without storages. The optimal storage capacity is for the same size of the energy that the FC station has to provide during the day.

The costs benefits analysis was carried out with the following hypothesis: 12 years lifespan, 4500 cycles (one per day), 90% of efficiency (both in charge/discharge processes) and storage installation cost proportional to the size.

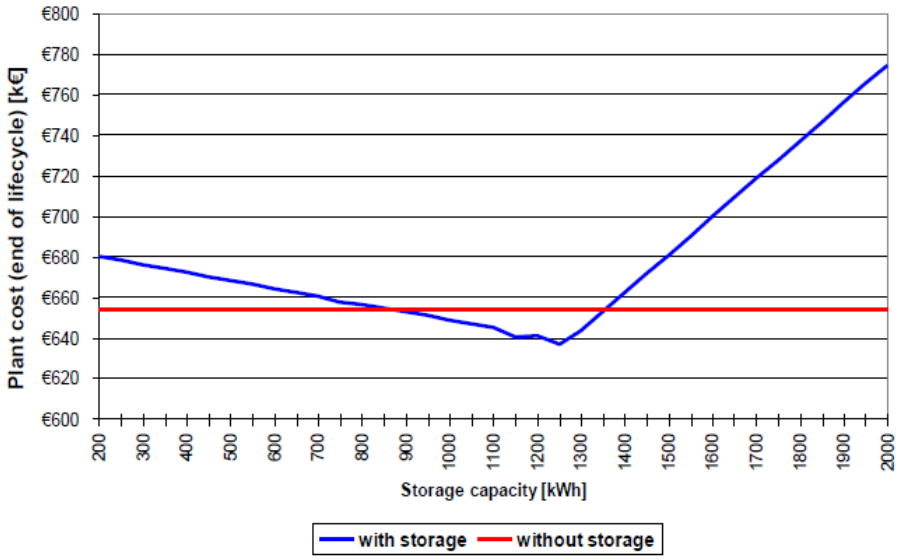

Figure 57: Plan cost comparison

10.1.3. Storage and Ancillary Services

Charging stations with storages are intrinsically capable of providing services to distribution utilities. This is mainly due to the presence of a voltage source converter as interfacing technology (converting AC into DC) and the presence of a storage system. The converter has the natural capability of de-coupled bidirectional control of the active and reactive powers as long as it is within its current capabilities. A storage of a fast charging station that provides (or draw) power to (from) the network is like a distributed generation applications capable of both drawing power and supplying it when required. The capability of the charging station to provide ancillary services to the distribution grid can be limited not only by the size and dynamics of the plant but also by the actual service that it has to guarantee for charging EVs. For this reason high capacity storages are more flexible to provide network services than low capacity storages.

Absorbing unpredictable production peaks from intermittent-not-programmable energy resources (for instance, photovoltaic plants have their production peak in middle hours of the day, when the energy demand is not at its maximum) can be achieve also by non-bidirectional system, like fast charging station with no implementation of auxiliary grid services. This task requires only the capability to control the power absorption to charge the storage systems. However to provide these service, the FC station shell be an active element in the smart grid and it needs a bi-directional communication with the smart grid control.

10.2. Impact on MV Grid

One of the main assumptions of this analysis is that electric vehicles will be charged on the same electrical distribution grids that today are used to provide energy to other kind of application. In other words, there is no reason to design from scratch a grid model specific for electric mobility.

Voltage drop is an aspect to consider for reliable operation of distribution networks since it can cause malfunction and damage of electrical equipment, and is particularly relevant in rural network where due to the long line lengths largest voltage drops usually arise.

Since electric mobility shall be an additional load to the grids that are already deployed in Europe, the study has started by the collection of distribution grid planning and operational rules used today [26] [27].

We considered voltage drops due to FC stations connected to MV lines. Our scenario assumes that existing gas stations, which are normally located where there is the actual need of fast charging, will be the best places to put FC systems, hence all present gas station are very likely to become “hybrid” gas stations. Taking this hypothesis we fine the position of all present gas station and connected each of them to the nearest (less than 150 meters) node of the MV grid. We considered a portion of the entire distribution grid in Milan, as shown in Figure.58 below, and virtually connected 28 “hybrid” refuelling stations to the 11 feeders of the MV grid.

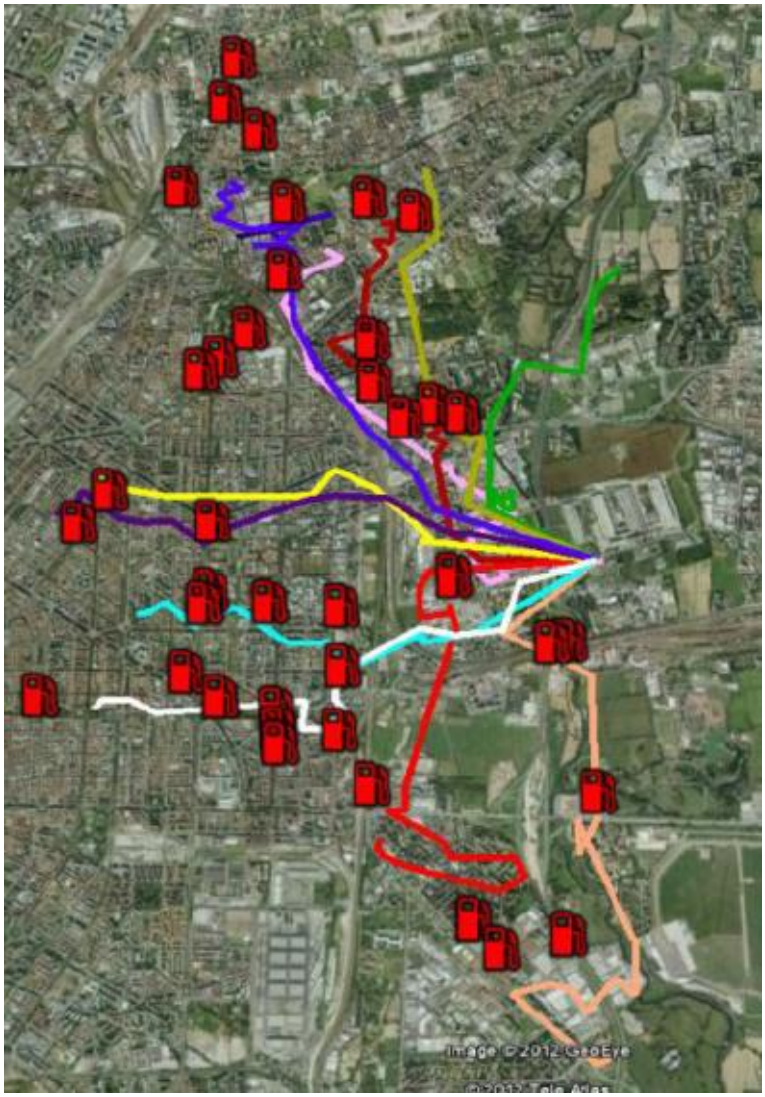

Figure 58: Milan MV distribution grid portion, with FC stations

Simulated voltage profile during a day along the most loaded MV line is shown in the next Figure.

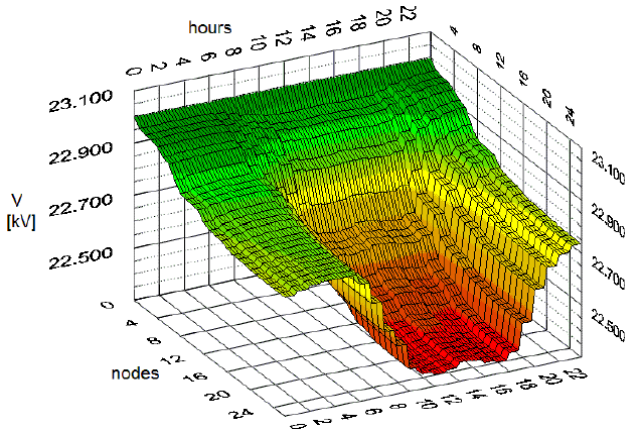

Figure 59: Voltage dropping along MV line

The maximum voltage drop in the farthest node is equal to 2.5% of nominal voltage; the legislation provides for the voltage drop a threshold of 10% of the nominal voltage level (EN50160).

We added to the pre-existing loads the EV load presented in Figure 59 and introduced a scale-factor parameter, which multiplies the power request in order to simulate different plant sizes.

We simulated the impact of the fast charge stations with a scale factor equals to 0 (base case: no EV charged), 1, 2 and 3. Figure 59 shows the difference between lines voltages compared to the base case simulation.

Voltages drop in all of them, following the curve of Figure 59, but the percentage of such drops is under 0.5 % (with reference to nominal voltage value); in the terminal node, the farthest from the MV/LV transformer, voltage difference is about -0.42 %. It is evident that the impact of fast charging station on the Milan MV distribution grid is imperceptible. This is due to the distribution grid planning rules: line cables are oversized to provide counter current power flow during maintenance operations or systems faults. As a result, the studied MV grid is able to support fast charge stations with no need of potentiate the existing distribution grid.

Storages systems previously presented can further elevate voltage level providing energy to the grid. Obviously this service must be integrated in a smart grid asset where a local voltage control is implemented high energy request for recharging EVs. This can bring to an overloading problem or a tension dropping that can be controlled using storage and power electronics. These issues occur mostly in rural distribution grids, due to the length of line cables. Storage systems inside FC stations can be used to store energy from intermittent-not-programmable energy resources, such as renewable energy for recharge EVs (green energy to green transport) or to give it back to the grid when it’s requested [28]. To provide such services a FC station requires a bi-directional communication to the smart grid control system.

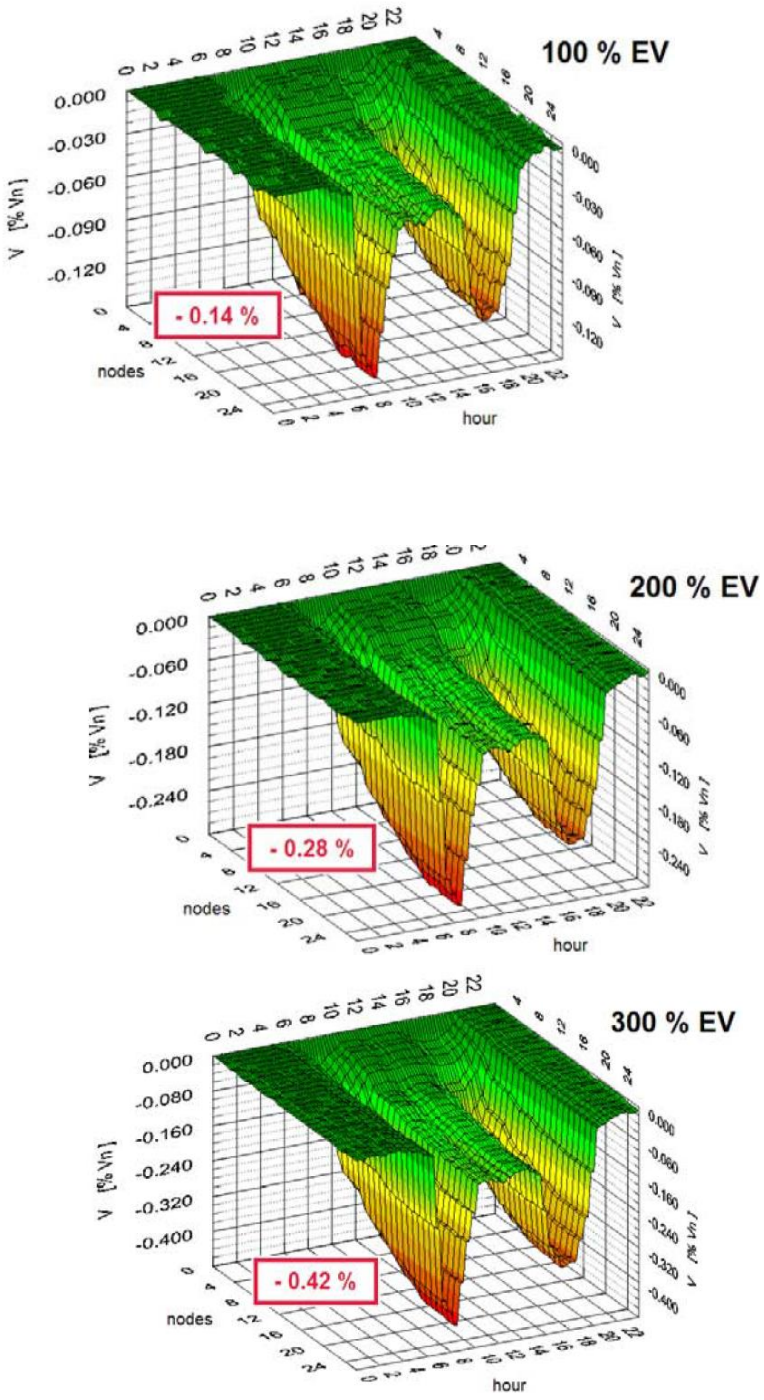

Figure 60: Multiple simulations of voltage drop impact on MV grid portion

11. Optimisation of Charging the Electric Vehicles

The charging of PHEVs and EVs can be a relatively large load in the electricity grid. If the charging is unmanaged the electricity grid can be affected negatively. Therefore, it is essential to study the impact of EVs on the electricity grid. The impact of the Electric Vehicles on the grid is discussed in the previous section. In the previous section we have learnt that the impact of the Electric Vehicles on the Distribution System Operators will be huge and the DSOs, who manage and operate the grid, therefore have an interest in supporting and managing EV charging if it avoids a massive reinforcement of the distribution grid.

In contrast, the EVs could potentially be an asset in the power system by providing ancillary services. Here we focus focuses on the centralized approach of directly controlling the EV charging. The EV aggregator is referred to as the charging service provider (CSP). The CSP controls the charging by calculating individual charging schedules for each EV. The CSP is separated from other power system players such as the retailer and the DSO [29]. A framework of letting the CSP, the retailer, and the DSO influence the charging schedules is proposed. For this thesis purpose, we have taken the results from the experiment conducted on the Danish island of Bornholm.

11.1. Uncoordinated Direct Charging

The first generation of EVs starts charging when the EV is plugged into the electricity network and stops when the battery is fully charged. This is referred to as direct charging. The aggregated load when using direct charging in the simulated system is shown in the figure below [30].

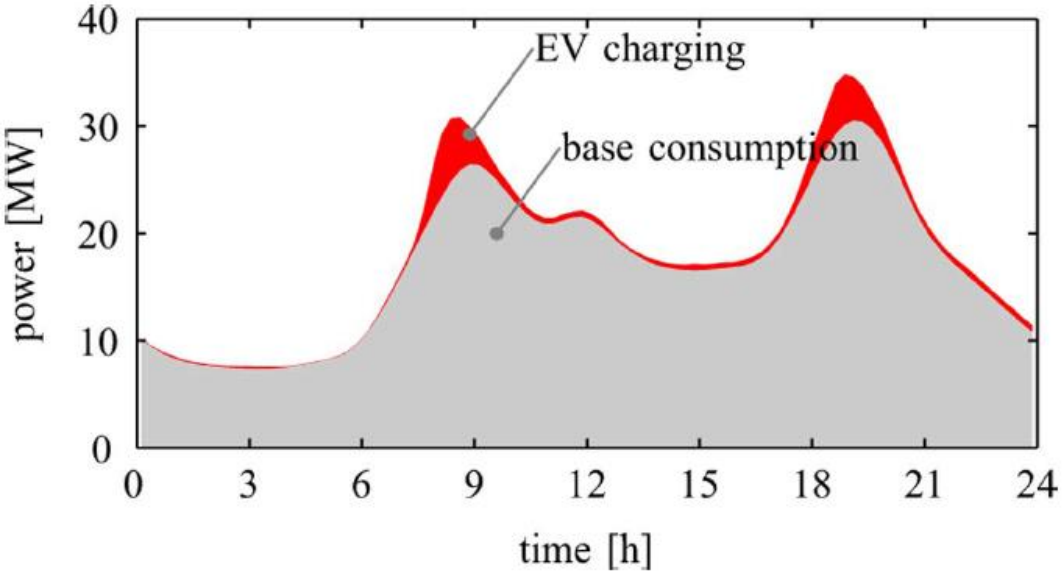

Figure 61: Base load of the system and total aggregated EV charging using uncoordinated direct charging of all EVs

The direct charging is therefore increasing the traditional daily peaks in demand because of the correlated usage patterns of commuter vehicles and traditional loads. The largest peak in demand is when EV drivers arrive at home in the evening, plug in the EV, and start cooking. This is one of the worst cases for the electricity grid because it is likely that reinforcements are needed to handle this high load [31]. Furthermore, the marginal power generated during the peak demand is in general expensive and intensive.

11.2. Charging Service provider

The overall planning model is shown in the below figure. The charging service provider (CSP) acts as aggregator of the EV fleet and interacts with the DSO and the electricity retailer (RET). By collecting statistics from the EV fleet and power usage propositions from the retailer and by interacting with the DSO, the CSP attempts to optimize the EV charging such that the owner's anticipated energy requirements are met, the retailer's suggested power profile is followed, and no grid bottlenecks appear during EV charging.

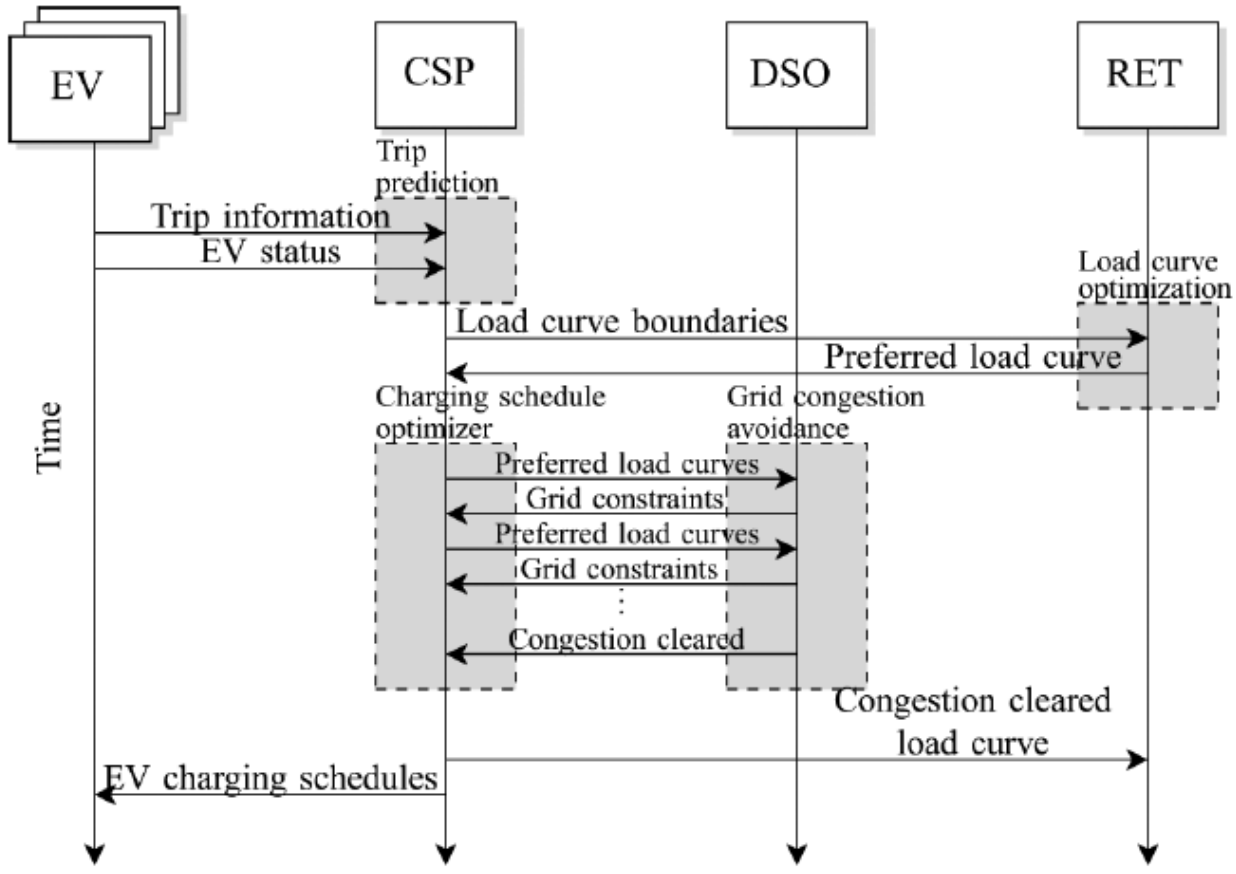

Figure 62: The flow of information between the charging service provider (CSP), the electric vehicles (EV), the distribution-system operator (DSO), and the retailer (RET)

The CSP has the following basic operational functions, omitting customer relationship and billing:

- **Data collection and storage:** The CSP collects historical trip data of all customer EVs. In addition, end customer information and billing information are stored.
- **Trip forecasting:** Trip forecasting is an essential part of the CSP's operation. It involves the prediction of near-future EV trips based on the historical trip data and possibly other parameters. Trip prediction is also used to define the load curve boundaries that are used to determine the preferred aggregated load curve.
- **Charging optimization:** This optimization is at the core of the CSP for computing individual charging schedules for each EV. To maximize EV utilization and minimize the cost of charging, the optimization should also be able to include other stakeholders' objectives. For example, allowing the retailer to decide on the aggregate load curve should result in an energy cost that is lower than the normal contractual pricing schemes offered by the retailer. Also, the CSP could assist the DSO in preventing distribution grid congestion and therefore potentially share the value of delayed expansion of the distribution grid [32].

Note that several important aspects are not addressed in this paper, for example, the communication infrastructure between EVs, the retailer, and the DSO is not described. However, the optimization methods and data needed to derive the charging schedules are described.

11.2.1. Trip Forecasting

The optimization of the EV charging depends on the energy needs of each vehicle. The end-user expects the EV to be sufficiently charged to drive the next trip. The most conservative strategy to achieve this is to use the direct charging. A good estimation of the future trip4 behaviour in the planning period is essential for the overall planning accuracy [29]. Thus, the following information is collected for each completed trip:

• Time-of-departure: a time stamp indicating when the trip started;

• Time-of-arrival: a time stamp indicating when the trip ended;

• State-of-energy at time-of-departure: the energy stored in the battery at the beginning of the trip;

• State-of-energy at time-of-arrival: the energy remaining in the battery at the end of the trip;

• Location at time-of-arrival: the physical location reached at the end of the trip, which becomes the starting location for the next trip.

Based on these historical data, the future trip behaviour is predicted for each individual vehicle. The data predicted includes time of departure, time of arrival, energy need, and location of each trip for each vehicle.

11.2.2. Charging Schedule Computation

A charging schedule is a pre-planned time series of the charging power. In this paper, the planning period is an entire day from midnight to midnight. It is divided into slots with a time step of t_s = 15 mins. An EV charging schedule therefore contains a charging power level for each of the 96 slots.

The goal of the optimization is to derive a charging schedule for each vehicle that ensures sufficient energy for the trips predicted. The CSP can buy the electricity on the wholesale markets only if it aggregates sufficient number of vehicles to meet the minimum bid volumes. The CSP is then required to optimize its bids according to the predicted demand and the available flexibility in time of charging.

If the CSP does not aggregate sufficient vehicles to enter these markets, it must be able to outsource the charging flexibility to an existing market player, such as a retailer. For example, the CSP can offer flexibility to the retailer in return for a shared profit realized with this flexibility. The retailer can, in turn, use this flexibility when optimizing its bids and interactions with the different electricity markets [33]. In this case, an appropriate communication infrastructure must be in place between the CSP and the retailer. The offered flexibility must be described and communicated to the retailer. In this paper the following list is used to describe the flexibility.

- E_0: an estimation of the initial energy stored in the fleet before the planning period.
- $\bar{E}$: a time series of the maximum integral of the allowed reference power.
- $\underline{E}$: a time series of the minimum integral of the allowed reference power.
- $\overline{P}$: a time series of the maximum allowed reference power.
- $\underline{P}$: a time series of the minimum allowed reference power.

The retailer optimizes its processes and computes a reference load curve $P_{ref,}$ which is a time series of the preferred aggregated charging power, while respecting the energy and power constraints

$$\underline{E}_j \leq E_{\mathrm{ref},j} \leq \overline{E}_j \quad \forall\, j = 1, 2, \ldots, N \tag{1}$$

$$\underline{P}_j \leq P_{\mathrm{ref},j} \leq P_j \quad \forall\, j = 1, 2, \ldots, N \tag{2}$$

Where the reference energy is given by the reference power

$$E_{\mathrm{ref},j} = E_0 + \sum_{\tau=1}^{j} t_s P_{\mathrm{ref},\tau} \quad \forall\, j = 1, 2, \ldots, N. \tag{3}$$

The preferred reference power series P_{ref} is communicated back to the CSP. An example of the load curve boundaries $\overline{E}$, $\underline{E}$, $\overline{P}$, and $\underline{P}$ in the figure below.
It clearly shows that during peak traffic times, i.e., in the morning and late afternoon, the available power $\overline{P}$, is reduced because many EVs are disconnected from the grid. Also, the aggregated minimum energy need is evident from the increases in before the peak traffic times.

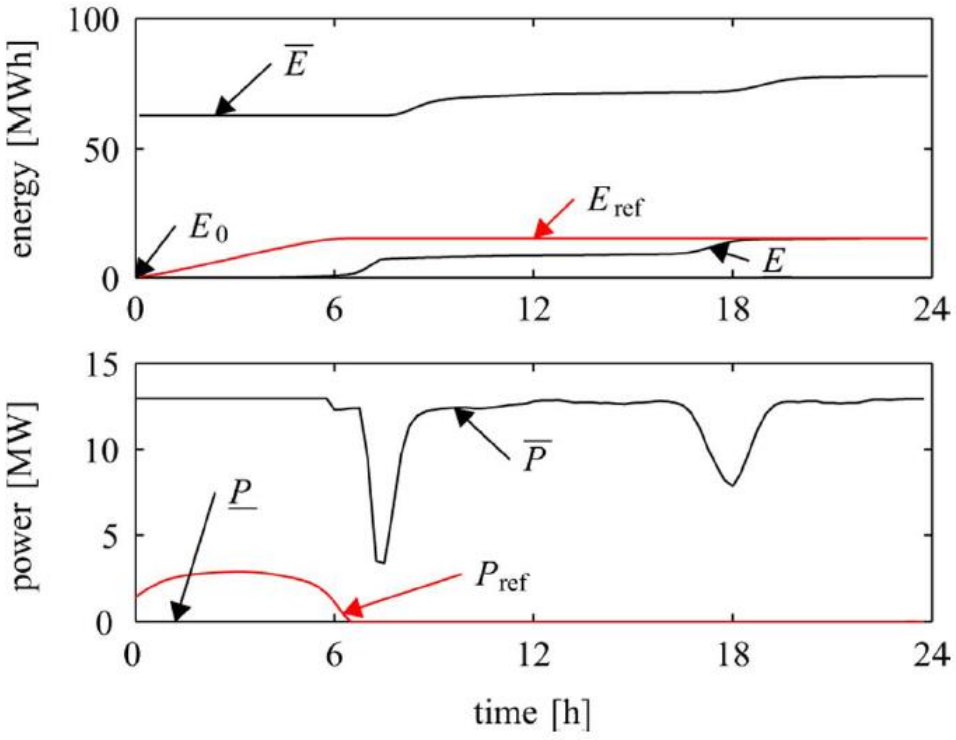

Figure 63: The initial fleet energy and the energy limits (upper graph) and power limits (lower graph). The reference energy trajectory, Eref is given by the cumulative sum of the reference power curve, Pref

It is assumed that the retailer optimizes and provides the aggregated load curve according to the boundaries specified by the CSP, while offering a competitive price on the overall energy [34]. The input from the retailer is the preferred charging curve P_{ref}. The objective for the optimization problem is to follow P_{ref} as closely as possible. If it is not possible to follow the reference curve exactly, there are several options for determining a solution. One way of achieving this is to minimize the sum of the quadratic difference and quadratic change of the difference

$$\min \sum_{j=1}^{N} \alpha_j d_j^2 + \sum_{j=1}^{N-1} \beta_j d_j'^2, \tag{4}$$

Where α_j and β_j are weighting coefficients, the difference between the preferred charging curve and the actual charging is

$$d_j = \sum_{i=1}^{N} P_{b,i,j} - P_{\mathrm{ref},j} \tag{5}$$

Where $P_{b,i,j}$ is the charging power in time slot *j* for vehicle *i* .
The change of this difference is

$$d'_j = d_j - d_{j-1}. \tag{6}$$

By including both terms it is possible to make the charging follow the fluctuations in the reference curve whenever the reference curve cannot be followed exactly. The weighting between these objectives has to be determined. Using the objective function (5) the problem becomes a quadratic programming problem.

Another way of specifying the objective function is to minimize the sum of the absolute differences. The linear program formulation is used to reduce computation time. However, the solutions of the two optimization problems are in general not the same, and the impact of the difference has to be studied further.

We denote the energy required by vehicle i for trip k as $E_{i,k}$ .Also, the vehicle's energy storage is limited by the maximum and the minimum energy $E_{max\ i}$ and $E_{min\ i.}$

The initial energy level in vehicle i is $E_{0,i}$. The resulting optimization problem is

$$\min_{P_b} \sum_{j=1}^{N} \alpha_j |d_j| + \sum_{j=1}^{N-1} \beta_j |d'_j| + \sum_{i=1}^{N} \sum_{k=1}^{K_i} \delta_{i,k} s_{i,k} \tag{7a}$$

Subject to (5),(6), and

$$\sum_{j=1}^{J_d(i,k)} t_s P_{b,i,j} - \sum_{\kappa=1}^{k-1} E_{i,\kappa} + E_{0,i} - E_{\min,i} + s_{i,k} \geq E_{i,k} \tag{7b}$$

$$\forall\, k = 1, 2, \ldots, K_i, \quad i = 1, 2, \ldots, M$$

$$\forall\, k = 1, 2, \ldots, K_i, \quad i = 1, 2, \ldots, M$$

$$s_{i,k} \geq 0 \tag{7c}$$

$$\forall\, k = 1, 2, \ldots, K_i, \quad i = 1, 2, \ldots, M \tag{7d}$$

$$0 \leq P_{b,i,j} \leq P_{\max,i,j}$$

$$\forall\, i = 1, 2, \ldots, M, \quad j = 1, 2, \ldots, N, \tag{7e}$$

Where $P_{max\ i,,j}$ is the maximum charging power for vehicle *i* in time slot *j*, which is zero if the vehicle is disconnected. Where is the maximum charging power for vehicle in time slot, which is zero if the vehicle is disconnected? The function $J_d(i,k)$ denotes the time slot prior to the start of trip *k* of vehicle *i*. For each trip energy constraint, a slack variable is added to handle situations in which individual trip requirements cannot be satisfied. The sum of the slack variables is minimized using a weighting factor $\delta_{i.k}$ for each slack variable. Hence, vehicles and trips can be prioritized by selecting the individual weights. However, in the examples here, the coefficients, α, β, and δ, and are all set to one. The minimum charging power is zero, because discharging power into the grid is not considered here in this thesis. If discharging were to be allowed, the optimization problem changes slightly. The energy constraints (7b)–(7c) have to be considered for each time step *j* instead of per trip*k*.

11.2.3. Retailer

The role of a retailer is to buy electricity on the wholesale market and resell it to end consumers. If the CSP is separate from the retailer, the CSP has to buy the power either from the retailer or on the wholesale market. The latter requires that the CSP aggregate a sufficient number of EVs to meet the minimum bid volume on the

wholesale market. Here, it is assumed that the retailer determines the reference load curve P_{ref} while respecting (1) and (2).

This section simplifies the retailer part because the focus is not on the details of the retailer but rather to demonstrate the interfaces needed by the CSP to outsource the calculation of $P_{ref.}$ One way of determining is to forecast the total inflexible base load P_{base} and to estimate the price sensitivity in the market. Assume, for example, that the price of electricity, c_j, depends quadratically on the total load at time slot j.

$$c_j = c_{0,j} \left(\frac{P_{\text{base},j} + P_{\text{ref},j}}{P_{0,j}} \right)^2, \tag{8}$$

Where $P_{base,j}$ is the inelastic base load, $P_{ref,j,}$ is the total charging power of the entire fleet at time slot j, and $C_{0,j}$, is the price of electricity when the load is equal to $P_{0,j.}$ In this study, the parameters, $C_{0,j}$, and $P_{0,j}$ are constant and do not influence the resulting optimal load curve in the optimization problem [35]. However, in a realistic situation the price sensitivity is not constant throughout the day. The reference load curve that minimizes the total cost is thus determined by solving the following nonlinear optimization problem:

$$\min_{P_{\text{ref}}} \sum_{j=1}^{N} t_s c_j \left(P_{\text{ref},j} \right) P_{\text{ref},j}, \quad \text{Subject to (1) and (2)} \tag{9}$$

The assumptions of a single market and a quadratic price sensitivity neglect, for example, the value of regulation power. In reality, several factors impact the way the retailer can determine the reference load curve. For example, the predicted price of electricity and the predicted value of regulation power influence the calculations. The retailer could, for example, allocate some charging in high-volatility hours throughout the day to ensure sufficient flexibility and available regulation power. Here, the reference power curve is determined by solving the optimization problem (9) for the base load $P_{base.}$

11.3. Distribution System operator

The DSO manages the distribution grid, and large-scale adoption of EVs may require costly grid reinforcements. This section describes a method to reduce potential grid overloading. The method allows the DSO to interact with the CSP and influence the charging schedules if overloading is detected. This may allow distribution-grid reinforcements and the associated costs to be avoided.

For this thesis, we consider that the CSP has a limited interaction with the DSO and only the necessary information is exchanged to solve the congestion. The distribution grid parameters and the conventional load profiles are assumed to be DSO confidential. Thus, the CSP has limited private information about other consumers than the EVs.

For an unconstrained grid, the charging schedules computation is done by solving the optimization problem (7) once. If the grid is constrained, the same optimization problem is solved and iteratively updated to include critical constraints of the distribution grid, which are computed by the DSO. A flow chart of the proposed algorithm is shown in Figure below. The details, where each step belongs to either the CSP or the DSO, are as follows.

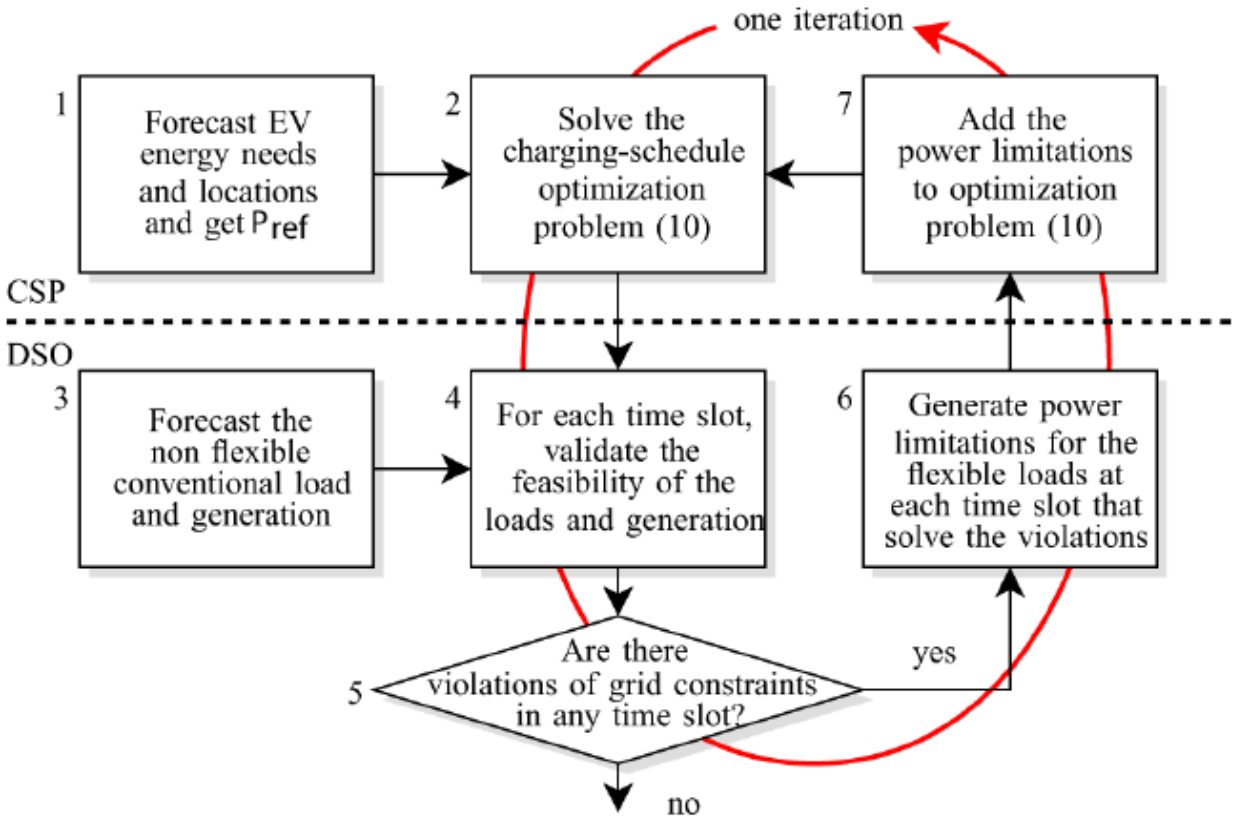

Figure 64: Flow chart of the algorithm that is jointly executed by the CSP and the DSO to derive the charging schedules under constrained grid conditions

The steps are numbered in the order they are executed. The notion of one iteration is also shown in the flow chart, where a new set of constraints is computed and added each time.

11.3.1. Forecast EV energy needs and locations and get P_{ref} (CSP)

The EV energy needs and locations are predicted using the trip history of each vehicle. The EV trip prediction contains the location and duration of the connection events and the minimum required state of energy after each charging interval. Also, the reference power curve P_{ref}, must be obtained either from an external partner or by computing it internally.

11.3.2. Solve the charging-schedule optimization problem (CSP)

Formulate the optimization problem in (7) based on the P_{ref} given and the EV trip forecasts. If this is not the first iteration, include the grid constraints calculated in the preceding iterations. Communicate the proposed individual charging schedules to the DSO.

11.3.3. Forecast the nonflexible conventional load and generation (DSO)

The base load, $P_{base,}$ is determined using generalized consumption profiles for a variety of consumer types, e.g., farms, households, etc. More detailed load forecasts can be obtained using nonintrusive appliance load monitoring together with usage pattern modelling. Distribution grid level generation, e.g., wind power and solar power, is also predicted.

11.3.4. For each time slot, validate the feasibility of the loads and generation (DSO)

The forecasted distributed generation and conventional loads are used together with a grid model to assess the feasibility of the proposed individual charging schedules. This can be done in several ways, depending on the needs and capabilities of the DSO.

11.3.5. Are there violations of grid constraints in any time slot? (DSO)

If the combination of the conventional loads, the distributed generation, and the proposed charging schedules is not feasible the algorithm continues. If the combination is feasible the CSP is notified that the proposed schedules can be implemented.

11.3.6. Generate power limitations for the flexible loads at each time slot that solve the violations (DSO)

Depending on the requirements of the DSO the power limitations are determined either from the maximum flow calculations or from the load flow analysis. An example of a power limitation is

$$\sum_{i \in \{1,4,8\}} P_{b,i,j} \leq 10^4, \quad j = 16 \tag{10}$$

Where cars 1, 4, and 8 can together only charge with 10kW at time slot 16 instead of three times the rated charging spot power 6.4 kW. The reason for the limitation of 10 kW can vary. For example, the local feeder transformer can be overloaded or the voltage in the local area can be too low.

11.3.7. Add the power limitations to the charging schedule-optimization problem (CSP)

Receive the new power limitations from the DSO and add them to the optimization problem formulation.

Note that the base load and the suggested variable load profiles are fixed for the DSO at each iteration of the algorithm. Hence, the computations for the time slots are independent of each other, and the DSO part of the algorithm is therefore inherently parallel.

11.3.7.1. Using the Flow Network method

If the DSO does not have the admittance matrix of the grid or if only the loading rate is of interest the charging power limitations can be computed using maximum flow minimum cut algorithm. In this case, the grid is represented by a flow network. The flow network is constructed for each time slot based on the grid connectivity and loading rate limitations. The flow network is defined as

$$F = \{(V, E),\ s, t \in V,\ c : V \times V \rightarrow \mathbb{R}^+\}, \tag{11}$$

Where(V, E), is a directed graph with edges E and nodes V and containing a source $s \in V$, a target?
$t \in V$, and a capacity $c(u, v) \in \mathbb{R}^+ \forall (u, v) \in E$ and $c(u, v) = 0 \forall (u, v) \notin E.$ The Flow of the network is a function $f : V \times V \rightarrow \mathbb{R},$ where

$$f(u,v) \leq c(u,v) \; \forall \; (u,\; v) \in V \times V \tag{12a}$$

$$f(u,v) = -f(v,u) \; \forall \; (u,v) \in V \times V \tag{12b}$$

$$\sum_{u \in V} f(u,v) = 0 \; \forall \; v \in V \setminus \{s,t\}. \tag{12c}$$

The capacities of the interior edges in the flow network,

$$\{c(u,v) \; | u,v \in V \setminus \{s,t\}\}, \tag{13}$$

are the maximum loading rates of the grid components. The flow network includes additional edges from a virtual source node *s* to all nodes representing generation units. The capacities of these edges are the generated power $P_{g,j}(u_j)$ for each generating unit u_g. Similarly, the flow network also includes additional edges from all nodes representing outlets to a virtual target node *t*. The capacities of these edges are the total power demand of each outlet u_c.

$$c(u_c,t) = P_{\text{base},j}(u_c) + \sum_{i \in \Omega(u_c)} P_{b,i,j}, \tag{14}$$

Where $P_{\text{base, j}}(u_c)$ is the conventional load at the outlet u_c for time slot *j* and is the set of vehicles that are connected to the outlet u_c at time slot *j*. The maximum flow through the network from the source to
the target can be formulated as a linear program (LP)

$$\max \sum_{u \in V} f(s,u) \tag{15}$$

Subject to (12a), (12b) and (12c)

After solving the maximum flow optimization the flow at each edge is known. If the flows over the edges to the target are equal to the capacities of these edges, the requested power levels at the outlets are feasible and can be delivered through the network. This criteria can be checked as follows:

$$f(u,t) = c(u,t) \; \forall \; u \in V. \tag{16}$$

If (16) is not true, a congestion exist and the requested power cannot be delivered to the outlets. In this case, there exists a minimum cut through the network where all edges

going through the cut are saturated. This cut partitions the set of nodes V in the flow network into (S, T) where $s \in S$ and $t \in T$.

To determine the power limitations for the EVs all the disjoint subnetworks are found in the network below the minimum cut, i.e., the part of the original flow network associated with *T*. For each of the disjoint subnetworks the following power limitation is created:

$$\sum_{(u,t)\in E'} \sum_{i\in\Omega(u)} P_{b,i,j}(u) \leq \sum_{\substack{(u,v)\in C \\ v\in V'}} f(u,v) - \sum_{(u,t)\in E'} P_{\text{base},j}(u), \tag{17}$$

Where $P_{base,j}$ (u) is the base load used to set up the flow network. Constraint (17) limits the total EV charging at all nodes in the disjoint subnetwork to the difference between the congested inflow to the subnetwork and the total base load of the outlets in the subnetwork.

11.3.7.2. Using the Load Flow Model

If the admittance matrix of the grid is known to the DSO, a traditional load flow analysis can provide more information than the flow network in the previous section. This section describes the method of deriving power limitations from the load flow analysis at each time step. There are several ways of determining these power limitations for the EV charging. Limitations can be derived from the maximum loading rate similarly as for the flow network. Moreover, limitations can be derived from parts in the grid where the voltage drops below a minimum allowed voltage.
Here, the 10-kV and 400-V networks are radial trees going out from the 60/10 kV substations. A power limitation for the charging of EVs for this part of the network is created by finding the critical line and the loads that are downstream from it. For example, assume that the load flow has been determined for time step *j* Denote the active power flow over a critical line in time step *j* as $P_{line,j}$ and the reactive power flow as $Q_{line,j}$. The maximum loading rate of the line is P_{line}^{max} and the set of outlets u_c downstream from the critical line is U_c. The set of EVs at those outlets is Ω (U_c).The total active load determined during the load flow computation is

$$P_{\text{load},j} = \sum_{i\in\Omega(U_c)} P_{b,i,j} + \sum_{u_c\in U_c} P_{\text{base},j}(u_c), \tag{18}$$

and the total reactive load is

$$Q_{\text{load},j} = \sum_{u_c \in U_c} Q_{\text{base},j}(u_c).$$

(19)

The new power limitation that needs to be handed over to the CSP in this example is

$$\sum_{i \in \Omega(U_c)} P_{b,i,j} \leq P_{\text{line}}^{\max} - \sum_{u_c \in U_c} P_{\text{base},j}(u_c) - P_{\text{line},j} + P_{\text{load},j}$$

(20)

where the total allowed charging power of the EVs in Ω (U_c) is limited to the right hand side of (20)

The distribution grid is dimensioned for a predefined maximum voltage drop. During this dimensioning process each transmission line is given a maximum voltage drop such that the overall voltage drop at each outlet is 7% during the peak of the conventional load. However, because the grid is not dimensioned to handle the EV fleet the charging can result in lines exceeding the allowed voltage drop.

If the maximum voltage drop is violated the EV charging in the downstream network must be reduced. A standard nose curve computation9 is used to compute the maximum active power that can be consumed by the loads. This maximum power depends on the allowed voltage drop, the reactive load in the downstream network, and the electrical characteristics of the line itself. The new power limitation that reflects the voltage drop limitation is

$$\sum_{i \in \Omega(U_c)} P_{b,i,j} \leq P_{\text{line}}^{\max}(Q_{\text{load},j}, \Delta U_{\max}, R, X) - \sum_{u_c \in U_c} P_{\text{base},j}(u_c) - P_{\text{line},j} + P_{\text{load},j},$$

(21)

Where ΔU_{max} is the maximum voltage drop, $Z = R + jX$ is the impedance of the Thevenin-equivalent circuit of the line. The constraint limits the total charging power of the EVs in Ω (U_c) to the right hand side of (21).

11.4. Analysis

Coordinated charging can solve some of the issues of uncoordinated charging. In this section, the charging is coordinated using the concepts described in the earlier sections [36]. The reference power curve optimization problem (9), the charging schedule optimization problem (7), and the maximum flow problem (15) are solved using IBM ILOG CPLEX10 library. The resulting simulated loads in the system is shown in the figures below.

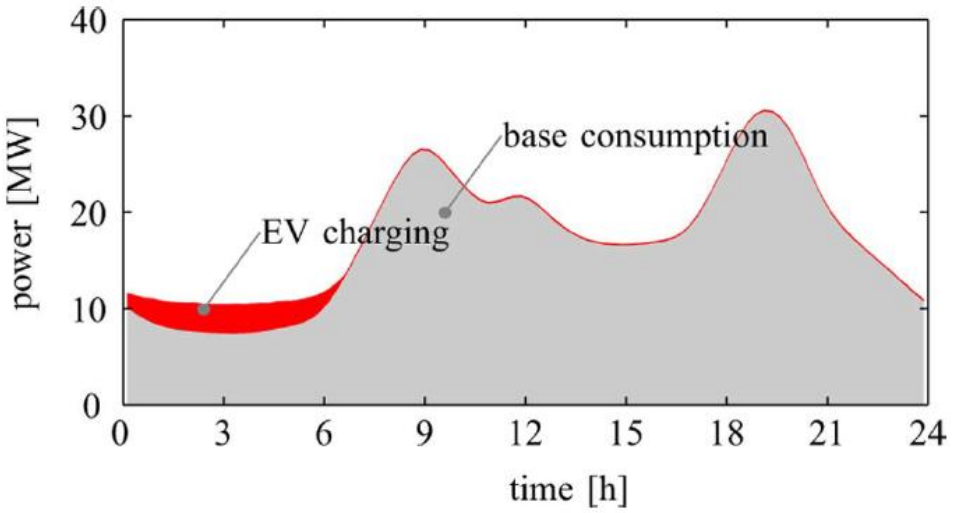

Figure 65: Base load of the system and total aggregated EV charging for the reference power curve Pref

EV charging is done during night because of the cost minimization used by the retailer. However, because the grid is not dimensioned for the EV charging a more detailed analysis of grid problems is required. The top graph of Fig. 65 shows the distribution of the relative loading rate of all simulated two ports in the entire grid throughout the day if the DSO is not included in the charging schedule computation. It can be seen that even though the charging is done during hours with low base load some parts of the grid are overloaded. This can be explained by the relatively low peak load for the outer parts of the low voltage grid. When several EVs are being charged simultaneously the grid in those areas is overloaded.
Consequently, there is a need to manage the charging of the EV fleet with the objective in preventing overload. The resulting relative loading using the maximum flow algorithm.

The resulting loading using the load flow analysis to compute power limitations is shown in the bottom graph of the figure below. In both cases, the overloading of the grid is reduced such that the maximum loading is around 100%. This is a consequence of iteratively adding new constraints to the optimization problem.

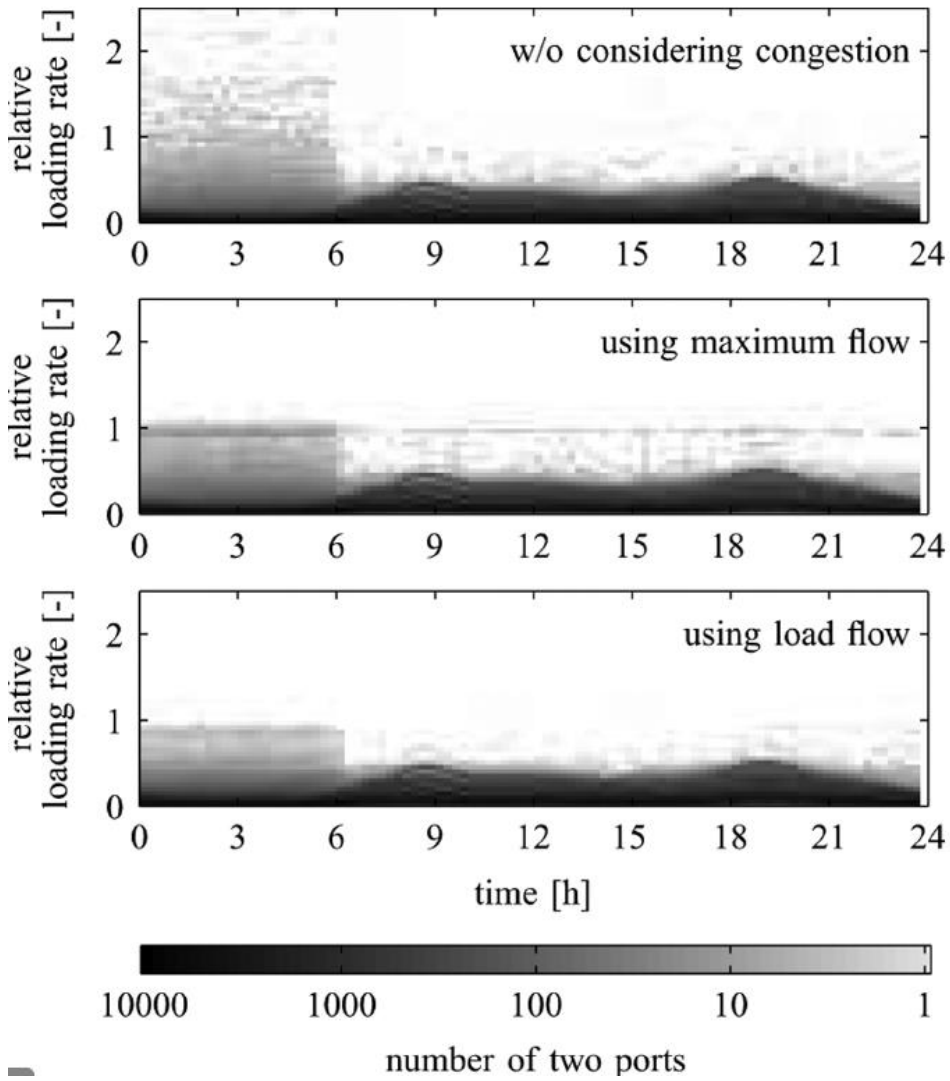

Figure 66: Grid load distribution, using reference power curve, without grid congestion, top graph, and grid congestion using the maximum flow algorithm, middle graph, and considering grid congestion using the load flow computation, bottom graph

The loading distribution, i.e., the number of two ports, is shown in a logarithmic colour scale. [37]

Because the maximum flow algorithm neglects voltage problems. It is important to also consider voltage problems. The set of figures below show the relative voltage distribution of all the nodes in the grid. The top graph shows the distribution if not considering congestion in the grid. It clearly shows that the voltages for several nodes are far below what is acceptable. Hence, it is even though the loading rate limitations are handled, as shown in the previous set of figures, the voltage still drops below an acceptable level for a large part of the grid [38]. This shows that solving the overloading problem does not guarantee that the voltages are within a feasible range.

The bottom graph in the below set of figures shows the relative voltage distribution using the load flow method. It shows that the method of computing load

flow solutions and generating new charging power constraints, as described in Load Flow Method, reduces the voltage problems. In fact, the voltage stays within acceptable limits during the charging of the electric vehicles.

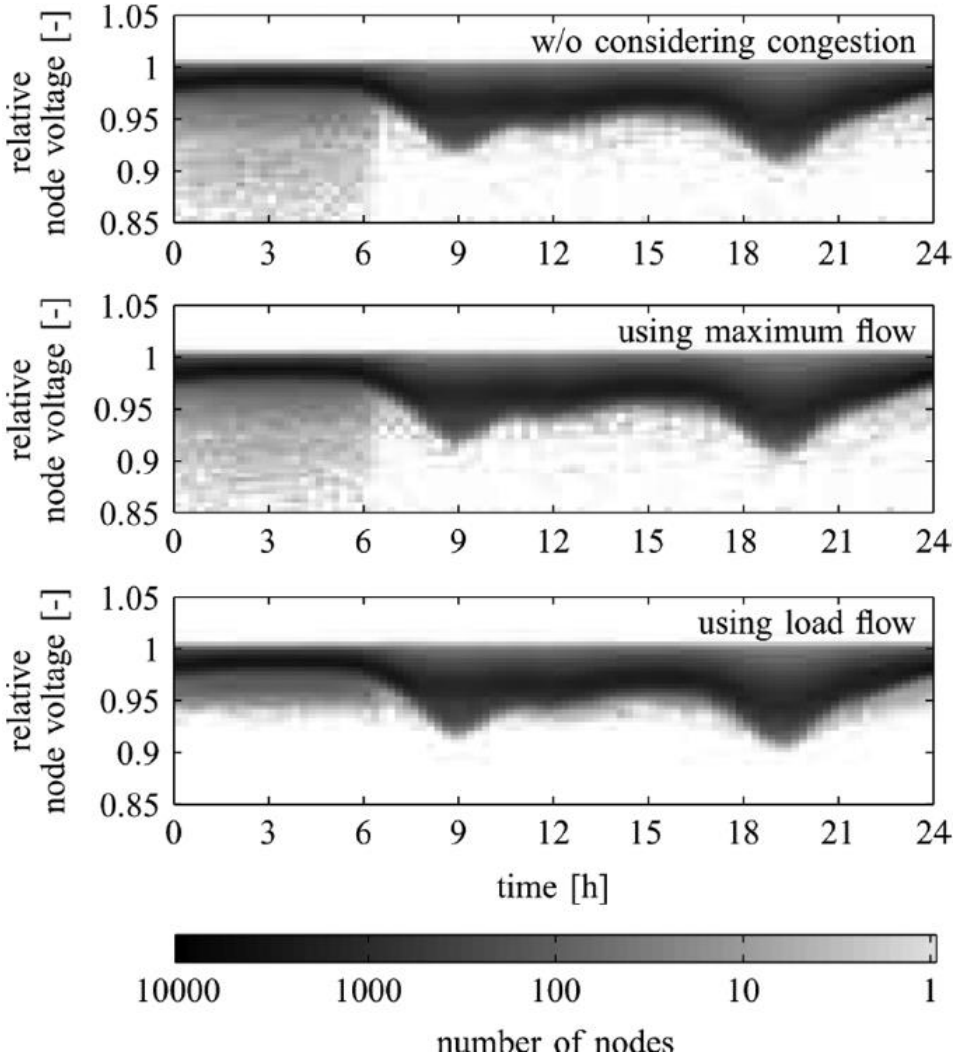

Figure 67: Relative voltage distribution in the grid, using reference power curve Pref, without grid congestion, top graph, and grid congestion using the maximum flow algorithm, middle graph, and grid congestion using the load flow computation, bottom graph

The relative voltage distribution, i.e., the number of nodes, is shown in a logarithmic colour scale.

As the charging schedules have been changed to avoid both overload and voltage drop limitations, it is important to quantify the resulting changes at the aggregated level. As mentioned in Section titled RETAILER, the CSP committed to follow a reference load curve at the aggregated level. The resulting aggregated EV charging is shown in the below figure.

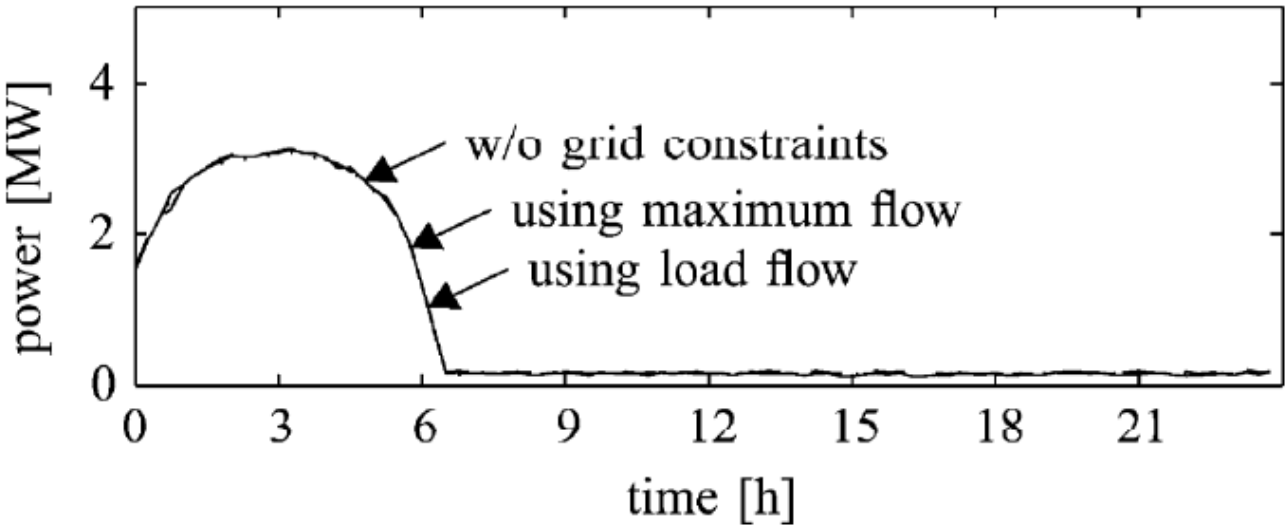

Figure 68: The aggregated EV charging without considering grid congestion, the aggregated EV charging when considering grid congestion using the maximum flow algorithm, and the aggregated charging when considering grid congestion using the load flow computation

It shows the resulting charging without considering grid congestion, using the maximum flow algorithm, and using the load flow analysis. It shows that the aggregated load curve does not change significantly (the three curves are therefore difficult to distinguish in the figure) when the grid congestion is included in the optimization.

However, the earlier set of 2 figures show that the charging is rescheduled on an individual EV level which solves both congestion and voltage problems. The individual EV charging is flexible enough to be rescheduled within the fleet without affecting the aggregated load [39]. If the grid has very low margins, it is likely that there will be a significant difference in the aggregated load curves if the preferred load curve P_{ref} is close to the maximum allowed power $\overline{P}$. This means that all EVs are charged simultaneously and the grid congestion can be impossible to solve without changing the charging on an aggregate level.

The method to avoid distribution grid constraints proposed is an iterative algorithm. It is important to also analyse the convergence of the algorithm. A proof of convergence and an upper bound of the number of iterations are not given in this thesis and are subject to future research. However, to get an idea of these issues, the total number of constraints that have been added to the original problem at each iteration is shown in the next figure below. It shows that using the maximum flow algorithm to avoid overloading only requires 11 iterations and 1561 new constraints in the charging schedule optimization. Using the load flow analysis to handle both overloading and low voltage problems requires 30 iterations and 23087 new constraints in the charging schedule optimization.

The figure below shows that the majority of the power limitations needed to solve the congestion, and the voltage problems when using the load flow, are added in the first third of the iterations. During the final two thirds only very few new power limitations are added.

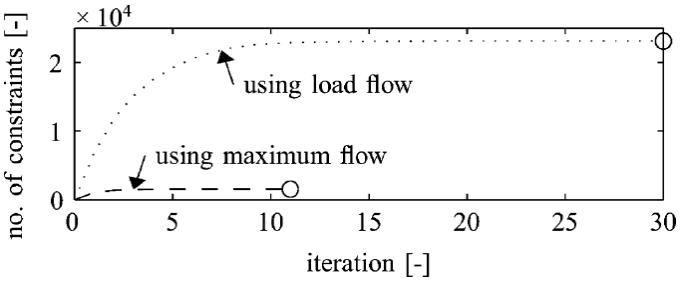

Figure 69: Number of iterations and total number of grid constraints in the schedule computation for the two methods of including grid constraints, using the maximum flow algorithm and using the load flow analysis

11.5. Optimization of Home Charging with Renewable Energy

With the use renewable energy, the charging of the Electric Vehicles can be done at home. This is a very good method of shaving off the peak load from the grid. Most electric vehicles (EVs) have an on-board charger that uses a rectifier circuit to transform alternating current from the electrical grid to direct current suitable for them. Cost and thermal issues limit how much power the rectifier can handle, so beyond around 240 VAC and 75 A it is better for an external charging station to deliver direct current DC directly to the vehicle's battery pack. Given these limitations, most conventional charging solutions are 240V/16A service in Europe [40]. The table below shows the different kind of charging and its ratings.

Summary of the different kind of charges

Charging time	Power supply	Voltage	Max current
6–8 hours	Single phase - 3.3 kW	230 VAC	16 A
2–3 hours	Three phase - 10 kW	400 VAC	16 A
3–4 hours	Single phase - 7 kW	230 VAC	32 A
1–2 hours	Three phase - 24 kW	400 VAC	32 A
20–30 minutes	Three phase - 43 kW	400 VAC	63 A
20-30 minutes	Direct-Current – 50 kW	400-500 VDC	100-125 A

Table 18: Different types of charging methods

The proposed system will be able to use renewable energy such as solar energy and wind power, to charge a set of batteries which will later be used for the vehicle. These batteries will be given dimension to allow a fast discharge with direct current from them to the electric vehicle.

One of the most interesting points of the system is its capability to be divided into several modules connected to a 400 V DC bus. This characteristic will allow adding as many elements as would be necessary in the future or for performing maintenance on certain modules without stopping the whole system. Another advantage is the possibility of having a hybrid pack of batteries.

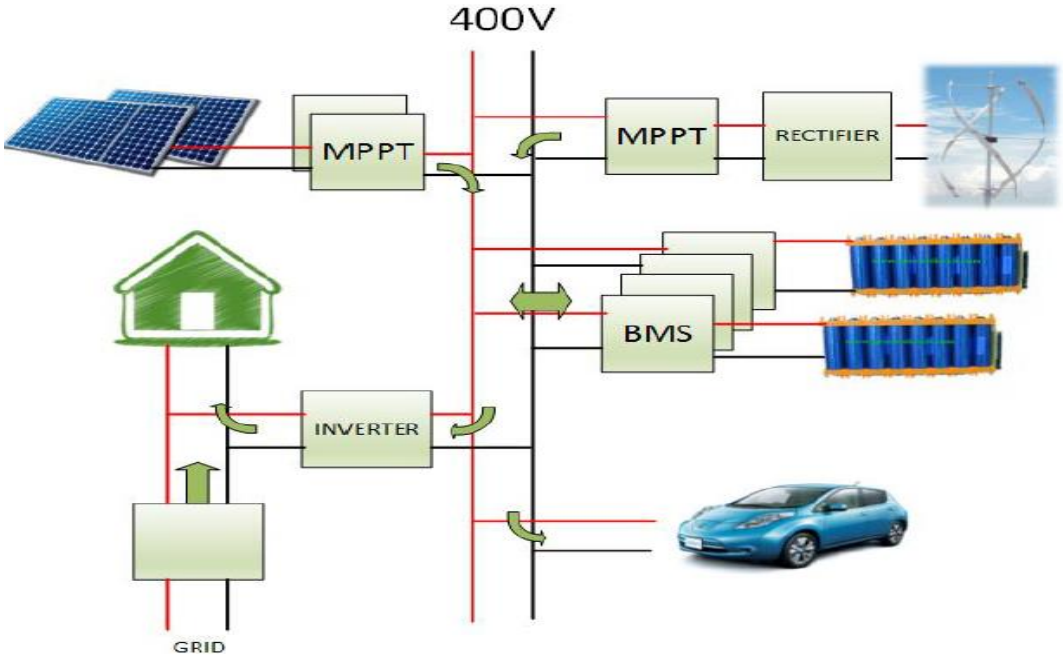

Figure 70: Schematic diagram of the system

In this thesis, we will discuss the BMS and the Inverter that connects the DC bus to the home in order to smooth the peak power demand. In both the cases topology and the control scheme will be discussed. Since, the BMS has been already discussed in the earlier section of this thesis, less time will be on the same and we will directly talk about the topology of the BMS system.

11.6. Topology of BMS

There are many ways of implementing the battery management system. Here there are two examples explained: master and slaves and daisy chain

The master and slaves organizes the cells into several blocks when one slave manages each module [41]. In the example shown in fig.3, 16 X 3.2 volt cells are arranged in modules, each with an output voltage of 51.2 Volts, but other module sizes and voltages are possible.

The daisy chain ring topology, uses a small simple slave printed circuit board connected to each cell to accommodate the voltage and temperature sensors with an A to D converter, as well as a current bypass switch to enable cell balancing by charge shunting and a communications transceiver with built in capacitive isolation for receiving and transmitting data in digital form.

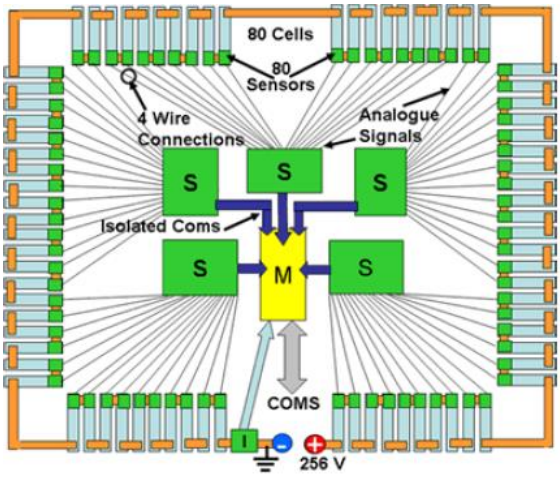

Figure 71: Master and Slave topology

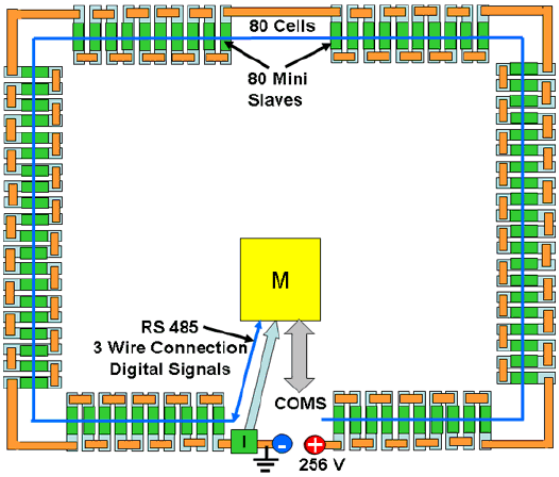

Figure 72: Daisy chain ring topology

Both topologies are based on a huge pack of batteries and a single BMS which is connected to a single, high power charger. This kind of system has a disadvantage that it is solved with the proposed system.

To manage the charge and discharge of the batteries a bidirectional DC-converter will be needed [42] [43]. There are several varieties such as buck-boost converter, reducer-buck raiser-boost converter and bidirectional fly back converter. Due to the huge voltage difference between the DC-bus (400V) and the batteries (3.2x10= 32 V), the last one was chosen for the design due to the ease of reducing/increasing the voltage thanks to the transformer.

11.6.1. Bidirectional Fly back

It is equivalent to that of a buck-boost converter with the inductor split to form a transformer. Therefore the operating principle of both converters is very similar.

When the transistor is closed, the primary of the transformer is directly connected to the 400 V DC bus. The primary current and magnetic flux in the transformer increases, storing energy in the transformer. Equation 1 shows max current value throughout the primary of the transformer. The voltage induced in the secondary winding is negative, so the diode is blocked. The output capacitor supplies energy to the output load.

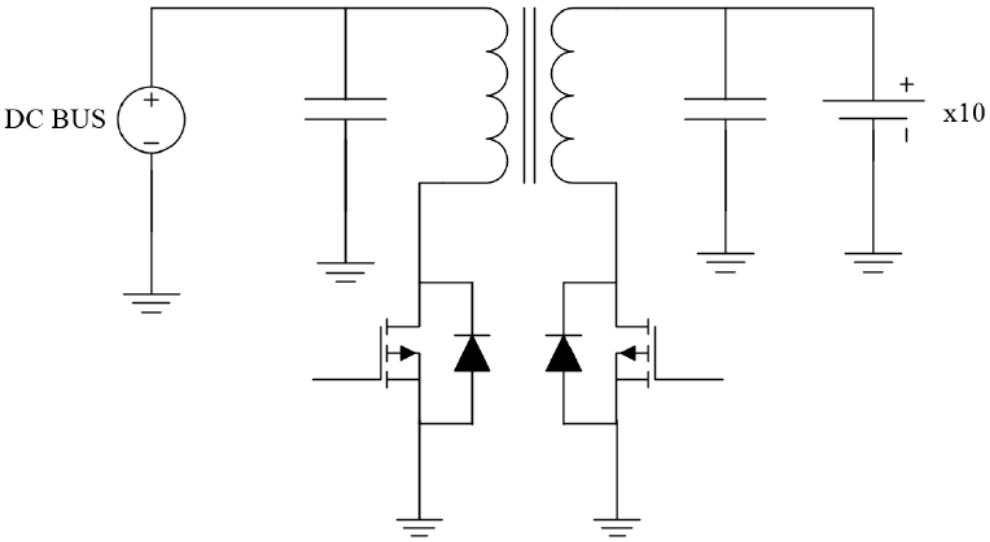

Figure 73: Equivalent circuit of fly back

$$Im = I0+Vbus*d*T/Lm \qquad (1)$$

Where Im and I0 are the maximum and the minimum current throughout the primary of the transformer, Lm is the magnetizing inductance, Vbus is the DC bus voltage, d is the duty cycle and T the period.

When the switch is opened the primary current and magnetic flux drops. The secondary voltage is positive, forward-biasing the diode, allowing current to flow from the transformer. The energy from the transformer core recharges the capacitor and supplies the load. During this period of time, the current throughout the transformer can be expressed as follows:

$$I0 = Im+nVbus/Lm(1-d)T \qquad (2)$$

Where n is the turn ratio.

Bus current (Ib), will therefore be the average value of the current through the transistor, namely:

$$Ib = (Im+I0)/2*d \qquad (3)$$

Moreover, the current with which the batteries will be charged (Ic), correspond to the average value of the diode, which is given by the expression:

$$Ic = n(Im+I0)/2*(1-d) \qquad (4)$$

Finally, the duty cycle necessary can be calculated thanks to the relationship between bus and batteries voltages:

$$Vbat/Vbus = d/(n(1-d)) \qquad (5)$$

11.6.2. Inverter

The system will have an inverter to transform direct current from the bus to the alternating current for use in the home. However, unlike other systems of self-consumption, it is not delivering power to the house without interruption but only doing so when the demanded power exceeds a reference value. Thus, the demand curve can be smoothed and allow reducing the power tariff contracted with the supplier.

To design the inverter, full bridge topology is chosen for several reasons. The most important of these is the ability to control the output amplitude. Modifying the slip angle, the amplitude of the fundamental harmonic in the output can be adjusted and thus control the power delivered, which is fundamental for our system.

11.6.2.1. Single phase full bridge

It consists of two arms with a two semiconductor switches on both arms with antiparallel diodes for discharging the reverse current. In case of resistive-inductive load, the reverse load current flow through these diodes. These diodes provide an alternate path to inductive current which continue so flow during the Turn OFF condition. The full-bridge inverter can produce an output power twice that of the half-bridge inverter with the same input voltage.

11.6.2.2. Unipolar SPWM switching

A SPWM unipolar voltage switching scheme is used (as the switching circuit of the inverter. By selecting the full bridge configuration, the minimal allowed DC-link voltage can be set to be the peak value of the AC grid voltage (plus margins).
Furthermore, using unipolar voltage switching scheme moves the first harmonic from order mf − 1 to the order of 2mf −1, where mf is the frequency modulation ratio. This means that it will can be easily reducer by the filter in the output.

11.7. Control

In many of the current battery management systems, there is a single large BMS that controls a sizeable number of cells. In this case, the control would not be a problem. The BMS module would be responsible for regulating the DC bus. Thus, the charge discharge will always be done properly depending on the other elements of the overall system.

When more BMS modules in parallel are added, this regulation system is no longer valid. Although it is true that all the modules, altogether, achieve a power balance, they don't do it in an equalized way. Namely, a single BMS could be discharging 90 W while two others are charging 60 W and 30W. Therefore, a global control system that solves this problem is completely necessary. One of the possible solutions to this problem is to create a master-slave system. In this kind of system, one of the BMS modules would be the master, which would be connected all the time to both renewable energy source modules and loads (inverter and electric car). Once it knows the data, it sends the reference to the other modules to get a balanced charge discharge between all of them. One of the drawbacks of this system is the total dependence on the master module. Any fault could throw off the entire system.

In this thesis, a new method for the correct equalization of all the modules is introduced based on the philosophy of droop control used in the distributed generation. Thanks to this system, the generator modules which inject power into the bus cause a voltage elevation proportional to the amount of power delivered. Moreover, the power demanded by both the car and the inverter will reduce the voltage. Based on this value, all BMS modules charge or discharge with a power proportional to the bus voltage.

The first advantage of this method is the fact that the dependence between modules will be avoided. Each and every one will be completely independent and they will charge and discharge in an identical way. The only problem with this system is that the bus voltage will not have a fixed value.

11.7.1. BMS Control

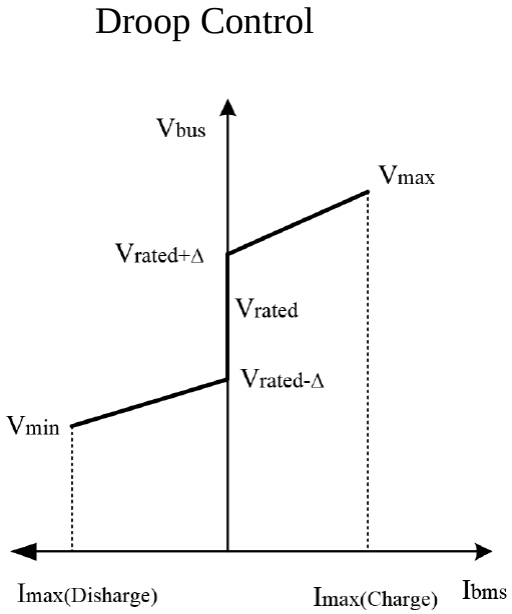

Figure 74: Operating ranges of Droop control

Three different areas of operation can be distinguished. The first one corresponds to a dead zone. Namely, not delivering power to the EV or the inverter nor storing energy. This area is designed primarily to ensure that the charge does not to overlap with the discharge. The second zone corresponds to the charge which is represented on the right side of the figure. Finally, to the left, the discharge area can be seen. The maximum and minimum voltages as well as the slope of the curves depend on the load requirements, specifically the car, which has the largest amount of power demand. Below, two possible operating modes will be explained.

11.7.2. Charge

Watching the charge area in the above figure, it can be said that the bus voltage will depend on the slope of the curve as well as the charging current. The following expression shows that value.

$$Vbus = Vbusrated+\Delta+(Vbusmax-Vbusrated+\Delta)/Ibusmax*Ibus \quad (6)$$

An equivalent circuit consisting of a resistance can be made, which will be named Rdc, with a value of the droop connected to a voltage source whose value is the voltage bus plus the desired increase.

11.7.3. Discharge

During the discharge the behaviour is similar to what occurs during the charge. In this case, the bus voltage would correspond to the following expression.

Vbus = Vbusrated-Δ-(Vbusrated-Δ-Vbusmax)/Ibusmax*Ibus (7)

Keeping in mind these two expressions and the comparison that has been made, the BMS system based on droop control could be represented in a simple circuit form as shown in the next figure.

Moreover, what it is really wanted, is the control of the delivered or consumed power, so what it is really needed to know is the current value. Once the value of the bus voltage is known, which depends on other modules as it was previously explained, we can calculate the necessary current isolating from the above expressions, which will be our reference.

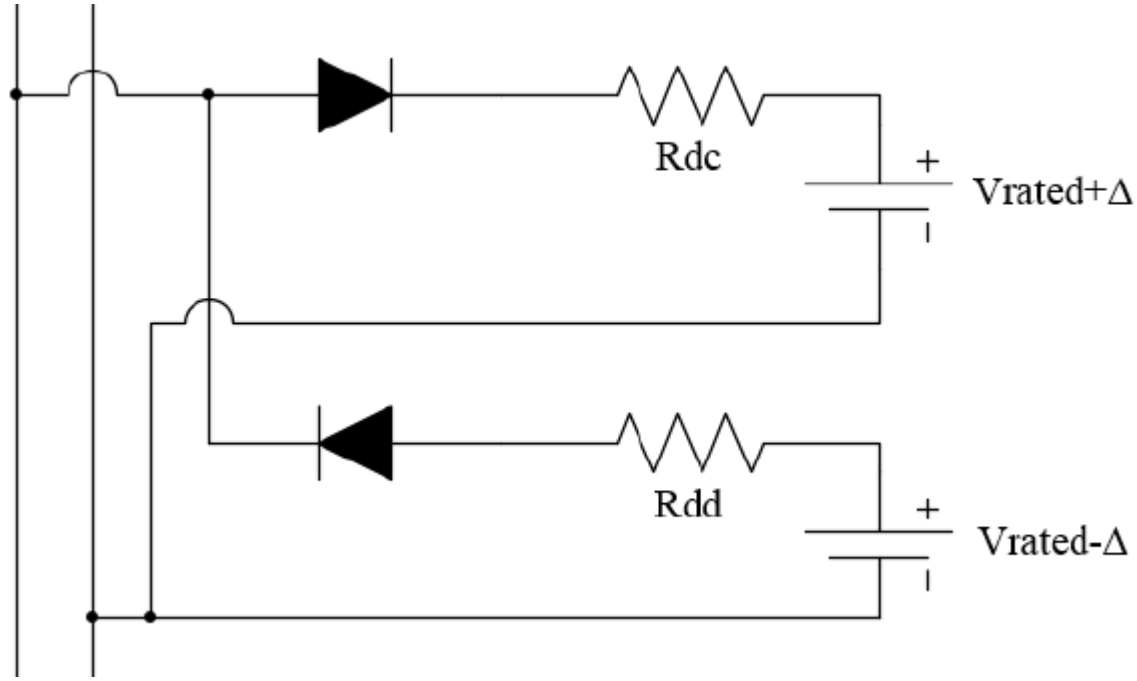

Figure 75: Schematic Circuit

11.7.4. Block Diagram

As in the previous section, the block diagram is divided in charge and discharge, although they are very similar. The first item to emphasize is the current reference that must be controlled. As was specified above, it depends on the bus voltage. During the charge, Vbusrated+Δ is subtracted and it is multiplied by the Rdc value, which is not more than the aforementioned droop. In the case of discharge, instead of subtracting,

we add the Vbusrated-Δ value and multiply by Rdd. This operation represents the droop control.

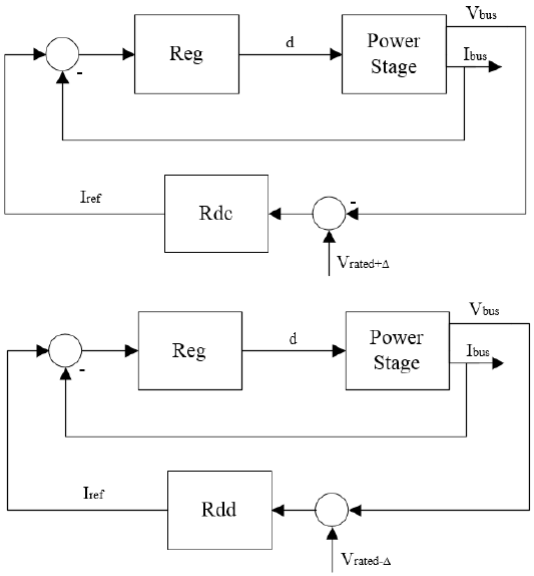

Figure 76: Block diagram during charge and discharge

The next element is the transfer function of the power system. To obtain them, we have used the expressions 1 to 5. For modelling, it has been taken into account that the input variable is the duty cycle, which is the only one that can be controlled at any time, while the output variable is the current delivered to the bus. As before, both the charge and discharge have their own function transfer that are shown in equation 8 and equation 9.

G(S) = n*Vbat*Ibus/Ce*Vbus*Lm*s2+Lm*Ibus*s+d2*Vbus (8)

G(S) = Vbat*Ibus/Ce*Vbus*n*Lm*s2+Lm*Ibus*s+d2*Vbus*n (9)

As can be seen, in both cases there are two poles whose position depends primarily on the values of the inductance of the transformer and the capacitor capacity.

Finally, the regulator that will be used in the system must be mentioned. It should be noted for the design that the transitory of the system is not critical, due to the fact that during the initial moments the duty cycle will be taken to its operation value without using the controller to avoid current peaks that can damage the components. The use of a PI controller is recommended to eliminate as much as possible the output error.

11.7.5. Inverter Control

In the proposed system the inverter will work as a grid-feed. This means that it will controlled to deliver the necessary active power to the load (home). As a future expansion, it can be designed to work as a grid-forming if there are any fault in the grid.

As showed in the following figure, the inverter module will always know the active power by measuring Vg and Ig that the home is consuming. If this one exceeds a rated value, the control and therefore the inverter will start to work for ensuring a constantly active power value delivering a controlled current.
So, this will be the system's reference.

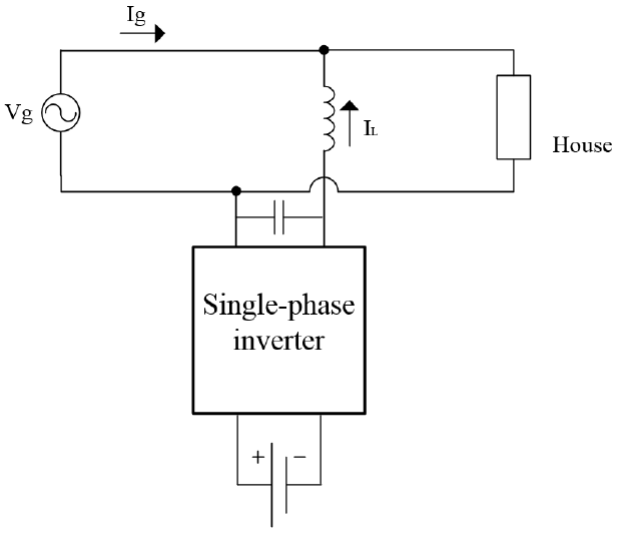

Figure 77: Schematic connection between the inverter and the grid

11.7.5.1. Grid Synchronization Method

Phase, amplitude and frequency of the utility voltage are critical information for the operation of the grid-connected inverter system. In such applications, an accurate and fast detection of the phase angle, amplitude and frequency of the utility voltage is essential to ensure a correct generation of the reference. The method that will be used is based on the detection of the zero crossing of the grid voltage.

11.7.5.2. Block diagram

The proposed control system is showed in the figure below. Three important parts can be observed on it.

The first of them corresponds to the reference current generator. This block performs two operations. On the one hand the measurement of current (Ig) and voltage (Vg). Thus, the active power that is consuming the house is calculated.

Moreover, it calculates the necessary current reference value (IL) that the inverter has to deliver to ensure that the active power will be always constant. The second one corresponds to the module that synchronize with the grid. That module is based on zero crossing abovementioned taking as reference the line voltage (Vg). This module will connect with the previous one in order to have a current reference synchronized at all times with the grid. Finally, the error in the current is calculated, which will be regulated by a PI controller to subsequently, establish the PWM required by the system.

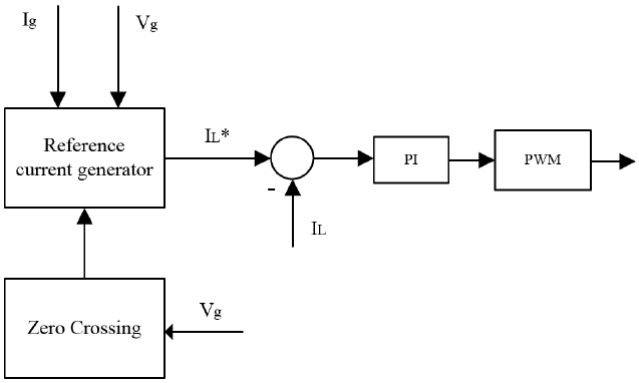

Figure 78: Block Diagram of Inverter

References

[1] 1. M. F. W. M. 1. M. 2. Z. C. W. 2. M. S. 3. S. 3. H. A. a. 4. A. M. A. 1Afida Ayob, "Review on Electric Vehicle, Battery Charger, Charging Station and Standards," *Research Journal of Applied Sciences, Engineering and Technology 7(2): 364-373, 2014,* p. 10, 2014.

[2] L. F. C. C. D. I. O. Veneri**, "Charging Infrastructures for EV:Overview of Technologies and Issues," **Electrical Engineering Department University Federico II of Naples, Via Claudio 21, 80125 Naples, (Italy),* pp. 1-6, 2012.

[3] Y. H.-j. L. C.-d. Xie Ying-hao1a, "Present Situation and Prospect of Lithium-ion Traction Batteries for Electric Vehicles Domestic and Overseas Standards," *1.Guangdong Brunp Recycling Technology Co., Ltd., Foshan 528244, China ； 2. Guangdong power battery & electric vehicle recycling research academician workstation, Foshan 528244, China,* pp. 1-4, 2014.

[4] U. O. F. i. B. M. -Y. C. Habiballah Rahimi-Eichi, "Battery Management System," *An Overview of Its Application in the Smart Grid and Electric Vehicles.*

[5] A. B. M. I. G. F. P. G. a. Antonio Affanni, "Battery Choice and Management for New-Generation Electric Vehicles," *IEEE TRANSACTIONS ON INDUSTRIAL ELECTRONICS, VOL. 52, NO. 5, OCTOBER 2005,* 2005.

[6] U. O. F. i. B. M. -Y. C. Habiballah Rahimi-Eichi, "Battery Management System," *An Overview of Its Application in the Smart Grid and Electric Vehicles,* 2013.

[7] Subaru vehicles, "http://www.chademo.com/," Protocol production, 2016. [Online].

[8] A. B. C. S. P. Dost, "On Analysis of Electric Vehicles DC-Quick-Chargers based on the CHAdeMO protocol regarding the connected systems and security behaviour," *Institute for Power Systems Technology and Power Mechatronics Ruhr-University Bochum.*

[9] J. L. a. K. C. 1. T.W. Ng, "A Review of International charging coupler Standards and its availability in Hong Kong," *Department of Electrical Engineering, The Hong Kong Polytechnic University, Hong Kong.*

[10] T. B. a. H. Chaudhry, "Overview of SAE Standards for Plug-in Electric Vehicle," *Center for Transportation Research, Energy Systems Division.*

[11] Tesla motors, "https://www.teslamotors.com/," Car manfacturer, 2016. [Online].

[12] D. S. C. F. D. S. Maria Carmen Falvo, "EV Charging Stations and Modes: International Standards," *International Symposium on Power Electronics,International Symposium on Power Electronics,.*

[13] L. F. O. Veneri**, "Charging Infrastructures for EV:Overview of Technologies and Issues," **Electrical Engineering Department University Federico II of Naples, Via Claudio 21, 80125 Naples, (Italy).*

[14] D. S. Maria Carmen Falvo, "EV Charging Stations and Modes:International Standards," *International Symposium on Power Electronics,.*

[15] L. W. a. M. A. Robert C. Green II, "The Impact of Plug-in Hybrid Electric Vehicles on Distribution Networks: a Review and Outlook," *IEEE,* 2010.

[16] E. R. Y. Yan Xiangwu, "Research on Power Supply Mode for Electric Vehicle Charging Devices in Residential Community," *School of Electrical and Electronic Engineering,North China Electric Power University,Baoding, China.*

[17] M. I. a. P. T. K. F. I. Murat Yilmaz, "Review of Charging Power Levels and Infrastructure for Plug-In Electric and Hybrid Vehicles," *Grainger Center for Electric Machinery and Electromechanics.*

[18] R. R. Y. H. Z. D. L. P. †. Y Chen*, "Standardization Progress Investigation on Electric Vehicle Charging Infrastructure in China," *ABB Corporate Research China, Power Systems Department, Beijing, China,ABB Corporate Research Sweden, Power Technologies, Vasteras, Sweden.*

[19] M. F.-F. S. M. I. a. M. R. S. M. I. Soroush Shafiee, "Investigating the Impacts of Plug-in Hybrid Electric Vehicles on Power Distribution Systems," *IEEE TRANSACTIONS ON SMART GRID, VOL. 4, NO. 3, SEPTEMBER 2013.*

[20] K. I. S. L. P. Csaba Farkas, "Impact Assessment of Electric Vehicle Charging on a LV Distribution System," *Cs. Farkas is MSc student at the Department of Electric Power Engineering, Budapest University of Technology and Economics, Egry J. u.18, H-1111 Budapest, Hungary.*

[21] S. D. Bundit Pea-da, "Impact of Fast Charging Station to Voltage Profile in Distribution System," *Department of Electrical Engineering,Faculty of Engineering, Kasetsart University,Bangkok, Thailand.*

[22] ∗. I. B. B. D. P. M. F. A. G. L. M. D. Sbordonea, "EV fast charging stations and energy storage technologies:A real implementation in the smart micro grid paradigm," *DIAEE – Electrical Engineering, University of Rome Sapienza, via Eudossiana 18, 00184 Rome, Italy, ENEA, Italian National Agency for New Technologies, Energy and Sustainable Economic Development, Via Anguillarese 301, 00123 Rome, Italy,* 2014.

[23] A. V. Giuseppe MAURI, "FAST CHARGING STATIONS FOR ELECTRIC VEHICLE: THE IMPACT ON THE MV DISTRIBUTION GRIDS OF THE MILAN METROPOLITAN AREA," *2nd IEEE ENERGYCON Conference & Exhibition, 2012 / Sustainable Transportation Systems Symp.*

[24] A. M. J. H. M. D. M. D. Satish Rajagopalan1, "Fast Charging: An In-Depth Look at Market Penetration,Charging Characteristics, and Advanced Technologies," *1Electric Power Research Institute (EPRI), USA.*

[25] Z. Y. L. T. C. X. S. o. E. I. &. E. E. Zheng Zhongqiao, "Analysis on Development Trend of Electric Vehicle Charging Mode," *International Conference on Electronics and Optoelectronics (ICEOE 2011).*

[26] H. M. Z. W. L. J. XIE FeiXiang, "Research on Electric Vehicle Charging Station Load Forecasting," *School of Electrical Engineering Beijing Jiaotong University, Beijing 100044, China.*

[27] P. Gary H. Fox, "Getting Ready for Electric Vehicle Charging Stations," *Senior Member, IEEE.*

[28] B. T.-E. E. F. Fouad Baouche and Romain, "Efficient Allocation of Electric Vehicles Charging Stations: Optimization Model and Application to a Dense Urban Network," *Université de Lyon, F-69000, Lyon, France, IFSTTAR, LICIT, F69675, Bron,ENTPE, LICIT, F-69518, Vaulx-en-Velin,.*

[29] A. V. –. I. Giuseppe MAURI, "THE ROLE OF FAST CHARGING STATIONS FOR ELECTRIC VEHICLES IN THE INTEGRATION AND OPTIMIZATION OF DISTRIBUTION GRID WITH RENEWABLE ENERGY SOURCES.," *CIRED Workshop - Lisbon 29-30 May 2012.*

[30] M. I. a. C. B. Olle Sundström, "Flexible Charging Optimization for Electric Vehicles Considering Distribution Grid Constraints," *IEEE TRANSACTIONS ON SMART GRID, VOL. 3, NO. 1, MARCH 2012.*

[31] Q. S. L. Z. F. W. J. H. Hui WANG1, "LOAD CHARACTERISTICS OF ELECTRIC VEHICLES IN CHARGING AND DISCHARGING STATES AND IMPACTS ON DISTRIBUTION SYSTEMS," *1School of Electrical Engineering, Zhejiang University, China (*fushuan.wen@gmail.com),2School of Electrical Engineering, University of Western Sydney, Australia (j.huang@uws.edu.au).*

[32] C. A. A. Jens Schmutzler and Christian Wietfeld, "Distributed Energy Resource Management for Electric Vehicles using IEC 61850 and ISO/IEC 15118," *2012 IEEE Vehicle Power and Propulsion Conference, Oct. 9-12,2012, Seoul, Korea.*

[33] C. Y. C. S. M. I. Y. N. a. R. Y. Lidan Chen, "Modeling and Optimization of Electric Vehicle Charging Load in a Parking Lot," *L. Chen , C. Y. Chung and Y. Nie are with the Computational Intelligence Applications Research Laboratory (CIARLab), Department of Electrical Engineering, The Hong Kong Polytechnic University, Hong Kong.*

[34] D. I. O. V. Clemente Capassoa, "DC Charging Station for Electric and Plug-In Vehicles," *The 6th International Conference on Applied Energy – ICAE2014.*

[35] D. H.-P. R.-R. D. M.-M. J. B.-J. M. Barnola-Sampera, "Charging/discharging process for electric vehicles:proposal and emulation," *Endesa, Research, Technology Development and Innovation Av. Vilanova, 12 - 08018 Barcelona, Spain.*

[36] K. Q. C. Z. M. I. B. G. S. M. I. a. D. M. H. M. I. Peng Zhang, "A Methodology for Optimization of Power Systems Demand Due to Electric Vehicle Charging Load," *IEEE TRANSACTIONS ON POWER SYSTEMS, VOL. 27, NO. 3, AUGUST 2012.*

[37] J.-W. G. H.-J. R. S.-R. J. Suk-Ho Ahn*, "Implementation of 60-kW Fast Charging System for Electric Vehicle," *Dept. of Energy Conversion Technology University of Science & Technology.*

[38] Y. T. H. S. V. S. K. N. S. D. Pranav Maheshwari, "A Review on Plug-in Electric Vehicles Charging:Standards and Impact on Distribution System," *Pranav Maheshwari, Yash Tambawala, H S V S Kumar Nunna, Suryanaraya Doolla,* 2014.

[39] K. L. K. B. Y. A. B. T. J. D. &. W. G. USMAN Muhammad*, "A framework for electric vehicle charging strategy optimization tested for travel demand generated by an activity-based model," *Transportation Research Institute (IMOB) University Hasselt, Diepenbeek, Belgium,* 2014.

[40] S. M. I. a. R. P. M. I. Zhanle Wang, "An Evaluation of Electric Vehicle Penetration under Demand Response in a Multi-Agent Based Simulation," *2014 Electrical Power and Energy Conference.*

[41] R. U. S.K. Biradar, "Energy Storage System in Electric Vehicle," *SES College of Engineering,Basaveshwar Engg. College,S .NIJ .P.S. N Polytechnic.*

[42] Y. J. B. Y. P. J. Y. Feng Nenglian, “Research on Battery Management System for Light Electric Vehicle,” *International Conference on Transportation, Mechanical, and Electrical Engineering (TMEE),* 2011.

[43] R. E. F. a. S. F. A. G. Mauri and P. Gramatica, “Recharging of EV in a typical Italian urban area: evaluation of the hosting capacity,” *IEEE Trondheim PowerTech,* 2011.